Smithsonian Institution
Scholarly Press

SMITHSONIAN CONTRIBUTIONS TO PALEOBIOLOGY • NUMBER 101

The Neogene Record of Northern South American Native Ungulates

Juan D. Carrillo, Eli Amson, Carlos Jaramillo, Rodolfo Sánchez, Luis Quiroz, Carlos Cuartas, Aldo F. Rincón, and Marcelo R. Sánchez-Villagra

SERIES PUBLICATIONS OF THE SMITHSONIAN INSTITUTION

Emphasis upon publication as a means of "diffusing knowledge" was expressed by the first Secretary of the Smithsonian. In his formal plan for the Institution, Joseph Henry outlined a program that included the following statement: "It is proposed to publish a series of reports, giving an account of the new discoveries in science, and of the changes made from year to year in all branches of knowledge." This theme of basic research has been adhered to through the years in thousands of titles issued in series publications under the Smithsonian imprint, commencing with Smithsonian Contributions to Knowledge in 1848 and continuing with the following active series:

Smithsonian Contributions to Anthropology
Smithsonian Contributions to Botany
Smithsonian Contributions to History and Technology
Smithsonian Contributions to the Marine Sciences
Smithsonian Contributions to Museum Conservation
Smithsonian Contributions to Paleobiology
Smithsonian Contributions to Zoology

In these series, the Smithsonian Institution Scholarly Press (SISP) publishes small papers and full-scale monographs that report on research and collections of the Institution's museums and research centers. The Smithsonian Contributions Series are distributed via exchange mailing lists to libraries, universities, and similar institutions throughout the world.

Manuscripts intended for publication in the Contributions Series undergo substantive peer review and evaluation by SISP's Editorial Board, as well as evaluation by SISP for compliance with manuscript preparation guidelines (available at https://scholarlypress.si.edu). For fully searchable PDFs of all open access series and publications of the Smithsonian Institution Scholarly Press, visit Open SI at http://opensi.si.edu.

SMITHSONIAN CONTRIBUTIONS TO PALEOBIOLOGY • NUMBER 101

The Neogene Record of Northern South American Native Ungulates

Juan D. Carrillo, Eli Amson, Carlos Jaramillo, Rodolfo Sánchez, Luis Quiroz, Carlos Cuartas, Aldo F. Rincón, and Marcelo R. Sánchez-Villagra

Smithsonian Institution
Scholarly Press
WASHINGTON D.C.
2018

ABSTRACT
Carrillo, Juan D., Eli Amson, Carlos Jaramillo, Rodolfo Sánchez, Luis Quiroz, Carlos Cuartas, Aldo F. Rincón, and Marcelo R. Sánchez-Villagra. The Neogene Record of Northern South American Native Ungulates. *Smithsonian Contributions to Paleobiology*, number 101, viii + 67 pages, 35 figures, 13 tables, 2018.—South America was isolated during most of the Cenozoic, and it was home to an endemic fauna. The South American Native Ungulates (SANUs) exhibited high taxonomical, morphological, and ecological diversity and were widely distributed on the continent. However, most SANU fossil records come from high latitudes. This sampling bias challenges the study of their diversity dynamics and biogeography during important tectonic and biotic events, such as the Great American Biotic Interchange, the faunal exchange between North and South America after the formation of the Isthmus of Panama. We describe new SANU remains from the Neogene of the Cocinetas (northern Colombia) and Falcón (northwestern Venezuela) Basins. In the Cocinetas Basin, the middle Miocene fauna of the Castilletes Formation includes *Hilarcotherium miyou* sp. nov. (Astrapotheriidae), cf. *Huilatherium* (Leontiniidae), and *Lambdaconus* cf. *L. colombianus* (Proterotheriidae). The late Pliocene fauna of the Ware Formation includes a Toxodontinae indet. and the putative oldest record of Camelidae in South America. In the Falcón Basin, the Pliocene/Pleistocene faunas of the Codore and San Gregorio Formations include *Falcontoxodon aguilerai* gen. et sp. nov. and Proterotheriidae indet. We provide a phylogenetic analysis for Astrapotheriidae and Toxodontidae. The new data document a low-latitude provinciality within some SANU clades (e.g., Astrapotheriidae, Leontiniidae) during the middle Miocene. This contrasts with the wide latitudinal distribution of clades of other mammals recorded in the fauna, including the sparassodont *Lycopsis padillai*, the sloth *Hyperleptus*?, and the proterotheriid *Lambdaconus* cf. *L. colombianus*. The Pliocene/Pleistocene tropical faunas from northern South America are characterized by the predominance of native taxa despite their proximity to the Isthmus of Panama (fully emerged by that time). Only one North American ungulate herbivore immigrant is present, a cf. Camelidae indet. The Pliocene and early Pleistocene faunas suggest that environmental changes and biotic interactions affected the diversity dynamics and biogeographic patterns of SANUs during the Great American Biotic Interchange.

Cover image: Detail from Figure 34, life reconstruction of the Ware Formation faunal assemblage, Cocinetas Basin, Colombia, by Stjepan Lukac.

Published by SMITHSONIAN INSTITUTION SCHOLARLY PRESS
P.O. Box 37012, MRC 957, Washington, D.C. 20013-7012
https://scholarlypress.si.edu

Library of Congress Cataloging-in-Publication Data

Names: Carrillo, Juan D. (Juan David), 1987– author. | Smithsonian Institution Scholarly Press, issuing body.
Title: The Neogene record of northern South American Native Ungulates / Juan D. Carrillo [and seven others].
Other titles: Smithsonian contributions to paleobiology ; no. 101. 0081-0266
Description: Washington, D.C. : Smithsonian Institution Scholarly Press, 2018. | Series: Smithsonian contributions to paleobiology ISSN 0081-0266 ; number 101 | Includes bibliographical references. | Compilation copyright 2018 Smithsonian Institution
Identifiers: LCCN 2018007367
Subjects: LCSH: Ungulates, Fossil—South America. | Paleontology—South America.
Classification: LCC QE882.U2 C37 2018 | DDC 569/.62098—dc23 | SUDOC SI 1.30:101
LC record available at https://lccn.loc.gov/2018007367

ISSN: 1943-6688 (online); 0081-0266 (print)

ZooBank registration: 5 July 2018 (LSID urn:lsid:zoobank.org:pub:E42FF7D0-4DCB-40EF-9843-BF9F7481AD40)

Publication date (online): 27 July 2018

♾ The paper used in this publication meets the minimum requirements of the American National Standard for Permanence of Paper for Printed Library Materials Z39.48–1992.

Contents

Figures

Tables

The Neogene Record of Northern South American Native Ungulates

Juan D. Carrillo,[1,2] Eli Amson,[3] Carlos Jaramillo,[2] Rodolfo Sánchez,[4] Luis Quiroz,[5] Carlos Cuartas,[2] Aldo F. Rincón,[6] and Marcelo R. Sánchez-Villagra[1]*

INTRODUCTION

South America was isolated during most of the Cenozoic Era and was home to a highly endemic fauna (Simpson, 1980; Wilf et al., 2013). This isolation was punctuated with dispersal events that introduced novel clades into the continent (Croft, 2012), such as the hystricognath rodents during the middle Eocene (ca. 41 million years ago [MYA]; Antoine et al., 2012) and platyrrhine monkeys during the late Eocene (Bond et al., 2015) (Figure 1), migrations referred to as the Trans-Atlantic Dispersal Interval (TADI; Croft, 2016). The isolation of South America's mammal fauna ceased during the late Neogene after the formation of the Isthmus of Panama, which facilitated a faunal exchange with North America known as the Great American Biotic Interchange (Figure 1).

Among mammals, the South American Native Ungulates ("SANUs"; Welker et al., 2015) are an important faunal element of the Cenozoic in the continent, with an extensive fossil record that extends from the early Paleocene (ca. 64 MYA, Tiupampan South American Land Mammal Age [SALMA]; Gelfo et al., 2009; Woodburne et al., 2014a) to late Pleistocene (ca. 11–7 KYA, Cione et al., 2003; ca. 11–13 KYA, Barnosky and Lindsey, 2010). The SANUs are recorded along a wide latitudinal range in South America reaching central and southern North America at least by late Pleistocene times (Lundelius et al., 2013). The SANUs exhibit a high taxonomic diversity, wide body mass range, and different degrees of hypsodonty (Madden, 2015; Bond, 2016; Gomes-Rodrigues et al., 2017).

Phylogenetic relationships among SANUs, and of SANUs to other placentals, have long been a subject of debate. The SANUs include the clades Litopterna, Notoungulata, Astrapotheria, Xenungulata and Pyrotheria, which have been hypothesized to be monophyletic (classified in Meridiungulata; McKenna, 1975; McKenna and Bell, 1997) or polyphyletic (O'Leary et al., 2013); and for some SANU clades, different affinities within placentals are proposed (Billet and Martin, 2011; Kramarz and Bond, 2014; Buckley, 2015; Welker et al., 2015; Westbury et al., 2017). Phylogenetic hypotheses include affinities of Litopterna and other closely related SANUs with an extinct group of North American ungulates known as Mioclaenideae, based on morphological evidence

[1] Paläontologisches Institut und Museum, Universität Zürich, Karl-Schmid-Strasse 4, 8006 Zurich, Switzerland. Present address: Department of Biological and Environmental Sciences, University of Gothenburg, Carl Skottsbergs gata 22B, SE 405 30, Gothenburg, Sweden.

[2] Smithsonian Tropical Research Institute, Apartado 0843-03092, Balboa, Ancon, Panama.

[3] Humboldt-Universität, AG Morphologie und Formengeschichte, Bild Wissen Gestaltung ein interdisziplinäres Labor & Institut für Biologie, Philippstrasse 12/13, D-10115, Berlin, Germany.

[4] Museo Paleontológico de la Alcaldía de Urumaco, Falcón, Venezuela.

[5] Department of Geological Sciences, University of Saskatchewan, Saskatoon, Saskatchewan S7N 5E2, Canada.

[6] Departamento de Física y Geociencias, Universidad del Norte, Km. 5 Vía Puerto Colombia, Barranquilla, Colombia.

* Correspondence: juan.david.carillo@gu.se

Manuscript received 24 July 2017; accepted 22 September 2017.

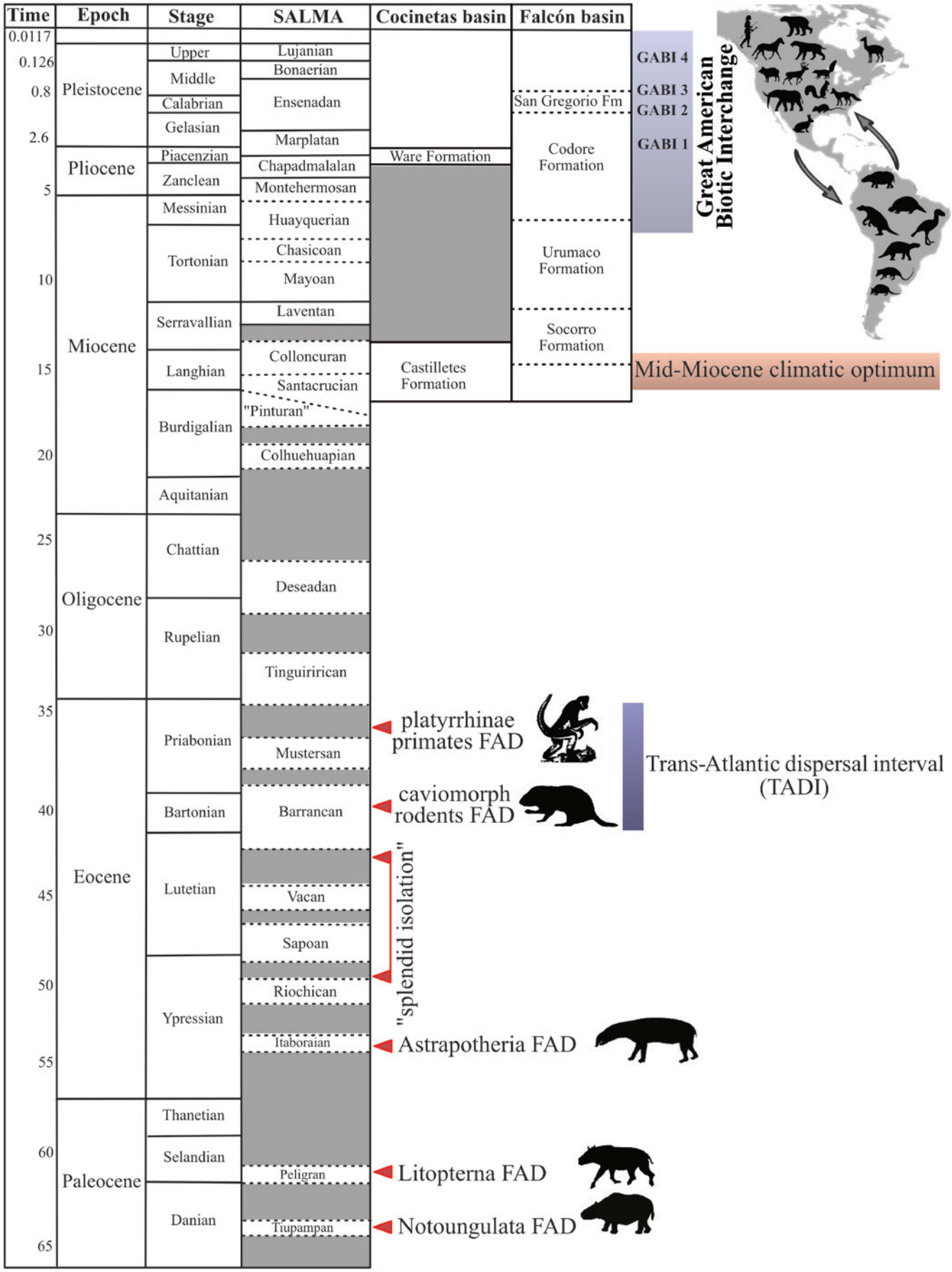
Time
Epoch
Stage
SALMA
Cocinetas basin
Falcón basin
0.0117
0.126
0.8
2.6
5
10
15
20
25
30
35
40
45
50
55
60
65
Pleistocene
Pliocene
Miocene
Oligocene
Eocene
Paleocene
Upper
Middle
Calabrian
Gelasian
Piacenzian
Zanclean
Messinian
Tortonian
Serravallian
Langhian
Burdigalian
Aquitanian
Chattian
Rupelian
Priabonian
Bartonian
Lutetian
Ypressian
Thanetian
Selandian
Danian
Lujanian
Bonaerian
Ensenadan
Marplatan
Chapadmalalan
Montehermosan
Huayquerian
Chasicoan
Mayoan
Laventan
Colloncuran
Santacrucian
"Pinturan"
Colhuehuapian
Deseadan
Tinguiririan
Mustersan
Barrancan
Vacan
Sapoan
Riochican
Itaboraian
Peligran
Tiupampan
Ware Formation
Castilletes Formation
San Gregorio Fm
Codore Formation
Urumaco Formation
Socorro Formation
GABI 4
GABI 3
GABI 2
GABI 1
Great American Biotic Interchange
Mid-Miocene climatic optimum
platyrrhinae primates FAD
caviomorph rodents FAD
Trans-Atlantic dispersal interval (TADI)
"splendid isolation"
Astrapotheria FAD
Litopterna FAD
Notoungulata FAD

(Cifelli, 1983; Muizon and Cifelli, 2000). Using postcranial data, Horovitz (2004) analyzed the relationships of SANUs with several other placentals and found no support for their monophyly. The SANUs were split between two separate clades of Holarctic ungulates ("Condylarthra"), one comprising Litopterna and Notoungulata and another comprising Astrapotheria. Using craniodental characters, Billet (2010, 2011) included Pyrotheria within Notoungulata and found this clade to be sister to Astrapotheria rather than Litopterna.

O'Leary et al. (2013) combined morphological characters and molecular sequences to evaluate the phylogenetic relationships within Placentalia, represented by 86 extinct and living species. According to this phylogeny, representatives of Notoungulata and Xenungulata are within Afrotheria, whereas representatives of Litopterna are within Laurasiatheria. In contrast, Welker et al. (2015) and Buckley (2015) used alpha 1 and 2 collagen chains to address the phylogenetic relationship of Notoungulata and Litopterna. Their results support the conclusion that Notoungulata and Litopterna form a clade as sister taxon to Perissodactyla, within Laurasiatheria. The close relationship of Litopterna with Perissodactyla is also supported by mitogenomic data (Westbury et al., 2017). Carrillo and Asher (2017) combined amino acid, collagen sequences, and morphological characters into a dataset including 182 fossil and living taxa in order to evaluate the relationship of Notoungulata and other SANUs within placentals. Their results yielded a limited number of possible phylogenetic relationships, but did not arbitrate between potential affinities with Afrotheria and Laurasiatheria.

Astrapotheria

Astrapotheria is a clade of SANUs recorded from the early Eocene (Itaboraian SALMA; Soria and Powell, 1981; Soria, 1987; Kramarz and Bond, 2013; Woodburne et al., 2014a,b; Kramarz et al., 2017) to the middle Miocene (12.76–13.6 mya, Laventan SALMA; Johnson, 1984; Johnson and Madden, 1997; Goillot et al., 2011; Vallejo-Pareja et al., 2015). The clade had a large body mass range between ~60 kg (*Albertogaudrya;* Vizcaíno et al., 2012) and ~4117 kg (*Parastrapotherium herculeum*?; Kramarz and Bond, 2011). Astrapotheres are characterized by canines developed as tusks, flattened astragalus, and calcaneus with secondary ectal facet and enlarged peroneal tubercle (Cifelli, 1993; Weston et al., 2004). In the more derived taxa the nasals are retracted, indicating the presence of a proboscis (Scott, 1937; Johnson, 1984; Johnson and Madden, 1997). Scott (1937) suggested amphibious habits for astrapotheres. Taphonomic evidence supports semiaquatic habits (Scott, 1937; Johnson, 1984; Marshall et al., 1990; Weston et al. 2004), and microanatomical features of long bones could support specializations to graviportality and semiaquatic habits in astrapotheres (Houssaye et al., 2016).

According to Cifelli (1993) two main clades are recognized within Astrapotheria: Trygonostylopidae and Astrapotheriidae. The latter comprises two clades: Astrapotheriinae, consisting of the southern taxa *Astrapotherium* and *Astrapothericulus*, and Uruguaytheriinae, which is composed of *Uruguaytherium, Granastrapotherium, Xenastrapotherium* and *Hilarcotherium*. The Uruguaytheriinae is supported by dental characters such as the absence of hypoflexid, absence of pillar in the lower molars, and absence of a labial cingulum (Johnson and Madden, 1997; Kramarz and Bond, 2009, 2011; Vallejo-Pareja et al., 2015).

Among Uruguaytheriinae, *Uruguaytherium beaulieui* is the oldest described taxon, being the sister taxa to the rest of the clade, and recorded in Uruguay but without precise provenance or known age (Kraglievich, 1928; Kramarz and Bond, 2011; Vallejo-Pareja et al., 2015). The earliest record of Uruguaytheriinae is a P4 of an undetermined genus collected in Alto Río Beu, near Santa Rosa, Ucayali, Peru (?late Oligocene; Antoine et al., 2016). Additional Uruguaytheriinae specimens are recorded in the early middle Miocene (Colloncuran SALMA) fauna of Cerdas, Bolivia (Croft et al., 2016). A Neotropical clade within Uruguaytheriinae comprises *Hilarcotherium castanedaii, Granastrapotherium snorki,* and five species of *Xenastrapotherium* (*X. kraglievichi, X. aequatorialis, X. chaparralensis, X. amazonense, X. christi*) (Kraglievich, 1928; Stehlin, 1928; Cabrera, 1929; Johnson and Madden, 1997; Vallejo-Pareja et al., 2015). *Hilarcotherium* is recorded in La Victoria Formation (middle Miocene), in the upper Magdalena valley, Colombia (Vallejo-Pareja et al., 2015). *Granastrapotherium* and *Xenastrapotherium* co-occurred in the middle Miocene (Laventan SALMA) faunas of La Venta and Fitzcarrald (Johnson and Madden, 1997; Goillot et al., 2011). *Xenastrapotherium* is widely distributed geographically and stratigraphically. It is recorded in Colombia, Venezuela, Ecuador, Brazil, and Peru, in sediments ranging from early to middle late Miocene in age (Goillot et al., 2011; Antoine et al., 2016).

FIGURE 1. (*Opposite page*) Geologic timescale of the Cenozoic Era illustrating the South American Land Mammal Ages (SALMAs), the chronology of the Cocinetas and Falcón Basins, the first appearance datums (FADs) of some South American clades, and the Cenozoic events of faunal exchange (Croft, 2016): TADI (Trans-Atlantic Dispersal Interval), the Great American Biotic Interchange, including the main dispersal events (GABI 1–4). The FAD of Litopterna is a minimum age, and the clade could be present since the Tiupampan SALMA (Muizon and Cifelli, 2000). The chronology of the latter follows Woodburne (2010): GABI 1 = ca. 2.4–2.6 mya, GABI 2 = ca. 1.8 mya, GABI 3 = ca. 0.8–1.0 mya, GABI 4 = ca. 0.125 mya.

Notoungulata

Notoungulata is a clade of SANUs with a high taxonomic diversity that includes more than 140 genera and 13 families (Croft, 1999), large morphological disparity (Giannini and García-López, 2014; Bond, 2016), and diverse dental eruption patterns, degrees of hypsodonty (Madden, 2015; Gomes-Rodrigues et al., 2017) and inferred diets (MacFadden, 2005; Croft and Weinstein, 2008; Townsend and Croft, 2008). Notoungulata is monophyletic (Roth, 1903; Cifelli, 1993; Billet, 2010, 2011) and is recorded during most of the Cenozoic in South America, from the early Paleocene (ca. 64 mya Tiupampan) (Muizon and Cifelli, 2000; Gelfo et al., 2009; Woodburne et al., 2014a) to the late Pleistocene (Cione et al., 2003; Barnosky and Lindsey, 2010). Together with Typotheria, Toxodontia is one of the main clades of Notoungulata. Toxodontia includes, among others, the clades Leontiniidae and Toxodontidae (Billet, 2011).

Leontiniidae are part of a clade within Toxodontia that also includes some Notohippidae and Toxodontidae (Cifelli, 1993; Billet, 2011). Leontiniidae are known from the late Eocene (Mustersan SALMA) (Bond and López, 1995; Ribeiro et al., 2010) to the middle Miocene (Laventan) (Villarroel and Colwell Danis, 1997). It attained its greater diversity during the late Oligocene (Deseadan SALMA) (Shockey et al., 2012; Cerdeño and Vera, 2015). Leontiniids have a medium-to-large body mass among Toxodontia. They are characterized by having mesodont (see Mones, 1982) cheek teeth and a tendency to form tusk-like incisors (Shockey et al., 2012). In the Miocene, leontiniids were widespread. They are represented by *Colpodon* from the various localities in central Patagonia, Argentina (Colhuehuapian SALMA; ca. 20.0–20.2 mya) and Laguna del Laja, Chile (early Miocene; ca. 19.5–19.8 mya) (Ré et al., 2010; Ribeiro et al., 2010; Shockey et al., 2012), and *Huilatherium* from La Venta, Colombia (Laventan) (Villarroel and Colwell Danis, 1997). The phylogenetic relationships within Leontiniidae are not fully resolved, but the Miocene taxa *Colpodon* and *Huilatherium* are hypothesized to belong to the same clade (Shockey et al., 2012; Cerdeño and Vera, 2015).

Toxodontidae is a clade of medium-to-large herbivores characterized by a specialized anterior dentition, ever-growing tusks, and hypsodont molars (Madden, 1997). Toxodonts were widespread in South America from the late Oligocene to late Pleistocene (Deseadan through Lujanian SALMAs) (Nasif et al., 2000). Within Toxodontidae two clades are recognized: Nesodontinae and Toxodontinae (Nasif et al., 2000; Forasiepi et al., 2015; Bonini et al., 2017a). Nesodontinae consists of early middle Miocene ("Pinturan" and Santacrucian SALMA) toxodontids from southern South America, whereas Toxodontinae comprises middle Miocene to late Pleistocene (Santacrucian through Lujanian) taxa widely distributed on the continent (Forasiepi et al., 2015). Toxodontinae representatives reached Central (Webb and Perrigo, 1984; Lucas et al., 1997; Lucas, 2014) and North America (~30°N) (Lundelius et al., 2013) during the late Pleistocene as part of the Great American Biotic Interchange (see below).

Litopterna

Litopterna is a diverse clade of SANUs recorded in South America from at least the late Paleocene (Peligran SALMA [Gelfo et al., 2009], although possibly they were present since the Tiupampan SALMA [Muizon and Cifelli, 2000]), to the late Pleistocene (Bond et al., 2001). Several clades are recognized within Litopterna: Protolipternidae, Notonychopidae, Adianthidae, Macraucheniidae, and Proterotheriidae (Cifelli, 1983, 1993; Schmidt, 2015; Forasiepi et al., 2016). The Sparnotheriodontidae has been variably treated as "Condylarthra" (Cifelli, 1983, 1993) or as a member of Litopterna (Soria, 2001).

Proterotheriids were small to medium-sized cursorial herbivores. They show different types of dentition, including brachyodont, mesodont, and protohypsodont (Soria, 2001; Villafañe et al., 2012; Schmidt, 2015). They are characterized by a reduction of the digits II and IV, acquiring a functional monodactyly (Cifelli and Villarroel, 1997; Ubilla et al., 2011; Schmidt, 2015). Proterotheriidae had a wide latitudinal distribution, and it is recorded from the early Eocene (Itaboraian) to the late Pleistocene (Bonaerian–Lujanian). It attained its maximum diversity during the Miocene (Santacrucian through Huayquerian SALMAs) (Bond et al., 2001; Villafañe et al., 2006; Scherer et al., 2009; Ubilla et al., 2011; Schmidt, 2015).

There are three main clades recognized within Proterotheriidae: Anisolambdinae, Megadolodinae, and Proterotheriinae; only the latter two are recorded in the Neogene (Cifelli, 1983; Cifelli and Villarroel, 1997; Soria, 2001; Villafañe et al., 2006). The Megadolodinae is known from the La Venta fauna (middle Miocene; Laventan) of Colombia (McKenna, 1956; Cifelli and Villarroel, 1997) and the Urumaco Formation (late Miocene) of Venezuela (Carlini et al., 2006b). The Proterotheriinae is recorded from the late Oligocene to the late Pleistocene (Deseadan through Lujanian) (Villafañe et al., 2006). They have a wide distribution (including northern South America) and reach their highest diversity during the Miocene (Santacrucian through Huayquerian) (Cifelli and Guerrero, 1997; Villafañe et al., 2006; Schmidt, 2011, 2015).

Study Sites

Cocinetas Basin

The Cocinetas Basin is located in the eastern Guajira Peninsula, in northern Colombia (Figure 2). The Neogene stratigraphy of the basin was revised by Moreno et al. (2015). The terrestrial mammal assemblages were collected from both the Castilletes and Ware Formations. The Castilletes Formation was deposited in a shallow marine to fluvio-deltaic environment and has been dated as 16.7–14.2 mya based on $^{87}Sr/^{86}Sr$ isotope

FIGURE 2. Geographic location of Cocinetas and Falcón Basins in Colombia and Venezuela, respectively.

chronostratigraphy and macroinvertebrate biostratigraphy (late early to early middle Miocene, upper Burdigalian–Langhian; Santacrucian/Colloncuran SALMAs; Hendy et al., 2015; Moreno et al., 2015). The Ware Formation is dominated by fluvio-deltaic environment deposits at the base and shoreface and nearshore deposits at the top. It is dated as 3.4–2.78 MYA based on $^{87}Sr/^{86}Sr$ isotope chronostratigraphy and macroinvertebrate biostratigraphy (late Pliocene, Piacenzan, Chapadmalalan/Marplatan SALMAs; (Hendy et al., 2015; Moreno et al., 2015).

The terrestrial mammalian fauna of the Castilletes Formation includes a sparassodont, a sloth, astrapotheres, litopterns, and notoungulates (Table 1; Amson et al., 2016; Suarez et al., 2016). The Castilletes Formation also records other terrestrial and marine fossils such as mollusks, echinoderms, arthropods, sharks, rays, bony fishes, snakes, turtles, crocodiles, cetaceans, and plants (Aguilera et al., 2013b; Cadena and Jaramillo, 2015a, 2015b; Hendy et al., 2015; Moreno et al., 2015; Moreno-Bernal et al., 2016; Aguirre-Fernández et al., 2017a). The mammalian fauna of the Ware Formation is characterized by an assemblage of sloths, cingulates, rodents, toxodontids, a procyonid, and a camelid (Table 1), the last two being immigrants from North America (Forasiepi et al., 2014; Moreno et al., 2015; Amson et al., 2016; Moreno-Bernal et al., 2016; Pérez et al., 2017). The Ware Formation also records crocodiles (Moreno-Bernal et al., 2016), turtles, bony fishes, fossil wood, and a diverse marine assemblage (Aguilera et al., 2013a; Hendy et al., 2015; Jaramillo et al., 2015; Moreno et al., 2015).

Falcón Basin

The Falcón Basin in northwestern Venezuela (Figure 2) has a long history of paleontological and geological studies (Sánchez-Villagra, 2010). The Urumaco sequence includes seven geological formations: Agua Clara, Cerro Pelado, Querales, Socorro, Urumaco, Codore and San Gregorio (Quiroz and Jaramillo, 2010). Four of these formations have reports of fossil mammals: Socorro, Urumaco, Codore (Sánchez-Villagra et al., 2010, and references therein), and San Gregorio (Table 2), which together extend from the middle Miocene to the late Pliocene (Quiroz and Jaramillo, 2010).

The Urumaco Formation is characterized by diverse faunal associations in terrestrial, estuarine, and marine environments of late Miocene age (Sánchez-Villagra and Aguilera, 2006; Quiroz and Jaramillo, 2010). The terrestrial mammal fauna of Urumaco includes giant rodents (Sánchez-Villagra et al., 2003; Horovitz et al., 2006, 2010; Geiger et al., 2013; Carrillo and Sánchez-Villagra, 2015) as well as a high diversity of sloths (Carlini et al., 2006a, 2006c, 2008a; Rincón et al., 2015). Coprolites of fossil vertebrates (including terrestrial mammals) are also recorded (Dentzien-Dias et al., 2018). The described SANUs include the megadolodine litoptern *Bounodus enigmaticus* (Carlini et al., 2006b) and a toxodontine *incertae sedis* (Bond et al., 2006). Linares (2004) provided a list of SANUs, none of which have been described (see Bond and Gelfo, 2010).

TABLE 1. Mammals from the Cocinetas Basin. BM = Body mass in kg. A dash (-) indicates data not available.

Clade	Subclade	Taxon	BM	Reference
		Castilletes Formation		
Sparassodonta	Borhyaenoidea	*Lycopsis padillai*	~22	Suarez et al. (2016)
Xenarthra	Megatherioidea	*Hyperleptus*?	-	Amson et al. (2016)
	Glyptodontidae	Glyptodontidae indet.	-	Moreno et al. (2015)
	Pampatheriidae	Pampatheriidae indet.	-	Moreno et al. (2015)
Astrapotheria	Uruguaytheriinae	*Hilarcotherium miyou* n. sp.	~6,456	This work
Notoungulata	Leontiniidae	cf. *Huilatherium*	-	This work
Litopterna	Proterotheriidae	*Lambdaconus* cf. *L. colombianus*	-	This work
		Ware Formation		
Xenarthra	Lestodontini	Gen. et sp. nov.	-	Amson et al. (2016)
	Scelidotheriinae	Gen. et sp. indet.	-	Amson et al. (2016)
	Megalonychidae	Gen. et sp. nov.	-	Amson et al. (2016)
	Megatheriinae	*Pliomegatherium lelongi*	~2,417	Amson et al. (2016)
	Nothrotheriinae	cf. *Nothrotherium*	~41	Amson et al. (2016)
	Glyptodontidae	Glyptodontidae indet.	-	Moreno et al. (2015)
	Pampatheriidae	Pampatheriidae indet.	-	Moreno et al. (2015)
Rodentia	Caviomorpha	*Hydrochoeropsis*? *wayuu*	~24	Pérez et al. (2017)
	Caviomorpha	Erethizontidae indet.	-	Moreno et al. (2015)
Notoungulata	Toxodontidae	Toxodontinae indet.	-	This work
Artiodactyla	Camelidae	Camelidae indet.	-	This work
Carnivora	Procyonidae	*Chapalmalania sp*.	-	Forasiepi et al. (2014)
Litopterna	Proterotheriidae	Proterotheriidae indet.	-	This work

TABLE 2. Mammals from the Falcón Basin.

Clade	Subclade	Taxon	Reference
		Codore Formation	
Notoungulata	Toxodontidae	*Falcontoxodon aguilerai* n. sp.[a]	This work
Litopterna	Proterotheriidae	Proterotheriidae indet.	This work
Xenarthra	Glyptodontidae	*Boreostemma pliocena*	Carlini et al. (2008)
	Pampatheriidae	Indet.	Carlini, pers comm.[b]
		San Gregorio Formation	
Carnivora	Procyonidae	*Cyonasua* sp.	Forasiepi et al. (2014)
Notoungulata	Toxodontidae	*Falcontoxodon* sp.	This work
Rodentia	Caviomorpha	cf. *Caviodon*	Vucetich et al. (2010)
		Hydrochoeropsis? *wayuu*	Vucetich et al. (2010); Pérez et al. (2017)
		Marisela gregoriana	Vucetich et al. (2010)
		Neoepiblema sp.	Vucetich et al. (2010)
Xenarthra	Dasypodidae	*Pliodasypus vergelianus*	Castro et al. (2014)
	Glyptodontidae	*Boreostemma*? sp. nov.	Zurita et al. (2011)
	Megatheriinae	aff. *Proeremotherium*	Carlini, pers comm.
	Pampatheriidae	Indet.	Carlini, pers comm.

[a] Body mass = 796 kg.
[b] A. A. Carlini, Museo de La Plata, personal communication.

The Codore Formation is early Pliocene in age. It is divided into three formal members: El Jebe, Chiguaje, and Algodones. The El Jebe and Algodones Members were deposited in a fluvial environment, whereas the Chiguaje Member represents a marine transgression (Quiroz and Jaramillo, 2010) and records cetaceans (Aguirre-Fernández et al., 2017a; 2017b). The terrestrial mammal fauna from Codore includes the glyptodon *Boreostemma pliocena* from the El Jebe Member (Carlini et al., 2008b) and a pampathere (A. A. Carlini, Museo de La Plata, personal communication).

The San Gregorio Formation is late Pliocene–early Pleistocene in age (Quiroz and Jaramillo, 2010). Fossil mammals come from the Vergel Member at the base of the San Gregorio and consist of caviomorph rodents (Vucetich et al., 2010), cingulates (Zurita et al., 2011; Castro et al., 2014), and a procyonid (Forasiepi et al., 2014).

The Great American Biotic Interchange

The Great American Biotic Interchange (GABI) is one of the greatest events of biotic exchange at a continental scale (Marshall et al., 1982; Webb, 1985, 1991). The traditional interpretation places the onset of the GABI ca. 3 mya, with some early mammal migrations ("heralds") during the late Miocene from South to North America by ca. 9 mya and from North to South America by ca. 7 mya (Webb, 2006; Woodburne, 2010; Leigh et al., 2014; Cione et al., 2015; O'Dea et al., 2016). Other studies using dated molecular phylogenies across a wide range of taxa in addition to mammals indicate that an important part of the interchange predated ca. 3 mya (Koepfli et al., 2007; Cody et al., 2010; Eizirik, 2012; Leite et al., 2014; Bacon et al., 2015; Stange et al., 2018).

The mammalian fossil record in South America shows that although the first immigrations are recorded during the late Miocene (ca.10–7 mya), the number of GABI participants rapidly increases after ca. 5–3 mya and this trend continues during the Pleistocene (Carrillo et al., 2015). Dated molecular phylogenies suggest a similar pattern for birds (Weir et al., 2009). For mammals, the core of the GABI is composed of a series of major migration "waves" during the Pleistocene (2.5–0.012 mya) (Woodburne, 2010). Climatic and environmental changes possibly influenced migration patterns during the Pleistocene (Webb, 1991; Bacon et al., 2016). Additional data on tropical paleoenvironments and paleofaunas from the Pliocene and Pleistocene are needed to test this hypothesis (Jaramillo, 2018).

The Neotropical fossil record is essential to reach a better understanding of the diversity dynamics and paleobiogeography during the GABI (Jaramillo, 2018). However, there is a fossil sampling bias in the continent, as our knowledge of the tropics is very scant when compared with that of the temperate faunas (Carrillo et al., 2015). The new findings from the Cocinetas and Falcón Basins serve to characterize changes of mammal assemblages in northern South America just before and during the GABI.

MATERIALS AND METHODS

We took standard linear measurements with a caliper to the nearest 0.1 mm, and with a metric tape for large elements (> 15 cm). For orientation of the dentition we follow Smith and Dodson (2003), where the four cardinal directions are mesial, distal, lingual, and labial (buccal). We follow the recommendations of Bengtson (1988) for the use of open nomenclature. The chronology of SALMAs follows Flynn and Swisher (1995), Madden et al. (1997), Cione and Tonni (1999, 2001), Tonni (2009), Kramarz et al. (2010), Shockey et al. (2012), Tomassini et al. (2013), and Woodburne et al. (2014a,b). Three-dimensional surface models of selected specimens of the described material are available in MorphoMuseuM (Carrillo et al., 2018a). Additional supplementary material is available from the Dryad Digital Repository (Carrillo et al., 2018b).

Abbreviations

Institutions

AMU-CURS	Alcaldía del Municipio de Urumaco, Colección Urumaco Rodolfo Sánchez, Venezuela
IGM	Museo Geológico José Royo y Gómez, Servicio Geológico Colombiano, Bogotá, Colombia
MACN	Museo Argentino de Ciencias Naturales, Buenos Aires, Argentina
MLP	Museo de La Plata, La Plata, Argentina
MNHN	Muséum national d'Histoire naturelle, Paris, France
MUN	Mapuka Museum, Universidad del Norte, Barranquilla, Colombia
NHMUK	Natural History Museum, London, UK
NMB	Naturhistorisches Museum Basel, Basel, Switzerland
PIMUZ	Paläontologisches Institut und Museum Universität Zürich, Zurich, Switzerland
STRI	Smithsonian Tropical Research Institute, Panama
UNEFM-CIAAP	Universidad Nacional Experimental Francisco de Miranda, Centro de Investigaciones Antropológicas, Arqueológicas y Paleontológicas, Coro, Venezuela
YPM	Yale Peabody Museum, New Haven, Conn., USA

Other Abbreviations

C, c	upper canine, lower canine
I, i	upper incisor, lower incisor
M, m	upper molar, lower molar
mya	million years ago
P, p	upper premolar, lower premolar
SALMA	South American Land Mammal Age
SANU	South American native ungulate

Comparative Anatomical Descriptions

Astrapotheriidae

The astrapothere material described here comes from the Castilletes Formation, in the Guajira Department, northern Colombia (Figure 3). Dental morphology and terminology follow Johnson (1984). We took craniodental measurements for astrapotheres following Johnson and Madden (1997) and Vallejo-Pareja et al. (2015). The craniodental material is described in comparison with other Uruguaytheriinae sensu Vallejo-Pareja et al. (2015), and postcranial elements are compared with

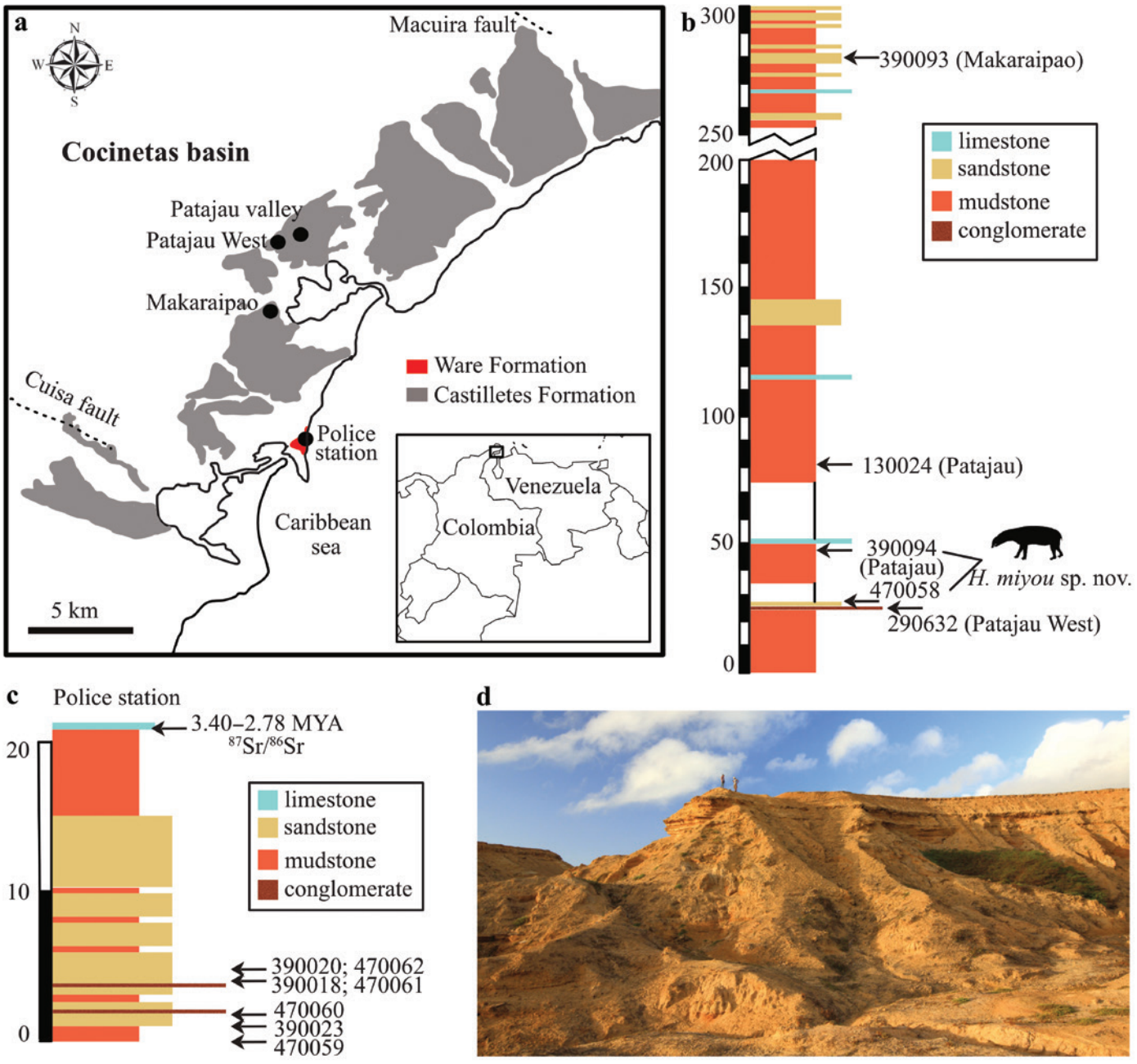

FIGURE 3. Geographic and stratigraphic occurrence of South American Native Ungulates (SANUs) in the Cocinetas Basin. (a) Map showing locations of fossiliferous localities with SANUs; (b) stratigraphic profile of the Castilletes Formation indicating the stratigraphic position of each locality; (c) stratigraphic profile of the Ware Formation indicating the stratigraphic position of each locality; both profiles are modified from Moreno et al. (2015); (d) landscape view at the Police Station locality (for scale, note two people standing at top of bluff); photo by Christian Ziegler.

astrapotheres whose postcranial anatomy is best known, in particular *Astrapotherium* and *Parastrapotherium* (Riggs, 1935; Scott, 1937).

Leontiniidae

The leontiniid molar comes from the Castilletes Formation (Figure 3); for its description, we considered recent systematic works on leontiniids (e.g., Villarroel and Colwell Danis, 1997; Shockey et al., 2012; Cerdeño and Vera, 2015). Dental terminology follows Ribeiro et al. (2010).

Toxodontidae

The toxodontid material described here comes from the Algodones Member of the Codore Formation and the Vergel Member of the San Gregorio Formation (Figure 4). Dental morphology and terminology follow Madden (1990, 1997). Craniodental material is described in comparison with other Toxodontinae sensu Nasif et al. (2000) and Forasiepi et al. (2015). Postcranial elements are described in comparison with toxodontids whose postcranial elements are best known, in particular *Nesodon imbricatus* and *Toxodon platensis*.

For the toxodontid foot bones, we measured the length and width of the calcaneus and tarsals. For the astragalus, we took nine measurements following Tsubamoto (2014), and we used these measurements in a Principal Component Analysis (PCA) to explore astragalar variation in toxodontids.

Proterotheriidae

The proterotheriid material described here comes from the Castilletes and Ware Formations in the Cocinetas Basin, and the Algodones Member of the Codore Formation in the Falcón Basin (Figures 3–4). Dental terminology follows Soria (2001) and Schmidt (2015). Dental and postcranial remains are described in comparison with recent systematic works on Proterotheriidae (Cifelli and Villarroel, 1997; Scherer et al., 2009; Schmidt, 2015). Postcranial measurements were taken following Schmidt (2013).

Camelidae

The camelid molar comes from the Ware Formation (Figure 3). Dental terminology follows Scherer et al. (2007) and Rincón et al. (2012). We follow Scherer (2013) and Gasparini et al. (2017) for the taxonomy of South American camelids.

Phylogenetic Analyses

Astrapotheriidae

We conducted a phylogenetic analysis using maximum parsimony. The analysis included 17 taxa and 64 characters; 61 characters were ordered and three unordered, following Vallejo-Pareja et al. (2015). Studies on simulated and empirical data showed that parsimony analyses with ordered states perform better when using characters that form morphoclines (Grand et al., 2013). Taxa included are *Eoastrapostylops* as the outgroup (Kramarz et al., 2017), and 16 astrapotheriids. We used the matrix presented by Vallejo-Pareja et al. (2015), and we added *Xenastrapotherium kraglievichi*, *Xenastrapotherium christi*, and the new Uruguaytheriinae from the Castilletes Formation. We excluded *Xenastrapotherium aequatorialis*, *Xenastrapotherium chaparralensis*, and *Xenastrapotherium amazonense*, because they are known only from fragmentary elements. We analyzed the character matrix with the program PAUP* 4.0 (Swofford, 2002). We used equally weighted characters, excluded uninformative characters, treated gaps as missing, and treated taxa with multiple states as polymorphic. We did a search using the branch-and-bound algorithm with a furthest addition sequence. A normal bootstrap resampling was performed, with 1000 replications. We provide the character–taxon matrix in supplementary materials (Carrillo et al., 2018b: appdx. 3).

Toxodontidae

We performed a maximum parsimony analysis on 28 notoungulate taxa and 59 morphological characters with PAUP* 4.0 (Swofford, 2002). We used the matrix presented by Forasiepi et al. (2015) and modified by Bonini et al. (2017a). We added *Piauhytherium* as described by Guérin and Faure (2013), and the new toxodontine from Codore Formation. We included *Xotodon cristatus* and *Xotodon major* as coded by Bonini et al. (2017a,b). We excluded uninformative characters, treated gaps as missing, and treated taxa with multiple states as polymorphic. Forasiepi et al. (2015) performed a phylogenetic analysis using implied and equal weights. In order to be comparable, we also used equally weighted characters and implied weighting with a concavity constant (k) value of 3. The implied weighting weights characters against homoplasy and improves the resampling metrics associated with the quality of the results (Goloboff et al., 2008; Goloboff, 2014). We did a heuristic search with a starting tree obtained via stepwise addition using the closest addition sequences and tree bisection reconnection (TBR), saving ten trees per round. A normal bootstrap resampling was performed, with 1000 replications. We provide the character–taxon matrix in supplementary materials (Carrillo et al., 2018b: appdx. 4).

Body Mass Estimations

To estimate the body mass in toxodonts, we used the multivariate regression functions proposed by Mendoza et al. (2006), based on craniodental measurements of living ungulates. For astrapotheres, we used the bivariate regression equation of the second lower molar length (m2) for non-selenodont

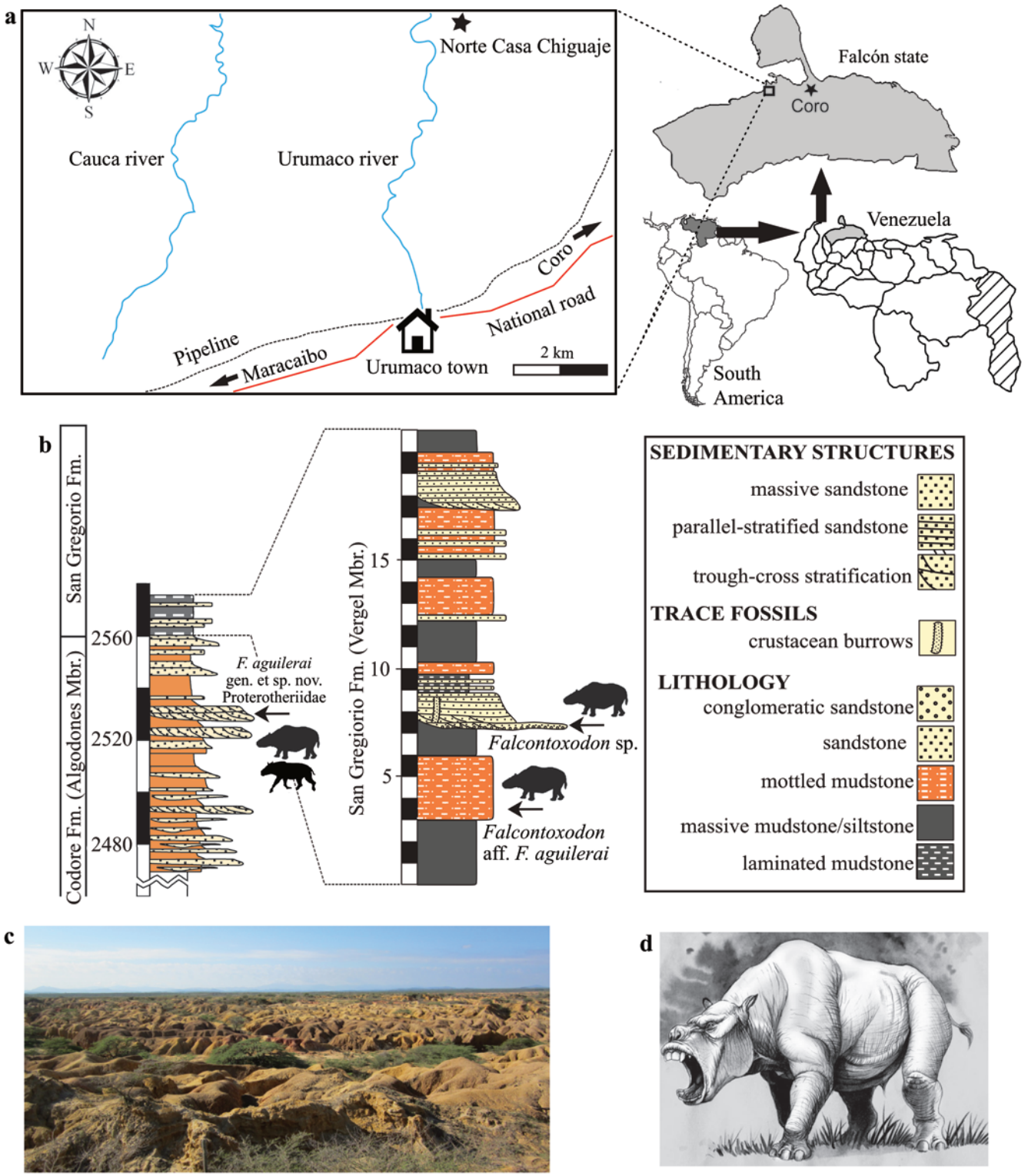

FIGURE 4. Geographic and stratigraphic occurrence of *Falcontoxodon* gen. nov. and Proterotheriidae: (a) location and (b) stratigraphic profile of localities from the Codore and San Gregorio Formations where specimens of *Falcontoxodon* and Proterotheriidae were found (Fm. = formation; Mbr. = member.); (c) landscape view in Norte Casa Chiguaje locality, of the Vergel Member, San Gregorio Formation; (d) artistic reconstruction of a toxodontid by Jorge González (modified from Sánchez-Villagra et al., 2010).

ungulates from Damuth (1990: tbl. 16.9), and the equation of the humerus length (H2) for all ungulates from Scott (1990: tbl. 16.7).

Chronostratigraphic Framework

The Neogene sequence of the Falcón Basin is one of the thickest and best exposed sedimentary sequences in the Neotropics, with more than 7 kilometers of stratigraphic thickness cropping out. Most of the sequence is highly fossiliferous and we expect that the paleontological exploration of this large region will continue for many decades to come. To help this and future studies in the region, we established a chronology for the region based on an extensive literature review, as this region has had many biostratigraphic studies over the past few decades. Most of these studies, especially in the western region, have been correlated to Bolli's zonal schemes in Trinidad (Bolli et al., 1994), which is the base for the biostratigraphy of tropical latitudes in the Americas. Furthermore, we include in supplementary materials (Carrillo et al., 2018b: appdx. 1), the lithological description of ten stratigraphic sections that encompass the entire Neogene sequence and could be used as a stratigraphic reference for future paleontological research.

RESULTS

Systematic Paleontology

Astrapotheria Lydekker, 1884

Astrapotheriidae Ameghino, 1887

Uruguaytheriinae Kraglievich, 1928, sensu Vallejo-Pareja et al. (2015)

Hilarcotherium Vallejo-Pareja et al., 2015

Type Species. *Hilarcotherium castanedaii* Vallejo-Pareja et al., 2015.

Hilarcotherium miyou sp. nov.

FIGURES 5, 6

Diagnosis. *H. miyou* differs from *H. castanedaii* in having lower canines, oval in cross section and implanted horizontally in lateral view; the absence of lingual cingulid in the lower molars; the absence of an anteroligual pocket in P4; and the absence of lingual cingulum in M2.

Etymology. The species is named after the word "miyo'u," which means big or large in Wayuunaiki (Captain and Captain, 2005), the language of the Wayuu community that inhabits in the Guajira Department.

Holotype. Specimen IGMp 881327, partial mandible with left ramus bearing left m3, m2, canines, and alveoli for the incisors. Fragment of the left condylar process, right M2 and distal portion of femur.

Referred Material. MUN-STRI 34216, fragmentary skull with portion of the occipitals, palatines, and left upper canine, associated P4 and M2, and fragmentary mandibular symphysis with the base of the lower canines and alveoli for left i3?, i2, and i1 and right i1 and i2. MUN-STRI 38073, left P4 and upper molar fragments.

Type Locality and Horizon. Patajau, Castilletes Formation. The holotype, MUN-STRI 34216 and MUN-STRI 38073 come from STRI locality 470058; 11.95062°N, 71.32370°W (Figure 3).

Description. The specimens are referred to Uruguaytheriinae based on the well-developed mesiolingual pocket in the upper molars, the absence of labial cingulum in upper molars, and the absence of hypoflexid and pillars in the lower molars (Johnson and Madden, 1997; Kramarz and Bond, 2009, 2011; Vallejo-Pareja et al., 2015; Croft et al., 2016). The material is further referred to *Hilarcotherium* based on the presence of three lower incisors, and the presence of a lingual cingulum in P4 (Figure 6; Vallejo-Pareja et al., 2015).

The width of the mandible (measured as the mediolateral width between the labial margin of the canines) of *H. miyou* is comparable to that of *H. castanedaii* and *Granastrapotherium snorki,* and larger than that of *Xenastrapotherium christi* (Table 3; Vallejo-Pareja et al., 2015). The symphysis is wide (Figure 5b) as in *H. castanedaii* (Vallejo-Pareja et al., 2015: fig. 4b) and *X. christi* (Figure 7b), and unlike *G. snorki,* where the symphysis is very narrow due to the absence of lower incisors (Johnson and Madden, 1997: fig. 22.5). In IGMp 881327 the most anterior portion of the mandible is not well preserved, but it is possible to identify at least three alveoli for the incisors, which are interpreted as the right and left i1 and the left i2 (Figure 5c). It is not possible to assess with confidence the size of the alveoli and the presence of i3. The alveoli size of lower incisors is a variable character in other uruguaytheriinae taxa (e.g., *Xenastrapotherium kraglievichi*; Johnson and Madden, 1997), and its significance as a diagnostic character needs to be further evaluated. MUN-STRI 34216 preserves the most anterior portion of the mandibular symphysis, which preserves four alveoli for the incisors, the base of the left i2, and the base of the left lower canine (Figure 6c,d). The incisors of uruguaytheriines are single rooted (Vallejo-Pareja et al., 2015: fig. 4f,g), and therefore the alveoli of MUN-STRI 34216 are interpreted as left i1, i2, i3 and right i1, i2 (Figure 6c,d). The alveolus of the right i3 and the right lower canine were not preserved.

The incisor alveoli of *H. miyou* are slightly larger (Table 3) than in *H. castanedaii* (Vallejo-Pareja et al., 2015). *Xenastrapotherium* has only two lower incisors. Johnson and Madden (1997) noted that in some specimens of *X. kraglievichi*, the lower incisors' alveoli were very small, "indicating that the lower incisors are either variably developed or may have worn out and

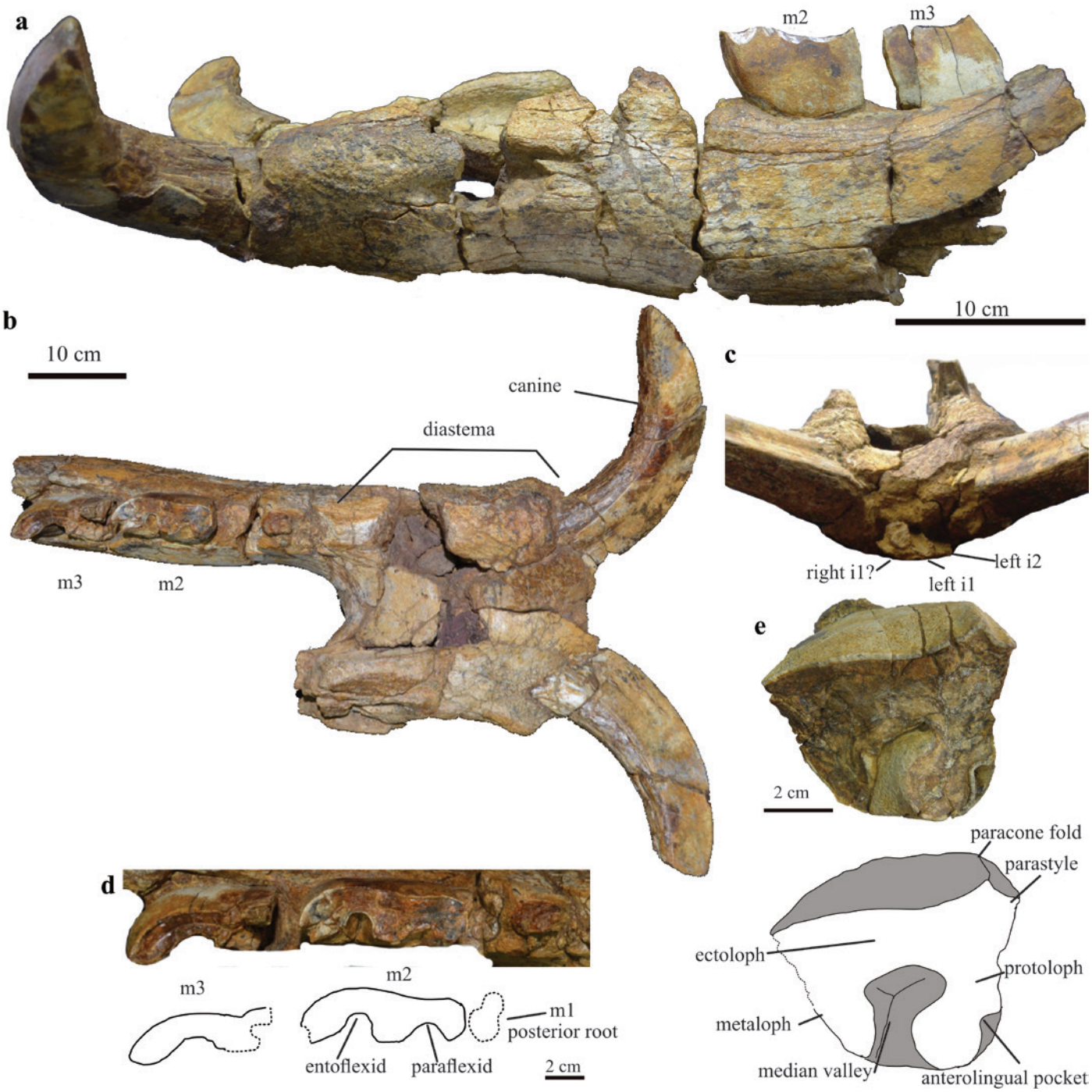

FIGURE 5. Mandible of *Hilarcotherium miyou* sp. nov. (Uruguaytheriinae, Astrapotheria) (holotype, IGMp 881327): (a) left lateral view; (b) occlusal view; (c) anterior view of symphysis indicating alveoli for incisors; (d) detail of dentition in occlusal view; (e) photograph and drawing of upper second molar (M2) in occlusal view.

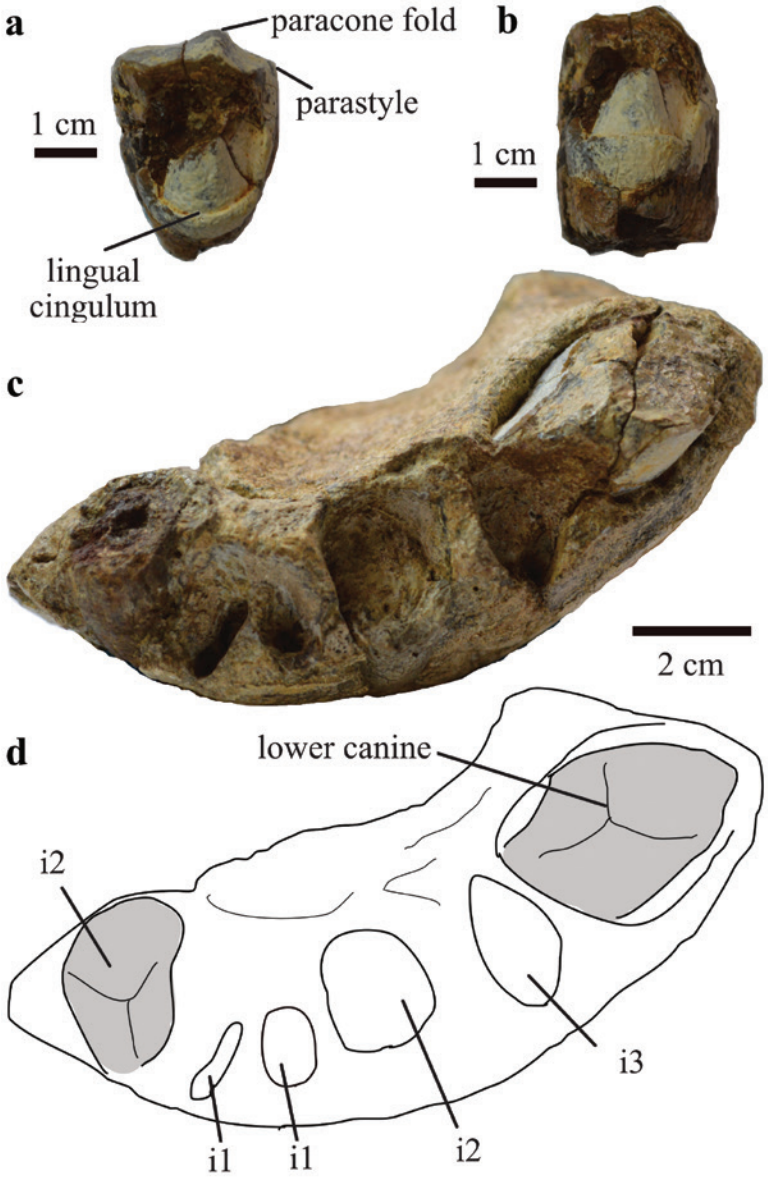

FIGURE 6. Upper fourth premolar (P4; MUN-STRI 38073) and mandibular symphysis (MUN-STRI 34216) of *Hilarcotherium miyou* sp. nov. (a) P4 in occlusal view; (b) P4 in lingual view; (c) mandibular symphysis in occlusal view; (d) drawing of mandibular symphysis showing canine and alveoli of incisors. The gray shading represents the base of the teeth.

been shed" (Johnson and Madden, 1997:360). There is intraspecific variation in the size of the incisors. This seems to be the case also in *H. miyou* (Figure 5c) and *X. christi* (Figure 7b), whose incisors have very small alveoli. *G. snorki* has no lower incisors (Johnson and Madden, 1997; Pardo-Jaramillo, 2010). The lower canines of *H. miyou* are oval in cross section, whereas in *H. castanedaii* they are triangular. In *H. miyou* the canines are implanted horizontally in lateral view and curved labially, unlike *H. castanedaii,* which has canines with a diagonal implantation in lateral view. Based on size differences and morphology of the canines, Johnson and Madden (1997) inferred sexual dimorphism in *Granastrapotherium*, with the larger (male?) morphotype having longer and nearly straight lower canines, and the smaller (female?) morphotype having shorter and more curved lower canines (Johnson and Madden, 1997).

Specimen IGMp 881327 preserves the left m2 and m3, and the root of m1, which is biradiculated, as in all astrapotheres (Figure 5d). They lack a hypoflexid, as is the case in *Hilarcotherium castanedaii*, *Uruguaytherium beaulieui*, and *Xenastrapotherium aequatorialis*. In *G. snorki* "the hypoflexid is indicated as a faint indentation opposite to the metalophid" (Johnson and Madden, 1997:371). In *X. christi* the hypoflexid is located opposite to the metalophid (Figure 7c,d), whereas in *X. kraglievichi* it is opposite to the paraflexid (Johnson and Madden, 1997). The m2 crown is undamaged in IGMp 881327 and is 40% larger than the m2 of *H. castanedaii* (Figure 8a; Vallejo-Pareja

TABLE 3. Dental measurements (mm) of *Hilarcotherium miyou* sp. nov. and *Hilarcotherium* cf. *H. miyou* from Castilletes Formation. Features: C, upper canine; i, lower incisor; m, lower molar; M, upper molar; p, lower premolar; P, upper premolar. Measurements follow Johnson and Madden (1997).

Taxon	Specimen	Feature	Side	Measurement	Value
H. miyou	IGMp881327	C	Left	Maximum diameter	64.0
				Transverse diameter	45.8
		C	Right	Maximum diameter	65.7
				Transverse diameter	48.4
		p4[a]	Left	Length	28.8
				Width	22.2
		m1[a]	Left	Length	52.6
				Width	28.2
		m2	Left	Length	81.8
				Width	28.8
		m3[b]	Left	Length	79.9
				Width	27.9
		M2	Right	Length	71.7
				Width	59.8
		Mandible	Left	Depth at m2	104.5
		Mandible	Left	Thickness at m2	78.2
		Mandible		Width between the labial margin of lower canines	125
	MUN-STRI 34216	i1[a]	Left	Anteroposterior length	21.0
				Transverse length	11.0
		i2[a]	Left	Anteroposterior length	18.0
				Transverse length	8.4
		i3[a]	Left	Anteroposterior length	19.8
				Transverse length	14.5
H. cf. *H. miyou*	MUN-STRI 16778	P4[a]	Left	Length	31.8
				Width	40.7
		M1[b]	Left	Length	59.2
				Width	65.4
		M2[b]	Left	Length	71.2
				Width	76.7
		M3[b]	Left	Length	73.6
				Width	60.1

[a] Measured at the alveolus.
[b] Tooth crown incomplete.

et al., 2015). The entoflexid is deeper linguo-labially in occlusal view than the paraflexid (Figure 5d), a feature related to wear and observed in other Uruguaytheriinae (Vallejo-Pareja et al., 2015). *H. miyou* has no lingual cingulid, unlike *H. castanedaii*, *X. christi*, and *X. aequatorialis* (Johnson and Madden, 1997; Vallejo-Pareja et al., 2015).

The P4 (MUN-STRI 34216 and MUN-STRI 38073) has a well-defined paracone fold, unlike *G. snorki*. The P4 of *H. miyou* shares with that of *H. castanedaii* the absence of a hypocone and the presence of a lingual cingulum (Vallejo-Pareja et al., 2015); however, in *H. miyou* the cingulum is continuous. Two M2 are referred to *H. miyou* (IGMp 881327 and MUN-STRI

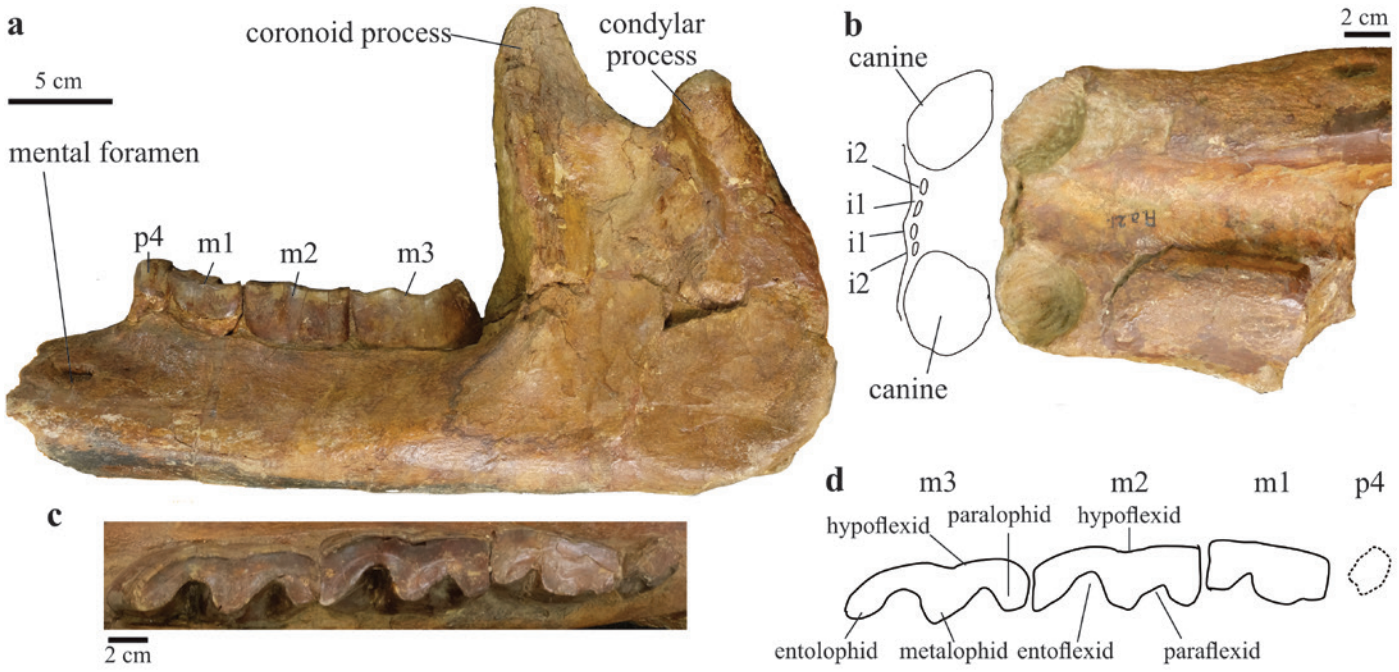

FIGURE 7. Mandible of *Xenastrapotherium christi* (Uruguaytheriinae, Astrapotheria) (NMB Aa21): (a) left lateral view; (b) dorsal view of symphysis showing the alveoli of canines and incisors; (c) left dentition in occlusal view; (d) drawing and dental features of dentition in occlusal view. Photos from NMB provided by L. Costeur.

34216), and these display a nearly quadrangular contour and the Y-shaped median valley, characteristic of the M2 in astrapotherids (Figure 5e). They lack a labial cingulum, which is present in *X. chaparralensis* (Johnson and Madden, 1997). *H. miyou* has a well-defined mesiolingual pocket, parastyle, and paracone fold (Figure 5e). There is no evidence of a lingual cingulum, as in *G. snorki*, and unlike *H. castanedaii* and other Uruguaytheriinae (Vallejo-Pareja et al., 2015).

Hilarcotherium cf. *H. miyou*

Referred Material. MUN-STRI 16777, almost complete left humerus, left radius with unfused and missing distal epiphysis, vertebral centrum, distal tibia and associated bone fragments. MUN-STRI 16778, left and right upper tooth rows highly fragmented bearing P4-M3. MUN-STRI 16779, lower canine. MUN-STRI 16785, three fragmentary caudal vertebrae. MUN-STRI 34212, patella. MUN-STRI 34217, sacrum, fragment of acetabulum, and thoracic vertebra. MUN-STRI 34221, atlas, almost complete left radius, metapodial, molar fragment, rib fragments and a fragment of a neural arch. MUN-STRI 34222, proximal portion of left humerus. MUN-STRI 34223, almost complete left ulna, distal epiphysis of left humerus, distal portion of left scapula, ribs, and vertebrae fragments. MUN-STRI 34225, distal portion of scapula. MUN-STRI 34229, partial right femur, tibia, and fibula. MUN-STRI 34292, patella. MUN-STRI 34310, distal portion of femur. MUN-STRI 36644, posterior portion of basicranium (cast PIMUZ A/V 5292). MUN-STRI 37384, dorsal portion of left scapula. MUN-STRI 37765, dorsal portion of scapula, partial radius and lunar. MUN-STRI 37390, distal tibia.

Locality and Horizon. Castilletes Formation. MUN-STRI 16777, 16778, 16779, 16785, 34217, 34221, 34222, 34223, 34225, 34229, 34310, 36644, 37384, and 37390 come from Patajau, STRI locality 390094; 11.9465°N, 71.3255°W. MUN-STRI 37765 comes from STRI locality 130024; 11.9348°N, 71.3344°W. MUN-STRI 34212 comes from Patajau west, STRI locality 290632; 11.9458°N, 71.3299°W. MUN-STRI 34292 comes from Makaraipao, STRI locality 930093; 11.9089°N, 71.3401°W (Figure 3).

Description. The isolated distal fragment of a canine (MUN-STRI 16779) has an oval wear facet that forms an acute chisel-like shape. MUN-STRI 16778 is a left upper tooth row with P4–M3. It is fractured, and not much can be discerned about crown morphology, although it is possible to clearly identify each tooth in situ. MUN-STRI 16778 has no P3, as in *Hilarcotherium* (Vallejo-Pareja et al., 2015) and *Granastrapotherium*, and unlike *Xenastrapotherium* (Johnson and Madden, 1997). The partial basicranium (MUN-STRI 36644) preserves

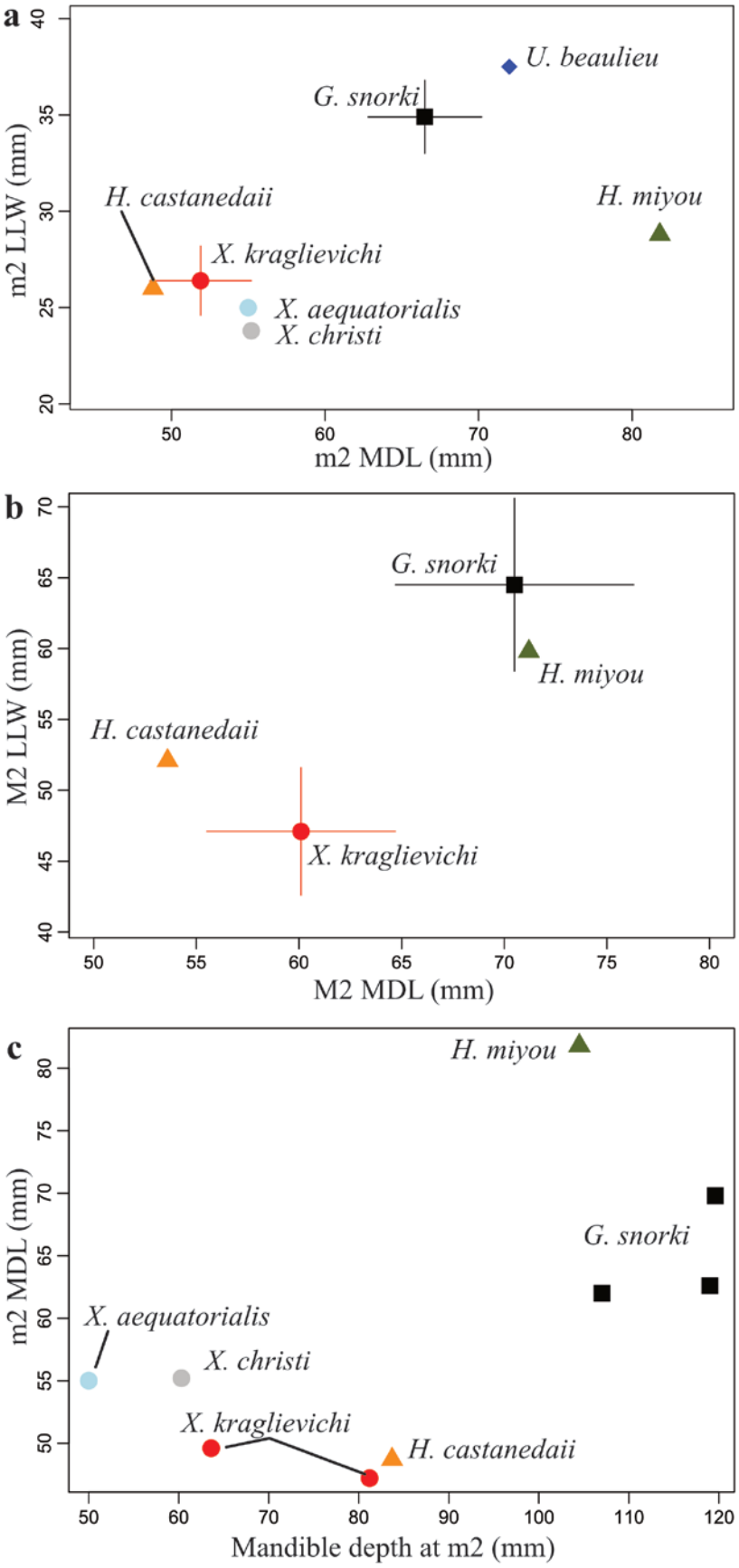

FIGURE 8. Bivariate plots with dental and mandible measurements of Uruguaytheriinae (Astrapotheria): (a) second lower molar (m2) mesiodistal length (MDL) vs. labiolingual width (LLW). In *G. snorki* and *X. kraglievichi*, the dot represents the mean and the bars the standard deviation provided by Johnson and Madden (1997); (b) second upper molar (M2) MDL vs. LLW. The values of *G. snorki* and *X. kraglievichi* are shown as explained in (a); (c) depth of the mandible at the level of m2 vs. m2 MDL.

the occipital condyles and part of the basioccipital and exoccipital (Figure 9a,b). The occipital condyles are large, measuring 85.5 mm in dorsoventral height, and the maximum width between the condyles is 153.5 mm. The foramen magnum is larger than in *H. castanedaii* (Vallejo-Pareja et al., 2015). It is almost circular, as in *Astrapotherium* (Scott, 1928). The foramen magnum's mediolateral width measures 54.7 mm and its dorsoventral height is 52.4 mm. In contrast, the foramen magnum in *Astraponotus* is considerably wider than high (Kramarz et al., 2011). The median notch at the dorsal margin of the foramen magnum is not as clearly differentiated as in *Astraponotus* (Kramarz et al., 2011). The exoccipital has a distinct process dorsal to the foramen magnum (Figure 9a,b).

The atlas (MUN-STRI 34221) preserves the cranial articular foveae, caudal articular surfaces, the neural and ventral arches, part of the transverse processes, and the transverse foramina (Figure 9c,d). It is comparable in size to that of *Parastrapotherium herculeum*? (Table 4; Figure 9e,f). The transverse process is wide as in *Astrapotherium* and *Parastrapotherium*. The cranial articular foveae for the occipital condyles are large, deeply

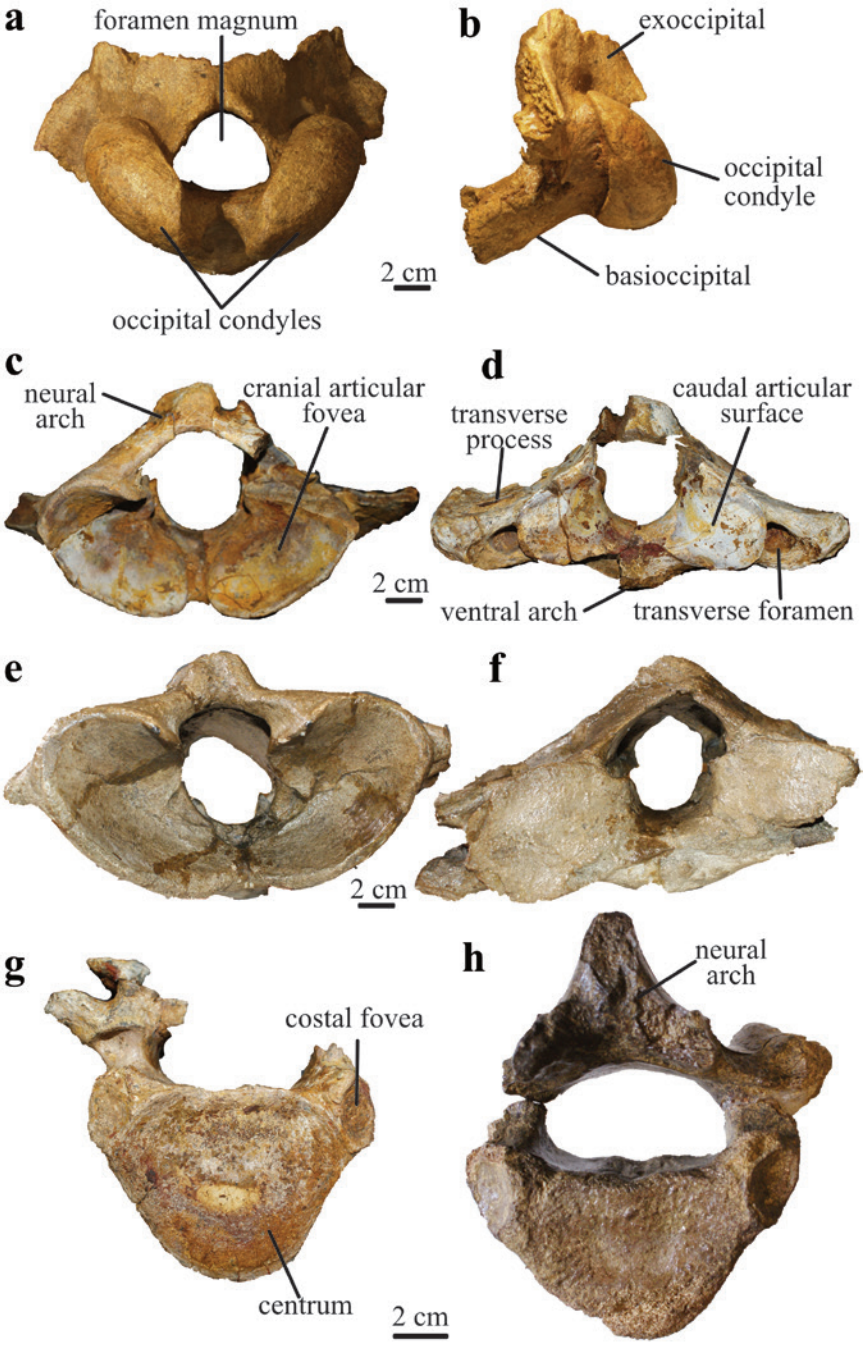

FIGURE 9. Basicranium and vertebrae of *Hilarcotherium* cf. *H. miyou* from the Castilletes Formation, and selected astrapotheres for comparison. *Hilarcotherium* cf. *H. miyou* basicranium (MUN-STRI 36644) in (a) caudal view, and (b) left lateral view. *Hilarcotherium* cf. *H. miyou* atlas (MUN-STRI 34221) in (c) cranial view, and (d) caudal view. *Parastrapotherium herculeum?* (MNHN COL 6) atlas, from the Colhuehuapian of Argentina in (e) cranial view, and (f) caudal view. (g) *Hilarcotherium* cf. *H. miyou* thoracic vertebra (MUN-STRI 34217) in caudal view; (h) *Parastrapotherium* sp. thoracic vertebra (MNHN DES 112) from the Deseadan of Argentina in caudal view.

TABLE 4. Postcranial measurements (cm) of Astrapotheriidae. An asterisk (*) indicates estimated value. For the humerus, the acronym used by Scott (1990) is in parentheses. A dash (-) indicates measurement could not be taken in the specimen.

Measurement	Data by taxon and specimen	
Atlas	***H.* cf. *H. miyou*** **MUN-STRI 34221**	***P. herculeum*?** **MNHN COL 6**
Anteroposterior length	15.6*	16.5
Dorsoventral height	12.9*	14.8
Mediolateral width	26.2*	27.4
Caudal vertebra	***H.* cf. *H. miyou*** **MUN-STRI 34217**	***Parastrapotherium* sp.** **MNHN DES 112**
Dorsoventral height of centra	7.65	6.27
Anteroposterior length of centra	5.95	5.19
Mediolateral width of centra	9.64	8.72
	H.* cf. *H. miyou	
Scapula	**MUN-STRI 34384**	**MUN-STRI 37765**
Dorsoventral width at distal end	10.28	-
Mediolateral thickness at distal end	-	12.0*
Humerus	***H.* cf. *H. miyou*** **MUN-STRI 16777**	***P. herculeum*?** **MNHN COL 127**
Length from head (H1)	65.0	-
Length from external tuberosity (H2)	67.5	-
Transverse diameter of the distal articulation surface (H4)	18.25	10.68
Transverse epicondylar diameter (H5)	25.5*	19.0*
Transverse diameter of the diaphysis below the deltoid process (H7)	9.1*	-
Anteroposterior diameter of the diaphysis below the deltoid process (H8)	13.1*	-

TABLE 4. (*Continued*)

Measurement	Data by taxon and specimen			
	H. cf. *H. miyou*	*P. hombergi*	*Parastrapotherium* sp.	*P. herculeum*?
Ulna	MUN-STRI 34223	MNHN DES 985	MNHN DES 1013	MNHN COL 128
Length	-	4.60	6.00	6.10
Median width of diaphysis	5.06	6.55	8.79	8.10
Olecranon height	6.34*	7.49	12.41	12.78
Olecranon thickness	-	6.60	9.31	9.17
Length of the trochlear notch	10.94	10.15	13.72	13.73*
Width at distal epiphysis	-	8.46	6.92	-
Thickness at distal epiphysis	-	6.92	-	-

	H. cf. *H. miyou*			*P. holmbergi*	*Parastrapotherium* sp.	
Radius	MUN-STRI 16777	MUN-STRI 34221	MUN-STRI 37765	MNHN DES 989	MNHN DES 1013	MNHN COL 129
Length	40.0	-	-	33.5	43.5	-
Width at proximal end	11.70	11.61	-	8.60	11.82	8.43
Thickness at proximal end	7.70	6.71	6.6*	5.27	6.95	5.28
Median width of diaphysis	5.72	4.34	-	5.18	8.71	-
Width at distal epiphysis	11.77	-	12.0*	9.00	11.07	-
Thickness at distal epiphysis	9.07	-	7.5*	5.57	8.14	-

	H. cf. *H. miyou*		*P. holmbergi*	*Parastrapotherium* sp.
Femur	MUN-STRI 34310	MUN-STRI 34229	MNHN DES 988	MNHN DES 1017
Length from head	-	104.0*	-	-
Length from greater trochanter	-	98.0*	-	-
Median width of diaphysis	11.05	13.94*	9.52*	-
Width at epicondyles	15.5*	-	-	17.2

concave, widely separated dorsally, and more proximate ventrally (Figure 9c), as in *Astrapotherium* (Scott, 1928, 1937) and *Parastrapotherium* (Figure 9e). The neural canal is circular in anterior and posterior view. The ventral side of the ventral arch is convex. The caudal articular surface is oval and nearly flat. The posterior opening of the large arterial foramen opens posteroventrally (Figure 9d), as in *Astrapotherium* (Scott, 1928). The thoracic vertebra (MUN-STRI 34217) preserves the centrum and a small fragment of the neural arch (Figure 9g). The centrum forms a triangle with rounded corners in anterior view, with the widest border on the dorsal side, as in *Parastrapotherium*. It has an oval articular surface for the rib on the dorsolateral edge of the centrum, also present in *Parastrapotherium* (Figure 9g,h).

The sacrum (MUN-STRI 34217) preserves three fused vertebrae of total length 26.8 cm. It is likely that the sacrum was formed by more vertebrae, given that in *Astrapotherium* it consists of four and probably five vertebrae (Scott, 1937). In anterior view the vertebral centrum is oval, but in the most caudal vertebra the centrum is strongly compressed dorsoventrally. The neural arches of the vertebrae are fused, forming a continuous plate. The transverse processes are also fused, and one sacral foramen is observed.

Three partial scapulae were recovered; they all represent the most dorsal portion of the scapula (Figure 10a,b). The scapula of astrapotheres is narrow anteroposteriorly, and does not have the bladelike appearance seen in most terrestrial mammals. In *Astrapotherium*, it narrows dorsally, but is wider anteroposteriorly than in the scapulae referred to *Hilarcotherium* cf. *H. miyou*, forming a more quadrangular end (Figure 10a,c; Scott, 1928, 1937). In *Hilarcotherium* cf. *H. miyou*, the dorsal end seems more bulbous. The fragmentary scapulae of *Hilarcotherium* cf. *H. miyou* show a spine that is wide and well developed laterally (Figure 10a,b), as in *Astrapotherium* and *Parastrapotherium* (Loomis, 1914).

One almost complete humerus (MUN-STRI 16777; Figure 10e–h) is large and comparable in size to *G. snorki* (Johnson and Madden, 1997: tbl. 22.6). The associated radius with unfused distal epiphysis (see below) indicates that this individual was not skeletally mature. The humerus is larger and more robust than in *H. castanedaii, A. magnum*, and *P. herculeum*? (Figure 10e–m; Table 4). The head is large and projects posteriorly to the plane of the shaft (Figure 10g), as in *H. castanedaii* and *A. magnum* (Scott, 1928, 1937; Vallejo-Pareja et al., 2015). The greater tubercle extends more proximally than the lesser tubercle (Figure 10e,i), as in *H. castanedaii* and *A. magnum*. The bicipital groove is broad and shallow, more than in *H. castanedaii* and *A. magnum*. The shaft is proportionally slender, but it has an elongated and marked delto-pectoral crest, which extends up to about two-thirds of the humeral length, as in *Parastrapotherium* (Loomis, 1914). The supinator crest is small and narrow. The radial fossa is large and deep, with no foramen (Figure 10e–f), as in *H. castanedaii* and *A. magnum* (Scott, 1928, 1937; Vallejo-Pareja et al. 2015). The capitulum is rounded and extends less distally than the trochlea, as in *H. castanedaii* and *A. magnum* (Figure 10e,j). The medial epicondyle is well developed as in *H. castanedaii* and unlike in *A. magnum* (Vallejo-Pareja et al., 2015).

An almost complete ulna (MUN-STRI 34223) was recovered and lacks only its most distal portion (Figure 11a–d). The shaft is anteroposteriorly deeper than mediolaterally wide. The olecranon is short and robust, as in *Parastrapotherium* (Figure 11a–f; Loomis, 1914). In anterior view, the olecranon projects more medially than the plane of the shaft (Figure 11a), but in lateral view the olecranon and the shaft are on the same plane (Figure 11c), as in *Parastrapotherium* (Figure 11e,f) and *A. magnum* (Scott, 1937). The length of the trochlear notch is similar to that in *P. holmbergi*, but smaller than in *P. herculeum*? (Table 4). The trochlear notch forms a semicircle in lateral view (Figure 11c). The coronoid process is large and is almost perpendicular to the axis of the shaft (Figure 11c,d), whereas in *Parastrapotherium* it is more oblique (Figure 11f). Distal and lateral to the coronoid process is the radial notch (Figure 11b), as in *Parastrapotherium* (Figure 11e).

Remains of several *Hilarcotherium* cf. *H. miyou* radii were recovered from Castilletes. The most complete (MUN-STRI 16777; Figure 11g,h) is from a juvenile, as determined from the unfused and missing distal epiphysis. It is comparable in size to the large specimens of *Parastrapotherium* (Table 4). The proximal end is wider than the shaft (Figure 11g–j) as in *Astrapotherium* and *Parastrapotherium* (Figure 11k,l). The articular surface

FIGURE 10. (*Opposite*) Scapulae and humeri of *Hilarcotherium* cf. *H. miyou* from the Castilletes Formation, and selected astrapotheres for comparison. *Hilarcotherium* cf. *H. miyou* scapulae, (a) MUN-STRI 38384 in lateral view; (b) MUN-STRI 34223 in anterior or posterior view; left scapula of *Astrapotherium magnum* from the Santa Cruz Formation, Argentina (YPM PU 15255) in (c) lateral view and (d) posterior view. *Hilarcotherium* cf. *H. miyou* left humerus (MUN-STRI 16777), (e) anterior view; (f) schematic drawing in anterior view; (g) medial view; (h) posterior view. *Hilarcotherium* cf. *H. miyou* partial humeri, (i) proximal portion of left humerus (MUN-STRI 34222); *Hilarcotherium* cf. *H. miyou* distal epiphysis of left humerus (MUN-STRI 34223), (j) anterior view and (k) posterior view. Left humerus of *Astrapotherium magnum* (YPM PU 15255) in (l) anterior and (m) posterior view.

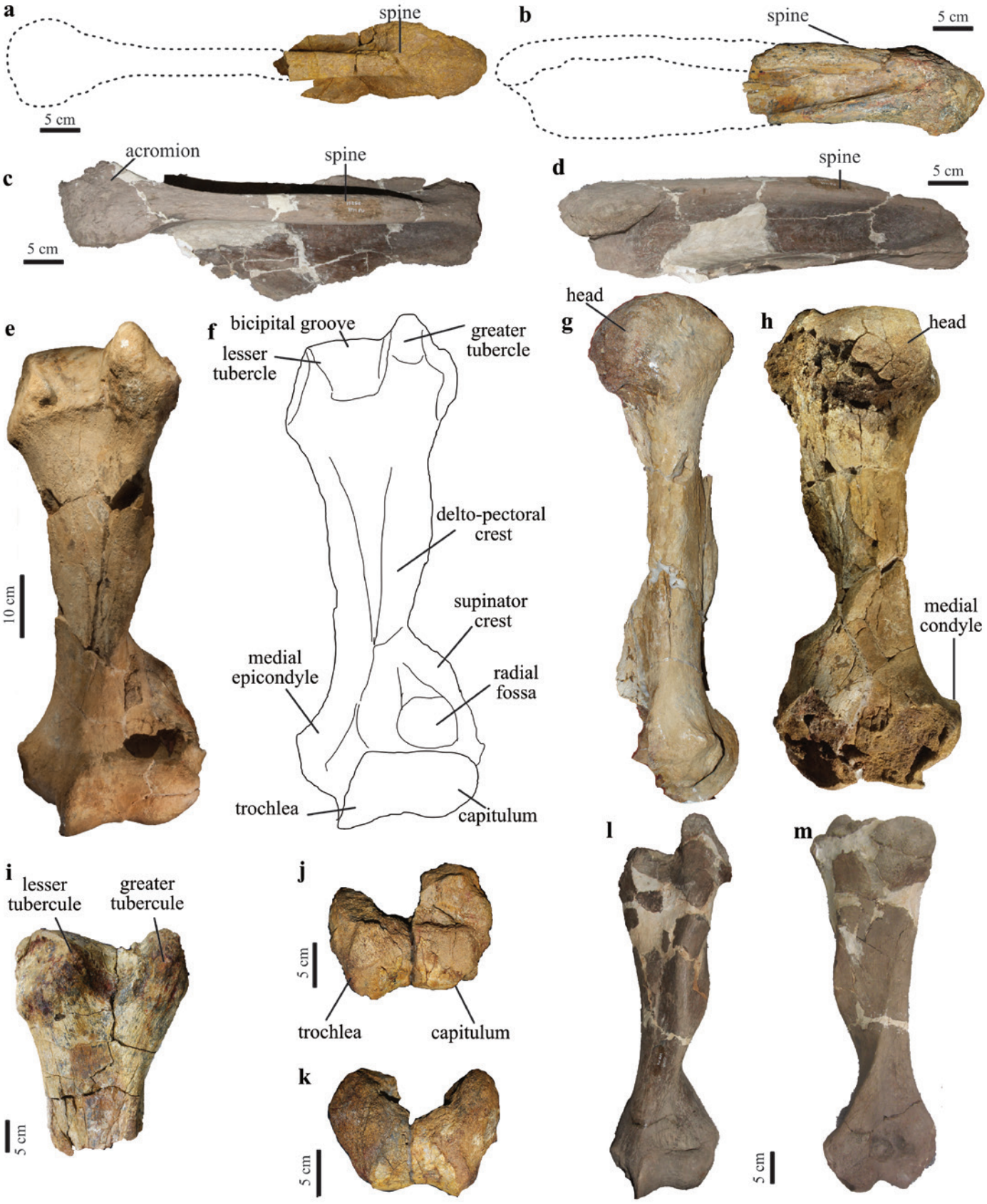
a
spine
5 cm
b
spine
5 cm
c
acromion
spine
5 cm
d
spine
5 cm
e
10 cm
f
bicipital groove
greater tubercle
lesser tubercle
delto-pectoral crest
supinator crest
medial epicondyle
radial fossa
trochlea
capitulum
g
head
h
head
medial condyle
i
lesser tubercle
greater tubercle
5 cm
j
5 cm
trochlea
capitulum
k
5 cm
l
m
5 cm

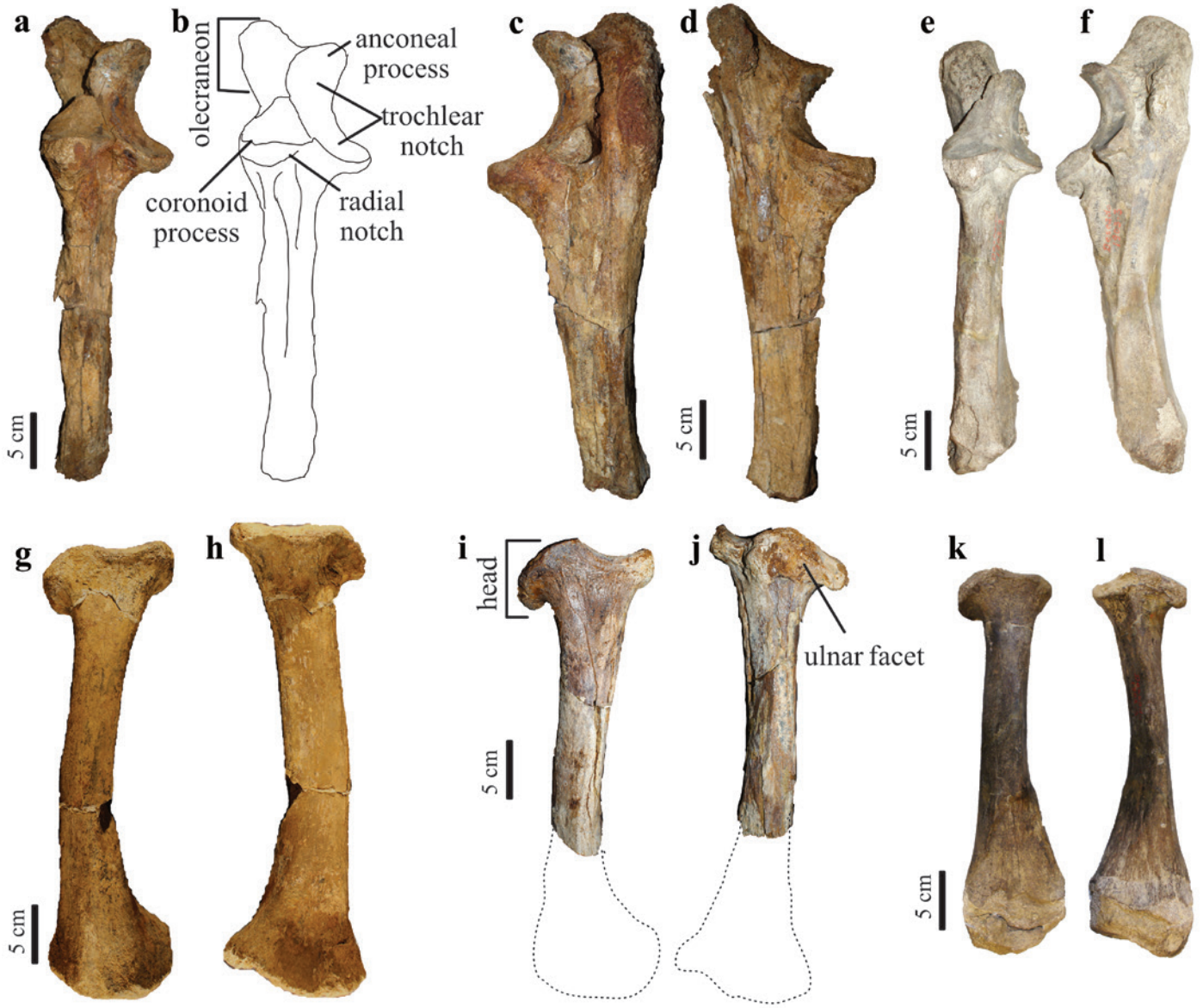

FIGURE 11. Antebrachial bones of *Hilarcotherium* cf. *H. miyou* from the Castilletes Formation, and selected astrapotheres for comparison. *Hilarcotherium* cf. *H. miyou* left ulna (MUN-STRI 34223), (a) anterior view; (b) schematic drawing in anterior view; (c) lateral view; (d) medial view. Left ulna of *Parastrapotherium holmbergi* (MNHN DES 985) from the Deseadan of Argentina in (e) anterior and (f) lateral view. Left radius of *Hilarcotherium* cf. *H. miyou* (MUN-STRI 16777), (g) anterior, and (h) posterior view. MUN-STRI 34221, (i) anterior, and (j) posterior view. Left radius of *Parastrapotherium holmbergi* (MNHN DES 989) in (k) anterior and (l) posterior view.

for the humerus is divided into two sections, the medial is concave and the lateral is saddle-shape, as in *A. magnum* (Scott, 1928, 1937). The anterior border of the proximal epiphysis is more proximal than the posterior one. The shaft is slightly curved (Figure 11g,h).

Two fragmentary femora were recovered from Castilletes. MUN-STRI 34229 is almost complete but badly preserved, and no details from the epiphyses can be observed. MUN-STRI 34310 preserves part of the shaft and the distal epiphysis. The median and lateral epicondyles project distally to the same level, and the articulation surface for the patella seems narrower than in *A. magnum* (Scott, 1937). The patella (MUN-STRI 34212) is oval and elongated proximodistally, narrowing at its distal end, as in *A. magnum* (Scott, 1937). It measures

15 cm in length. It is curved in lateral view, with a convex anterior border. The articular facet is quadrangular and measures 8.5 cm proximodistally and 6.2 cm mediolaterally. MUN-STRI 16777 includes a partial distal left tibia. The shaft is trihedral in cross section. The medial malleolus is broad, very similar to the condition of the tibiae reported from the Castillo Formation (Weston et al., 2004). MUN-STRI 34229 also includes a fibula, which is slender and straight, as in *A. magnum* (Riggs, 1935; Scott, 1937).

Body Mass Estimation

The body mass estimate from the m2 length of the holotype of *H. miyou* is ~6456.6 kg (Table 5). Previous studies used the m1–m3 length to estimate the body mass in astrapotheres (Johnson and Madden, 1997; Kramarz and Bond, 2011; Vallejo-Pareja et al., 2015). For other taxa, including the uruguaytheriines *H. castanedaii, G. snorki*, and *X. kraglievichi*, the body mass estimates from the m2 length are similar to those obtained from the m1–m3 length in the same specimen (Table 5), suggesting that if the lower molar row length could be measured in *H. miyou*, it would yield an estimate similar to the m2 length. The length of proximal limb bones is highly correlated with body mass in ungulates (Scott, 1990). The humerus length of a specimen tentatively referred to *Hilarcotherium* cf. *H. miyou* (MUN-STRI 16777) yields an estimate of ~4985.0 kg (Table 5), 23% less than the value obtained from the m2 length in *H. miyou*. For *G. snorki* the difference was observe to be 23% more (Table 5).

Phylogenetic Analysis of Astrapotheriidae

The cladistic analysis resulted in 10 most parsimonious trees of 128 steps, with a consistency index of 0.680 and retention index of 0.759. Ten characters were parsimony uninformative. The strict consensus (Figure 12) differs from the topologies presented by Vallejo-Pareja et al. (2015; fig. 6) in the

TABLE 5. Body mass (BM) estimates of astrapotheres (in kg). % PE = percent of error. The estimations from the m2 length and the m1–m3 length use equations of non-selenodont ungulates (Damuth, 1990). For m2 length, log(BM) = 2.98 * log(m2 length) + 1.11, with r^2 = 0.97 and % PE = 30.61. For m1–m3 length, log(BM) = 3.03 * log(m1–m3 length) – 0.39; with r^2 = 0.96 and % PE = 37.19. Estimates from the humerus length follow the equation of all ungulates for H2 in Scott (1990): log(BM) = 3.4026 * log(H2) – 2.513; with r^2 = 0.9196 and % PE = 29.

Taxon	Specimen(s)	Length	Estimated BM	BM+PE	BM–PE
		BM estimates from m2 length			
Hilarcotherium miyou	IGMp 881327	81.8 mm	6,456.6	8,433.0	4,480.2
Hilarcotherium castanedaii[a]	IGM p881231	48.8 mm	1,385.1	1,809.1	961.1
Granastrapotherium snorki[b]	mean of 9 specimens	66.5 mm	3,483.4	4,549.7	2,417.2
Xenastrapotherium kraglievichi	MLP 12-96	49.3 mm	1,427.9	1,864.9	990.8
Parastrapotherium martiale	MACN A 52604	66.9 mm	3,546.3	4,631.8	2,460.7
Astrapotherium giganteum	MACN-A 3274-3278	64.6 mm	3,195.2	4,173.2	2,217.1
		BM estimates from m1–m3 length			
Hilarcotherium castanedaii[a]	IGM p881231	140.2 mm	1,302.7	1,787.1	818.2
Granastrapotherium snorki[b]	UCMP 40017	187.5 mm	3,141.9	4,310.4	1,973.4
Xenastrapotherium kraglievichi[c]	MLP 12-96	141 mm	1,324.7	1,817.4	832.1
Parastrapotherium martiale[c]	MACN A 52604	194 mm	3,483.7	4,779.3	2,188.1
Astrapotherium giganteum[c]	MACN-A 3274-3278	196 mm	3,593.7	4,930.1	2,257.2
		BM estimates from humerus length			
Hilarcotherium castanedaii[a]	IGM p881231	45.5 cm	1,306.5	1,685.4	817.7
Hilarcotherium cf. *H. miyou*	MUN-STRI 16777	70 cm	4,985.0	6,430.7	3,120.1
Granastrapotherium snorki[b]	UCMP 40192	65.5 cm	4,501.1	5,806.4	2,817.3
Astrapotherium magnum[b]	FMNH 14251	52.3 cm	2,096.5	2,704.4	1,312.2

[a] Reported by Vallejo-Pareja et al. (2015).
[b] Reported by Johnson and Madden (1997).
[c] Reported by Kramarz and Bond (2011).

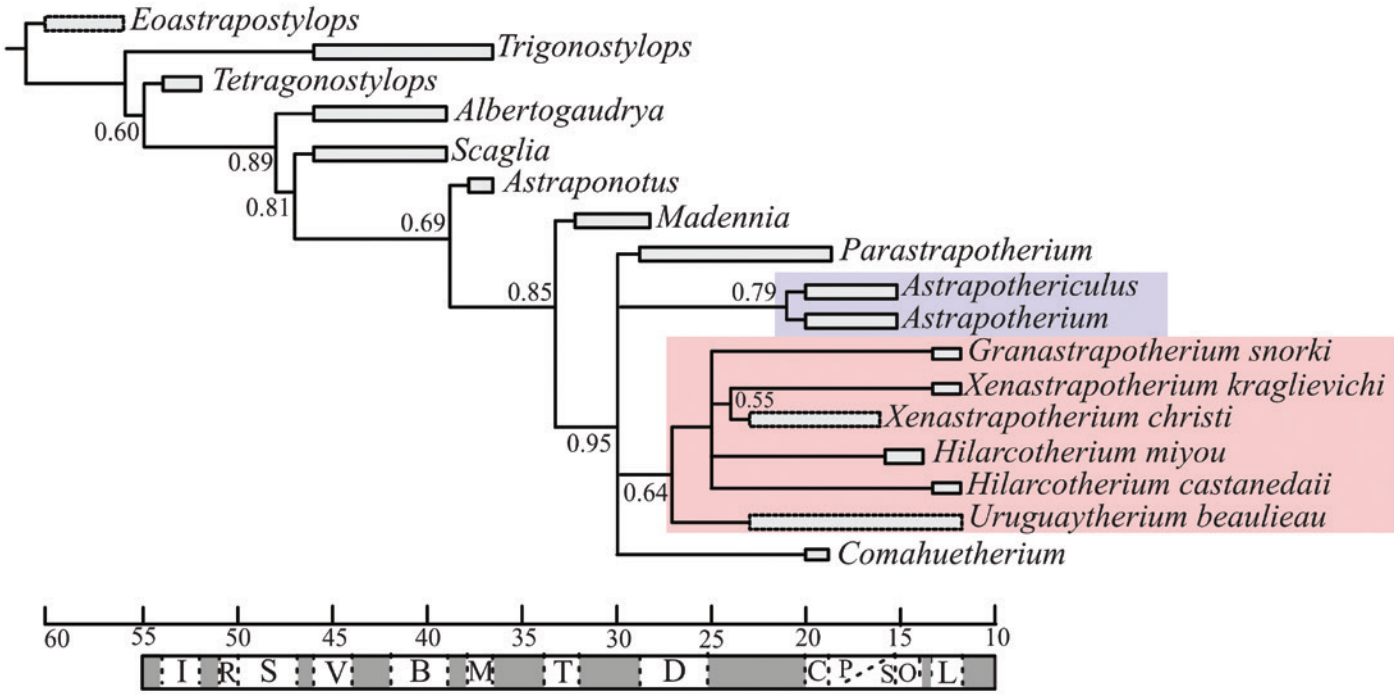

FIGURE 12. Hypothesis of phylogenetic relationships within Astrapotheriidae. Time-calibrated topology of the strict consensus resulting from the analysis with PAUP* 4.0. Bootstrap values higher than 0.50 are indicated for several nodes. Blue tint = Astrapotheriinae; red tint = Uruguaytheriinae. Letters below time line (MYA) denote SALMAs (from left to right): I = Itaboraian; R = Riochican; S = Sapoan; V = Vacan; B = Barrancan; M = Mustersan; T = Tinguirican; D = Deseadan; C = Colhuehuapian, P = "Pinturan"; S = Santacrucian; O = Colloncuran; L = Laventan.

position of *Comahuetherium*, and the relationships of northern Uruguaytheriinae. In the strict consensus, *Comahuetherium, Parastrapotherium*, and the clades Astrapotheriinae and Uruguaytheriinae form a polytomy (Figure 12), whereas Vallejo-Pareja et al. (2015) recovered *Comahuetherium* as the sister taxon of a clade including *Parastrapotherium*, Astrapotheriinae and Uruguaytheriinae.

We recovered the main clades previously recognized within Astrapotheriidae. The Astrapotheriinae (*Astrapotherium*, *Astrapothericulus*) clade has a bootstrap value of 0.79 and is supported by four unambiguous synapomorphies that concern the molars: deep hypoflexid (character state 0 of character 26; 26[0]), the presence of a lingual cingulid (30[1]), a rounded hypocone (40[0]), and an ephemeral median fossette (44[1]). The Uruguaytheriinae clade has a bootstrap value of 0.64 and is supported by two unambiguous synapomorphies: the absence of molar hypoflexid (26[2]) and the absence of labial cingulum in the molars (27[0]). The Uruguaytheriinae from northern South America (*Hilarcotherium, Granastrapotherium*, and *Xenastrapotherium*) form a clade supported by one unambiguous synapomorphy, the presence of a superficial paraflexid on the lower molars (28[1]). Finally, *X. kraglievichi* and *X. christi* form a clade supported unambiguously by the absence of i3 (3[1]) and the presence of a superficial hypoflexid (26[1]). Within the 10 most parsimonious trees obtained, *H. miyou* is recovered as the sister taxon of *H. castanedaii* in one, as the sister taxon of *G. snorki* in five, and as the sister taxon of a (*Xenastrapotherium*, *Granastrapotherium*) clade in four. The inclusion of additional taxa and more complete material is necessary to futher test the monophyly of the two *Hilarcotherium* species.

NOTOUNGULATA ROTH, 1903

TOXODONTIA OWEN, 1853

LEONTINIIDAE AMEGHINO, 1895

cf. *Huilatherium* Villarroel and Guerrero, 1985

TYPE SPECIES. *Huilatherium pluripicatum* Villarroel and Guerrero, 1985.

REFERRED MATERIAL. MUN-STRI 34312 right m3 (cast PIMUZ A/V 5290).

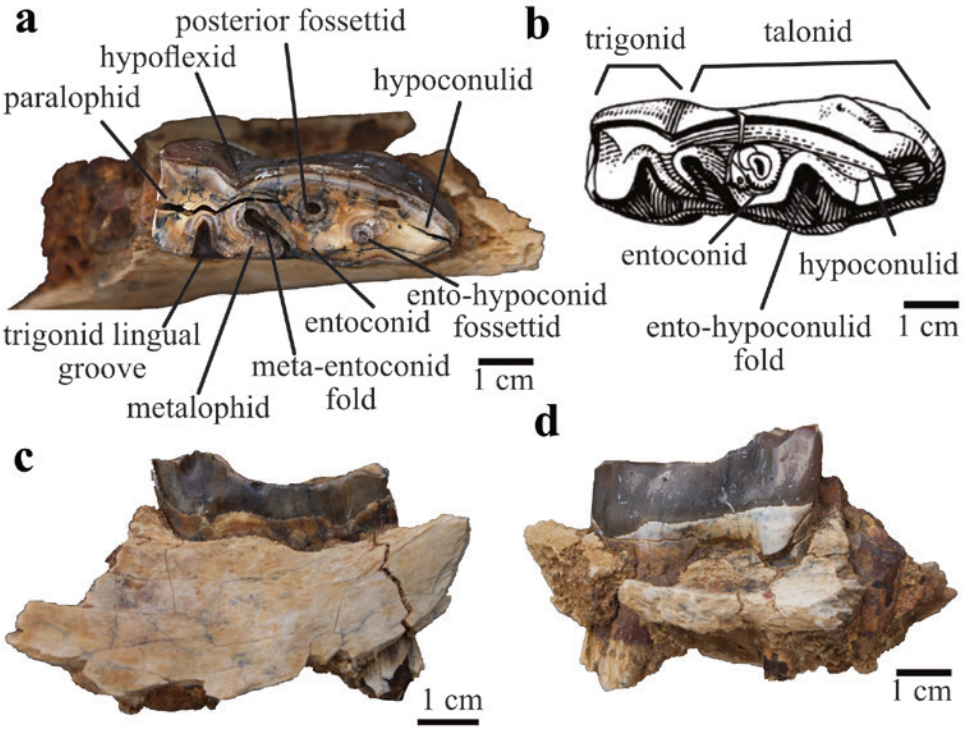

FIGURE 13. Leontiniidae (Notoungulata) right m3: (a) cf. *Huilatherium* (MUN-STRI 34312) in occlusal view; (b) *H. pluripicatum* (UCMP 40280), modified from Villarroel and Colwell Danis (1997); (c) MUN-STRI 34312 in lingual and (d) labial view.

Locality and Horizon. MUN-STRI 34312 comes from Patajau, Castilletes Formation, STRI locality 340094; 11.9465°N, 71.3255°W (Figure 3).

Description. The isolated tooth is interpreted as an m3 because of its elongate talonid that narrows distally (Figure 13a). It is protohypsodont (rooted teeth, crown height <50% of mesiodistal length; Pérez and Vucetich, 2012), with a mesiodistal length of 40.4 mm and labiolingual width of 14.5 mm, approximately 30% smaller than the m3 of *H. pluripicatum* (Villarroel and Colwell Danis, 1997: tbl. 19.4). The crown height measured at the labial side is 14.4 mm, yielding a hypsodonty index of 0.4, although this value may be an underestimation for this animal, as the appearance of the ento-hypoconulid as a fossettid indicates high wear in the specimen (Figure 13 a,b; see below).

The paralophid is wide and perpendicular to the mesiodistal axis of the crown. The trigonid lingual groove is well developed and straight, projecting from the lingual to the labial side of the crown. The metalophid is wider than in *H. pluripicatum* and it is oblique. The meta-entoconid fold is well developed and projects linguomesially, as in *H. pluripicatum* (Figure 13a). It has a posterior fossettid, which is rounded and not U-shaped, as in *H. pluripicatum* (Figure 13a,b). Due to wear, the ento-hypoconid fold appears as a fossettid between the entoconid and the hypoconulid (Figure 13a). According to Villarroel and Colwell Danis (1997), in *H. pluripicatum* the ento-hypoconid fold (treated as "entoflexid" by these authors) appears as a "large rounded pit" with extensive wear. The hypoconulid is large and almost parallel to the mesiodistal axis of the tooth, as in *H. pluripicatum* (Villarroel and Colwell Danis, 1997). There are neither lingual nor labial cingulids (Figure 13c,d). In *H. pluripicatum* and *Colpodon distinctus,* the labial cingulid is absent, and the lingual cingulid is present but reduced (Villarroel and Colwell Danis, 1997; Ribeiro et al., 2010). In *Henricofilholia* the labial and lingual cingulids are variably developed (Ribeiro et al., 2010), and *Martinmiguelia*, *Scarritia, Elmerriggsia* and *Gualta* have both lingual and labial cingulids (Ubilla et al., 1994; Bond and López, 1995; Ribeiro et al., 2010; Shockey et al., 2012; Cerdeño and Vera, 2015).

Toxodontidae (Gervais, 1847)

Toxodontinae (Trouessart, 1898)

Falcontoxodon gen. nov.

Type Species. *Falcontoxodon aguilerai* sp. nov.
Diagnosis. As for the type and only species.

Falcontoxodon aguilerai sp. nov.

FIGURES 14, 16

Etymology. The genus name is for the Falcón state in Venezuela, where the holotype was found. The species name is after Orangel Aguilera, in recognition of his lifetime contribution to paleontology in Venezuela.

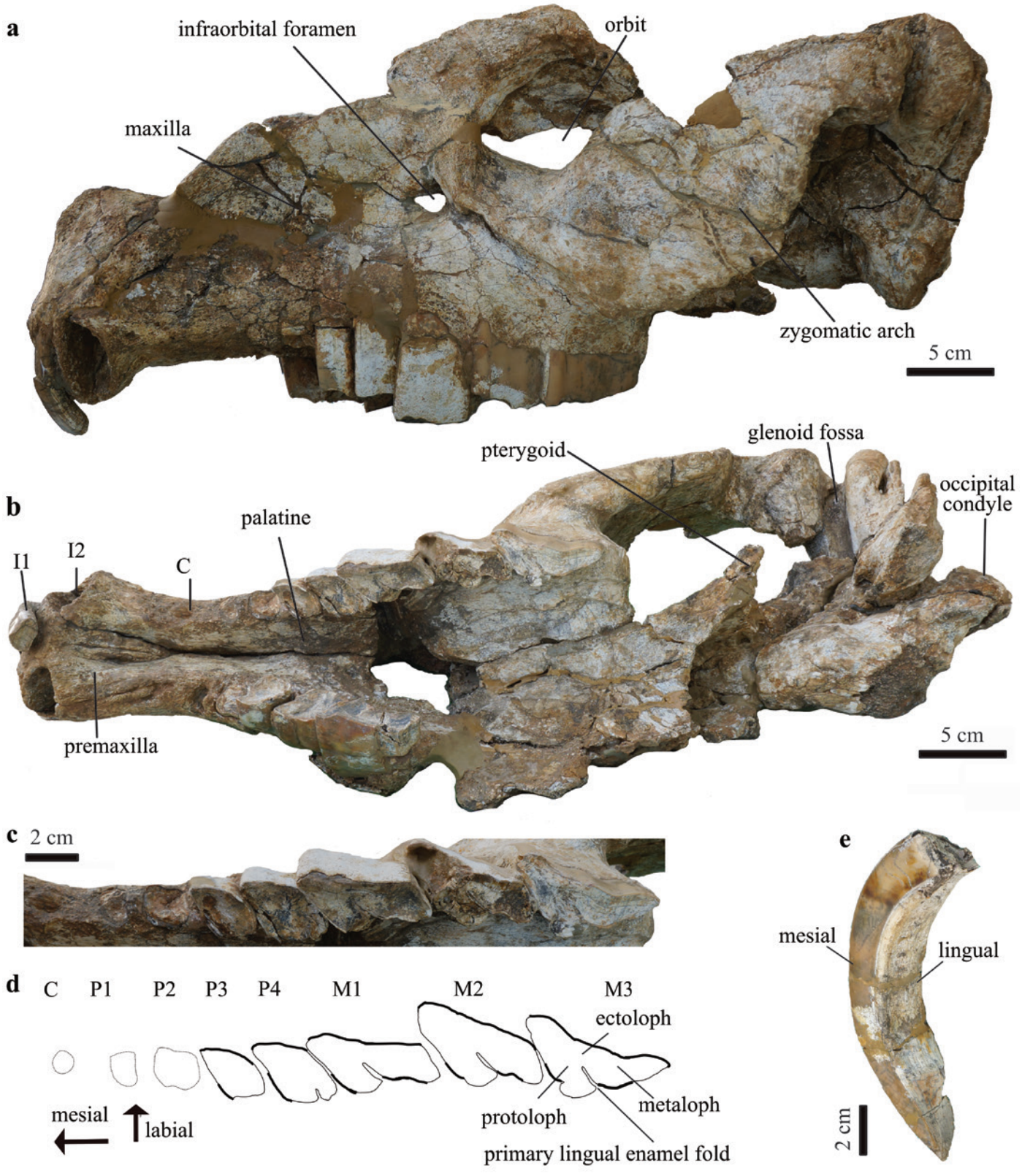

FIGURE 14. Skull of *Falcontoxodon aguilerai* gen. et sp. nov. (Toxodontidae, Notoungulata) (holotype, AMU-CURS 765): (a) left lateral view; (b) ventral view; (c) detail of the upper left dentition in occlusal view; (d) schematic drawing of dentition: distribution of enamel is shown by thick lines; (e) right I2 in mesiolingual view.

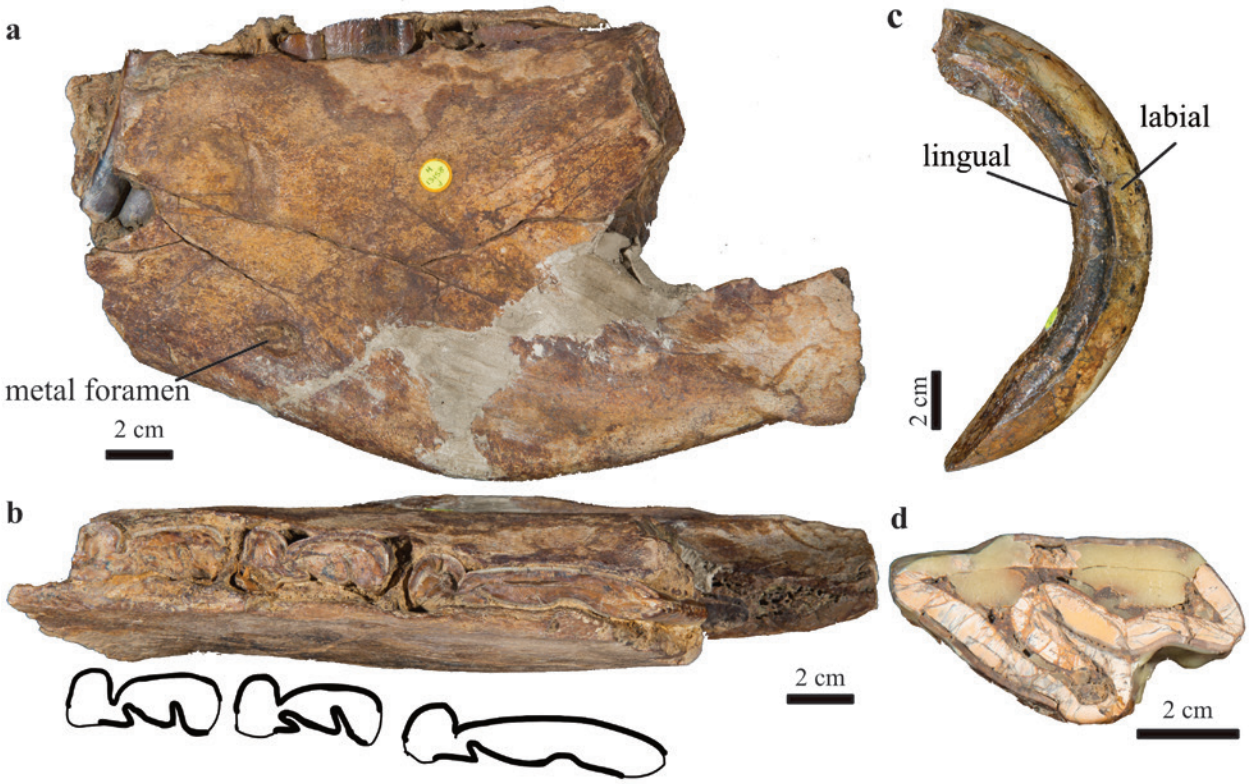

FIGURE 15. *Gyrinodon quassus* (Toxodontidae, Notoungulata) (holotype, NHMUK PV M 13158): (a) right partial mandible in lateral view; (b) top, right partial mandible in occlusal view; bottom, schematic drawing of m1–m3: distribution of enamel is shown by thick lines; (c) right I2 in labial view; (d) cross section of M1or M2. Photos by Lucie Goodayle; courtesy of Natural History Museum, London.

HOLOTYPE. AMU-CURS 765, fairly complete skull with left I1 and P3–M3 and right P3–M1 in situ, and associated right I2, M2, and M3. Alveoli of the other teeth are preserved. Mandible with complete dentition excepting left i2 and right i1, i2.

REFERRED MATERIAL. AMU-CURS 70, left m3.

TYPE LOCALITY AND HORIZON. The holotype and AMU-CURS 70 were collected in the Algodones Member, Codore Formation, Urumaco, Falcón State, Venezuela. 11°17′39.8″N 070°14′15.6″W (Figure 4a,b).

DIAGNOSIS. The dental formula is i 2/3, c 1/0, p 4/4, m 3/3. Mandibular symphysis reaches the level of m1–m2. Comparable in size to *Pericotoxodon*, larger than *Nesodon* and *Xotodon*, and smaller than *Toxodon* and *Mixotoxodon*. Upper molars have simple enamel lingual fold. Well-defined protoloph lingual column present only in M3. It differs from *Gyrinodon* in the sigmoid shape of the zygomatic arch in lateral view, the broad metaloph, and the absence of a ventral extension of the dentary. It differs from *Mixotoxodon* in having a short diastema posterior to i3, lingual enamel band of m1 restricted between the anterior fold and the hypoconulid, a less developed lower molar anterior fold, and less procumbent lower incisors. It differs from *Trigodonops* in the absence of a labial groove in p3 and p4. It differs from *Piauhytherium* in having a long nasal and the presence of an upper canine. It differs from *Pericotoxodon* in the position of the infraorbital foramen, widely separated from the zygomatic arch, the absence of I3, the upper molars with a simple enamel fold, and the absence of a ventral extension of the horizontal ramus of the mandible. It differs from *Andinotoxodon* in the presence of p1, absence of lingual enamel in the lower premolars, and in having a labiolingually narrower entolophid. It differs from *Hoffstetterius* in the presence of the upper canine and P1, and the absence of a mandibular ventral extension. It differs from *Paratrigodon* and *Trigodon* in the presence of P1 and lingual enamel in P3 and P4. It differs from *Calchaquitherium* in the rounded angle of the posteroventral border of the vertical ramus of the mandible, the incisors being at the same level as the cheek teeth, and the absence of a median symphyseal labial keel.

DESCRIPTION. The skull is pyriform in ventral view (Figure 14b), and the nasal is long as in most toxodontids (Forasiepi et al., 2015). The premaxilla is not expanded laterally, as in most Toxodontinae except for *Toxodon* (Owen, 1840) and *Hoffstetterius* (Saint-André, 1993). The infraorbital foramen is distant

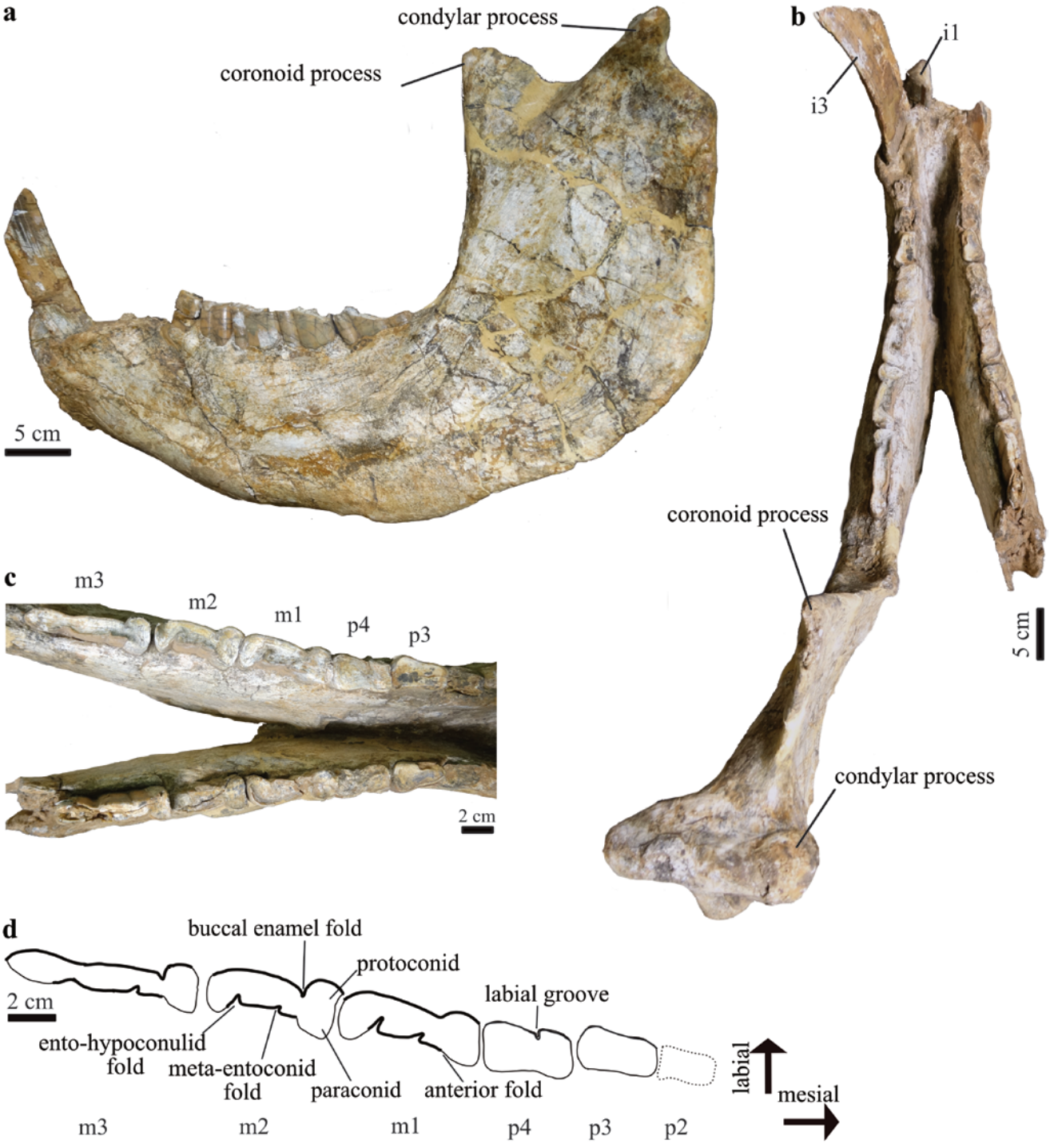

FIGURE 16. Mandible of *Falcontoxodon aguilerai* gen. et sp. nov. (holotype, AMU-CURS 765): (a) left lateral view; (b) dorsal view; (c) detail of dentition and symphysis in occlusal view; (d) schematic drawing of left dentition: distribution of enamel is shown by thick lines.

from the zygomatic arch (Figure 14a), as in *Adinotherium*, *Nonotherium*, *Nesodon*, *Palyeidodon*, *Hoffstetterius*, *Gyrinodon*, and *Toxodon*, and unlike *Pericotoxodon*, *Posnanskytherium*, *Trigodon*, *Piauhytherium*, *Paratrigodon*, and *Xotodon* in which the infraorbital foramen is in close proximity to the zygomatic arch (Madden, 1997; Guérin and Faure, 2013; Forasiepi et al., 2015). The zygomatic arch is sigmoid (Figure 14a), unlike the condition in *Gyrinodon*, *Toxodon*, *Hoffstetterius*, *Palyeidodon*, and *Trigodon*, and the root of the zygomatic process of the squamosal is located dorsal to the M3 (Figure 14a,b), as in most toxodontids except for *Posnanskytherium*, in which it is positioned dorsal to the M2 (Madden, 1997).

The palate is widest at the level of M3 and narrows toward P1. Anterior to P1 the palate is elongate and the lateral borders are parallel (Figure 14b). The I1 is approximately oval in cross section, similar to *Calchaquitherium* (Nasif et al., 2000). The I2 is developed as a tusk. It has enamel only on the labial side of the crown (Figure 14e), as in *Gyrinodon* (Figure 15c). The I3 is absent, unlike in *Pericotoxodon*, *Trigodon*, *Pisanodon*, *Palyeidodon*, and *Nesodon*. There is a diastema of 51 mm between I2 and C (Figure 14b), and a shorter diastema between C and P1 (Figure 14d), as in *Pericotoxodon* (Madden, 1997). The upper canine is greatly reduced, as shown by the size of the alveolus, with a diameter of approximately 7 mm (Table 6).

The upper and lower cheek teeth are hypselenodont (rootless) as in most toxodontids (Forasiepi et al., 2015). Only the alveoli of P1 and P2 are preserved. The P3 does not have a lingual enamel fold, but one is present in P4 (Figure 14d), as in *Mixotoxodon* and *Piauhytherium* (Van Frank, 1957; Guérin and Faure, 2013). The P4, and in a lesser degree the P3, are elongate mesiolabially, resulting in teardrop shape in cross section (Figure 14d), similar to *Pericotoxodon* and *Mixotoxodon* (Van Frank, 1957; Madden, 1997). In occlusal view, there is a broad labial enamel band that reaches the mesiolabial corner, and a second enamel band in the mesiolingual portion of the P3–P4 (Figure 14d) as in *Pericotoxodon* and *Mixotoxodon*. Madden (1997) noted that this band is obliterated in advanced stages of wear in *Pericotoxodon*.

The upper molars have a simple, persistent primary lingual enamel fold, which separates the protoloph from the metaloph (Figure 14d; see also Madden, 1990; 1997), as observed in individuals of *Pericotoxodon* with an advanced stage of dental wear (Madden, 1997: fig. 21.5), as well as in *Andinotoxodon* (Madden, 1990), *Mixotoxodon* (Laurito, 1993), *Piauhytherium* (Guérin and Faure, 2013), and *Gyrinodon* (Figure 15d). The protoloph does not support a lingual column in M1 and M2, but one is present in M3 (Figure 14d). In contrast, the lingual column is present in all molars in *Pericotoxodon* (Madden, 1997), and it is absent in *Mixotoxodon* (Laurito, 1993) and *Andinotoxodon* (Madden, 1990). The metaloph is broad and does not taper distally, as in most specimens of *Pericotoxodon* (Madden, 1997).

The horizontal ramus of the mandible of *Falcontoxodon* does not have a ventral extension (Figure 16a), in contrast to the presence of this feature in *Pericotoxodon* (Madden, 1997) and *Gyrinodon* (Figure 15a). The vertical ramus is wide and has a rounded caudoventral border (no distinct angular process), in contrast with the right-angle border of *Pericotoxodon* and *Calchaquitherium* (Madden, 1997; Nasif et al., 2000). The coronoid process is at the same level as the condyle, as in *Mixotoxodon* (Van Frank, 1957). There is no median symphyseal labial keel, unlike in *Nesodon* and *Calchaquitherium* (Nasif et al., 2000; Forasiepi et al., 2015). The symphysis extends caudally up to the level of m1–m2 (Figure 16b), in contrast to *Trigodonops*, *Piauhytherium*, *Mixotoxodon*, and *Gyrinodon* where it extends until the p4–m1.

The i1 is triangular in cross section, with a broad labial enamel band and a narrow lingual band, as in *Mixotoxodon* (Van Frank, 1957; Laurito, 1993). Only the alveolus of i2 is preserved. The i3 is tusk-like, with broad labial and lingual enamel bands (Figure 16c). There is a short diastema between i3 and p1. The c is absent, as in *Mixotoxodon*, *Calchaquiterium*, *Paratrigodon*, *Trigodon*, and *Piauhytherium* (Guérin and Faure, 2013; Forasiepi et al., 2015). Only the alveoli of p1 and p2 are preserved. The p3 and p4 are approximately rectangular in cross section. There is no labial groove in p3 but one is present in p4 (Figure 16d), similar to *Mixotoxodon* (Van Frank, 1957), and unlike *Trigodonops* and *Piauhytherium*, which have a marked labial groove in both p3 and p4 (Paula Couto, 1979; Guérin and Faure, 2013).

The lower molars are bicrescentic and ever growing, with a well-defined labial enamel fold (Figure 16c,d). The m1 has a lingual enamel band between the anterior fold and the hypoconulid (Figure 15d). In contrast, the lingual enamel of the m1 of *Mixotoxodon* is between the meta-entoconid fold and the hypoconulid (Van Frank, 1957; Rincón, 2011). The m1 and m2 have a shallow mesial fold at the same level as the labial fold, as in *Mixotoxodon* and *Gyrinodon* (Hopwood, 1928; Van Frank, 1957). The meta-entoconid and ento-hypoconulid folds are well defined in m1, but in the m2 the meta-entoconid fold is shallow, as in *Mixotoxodon* (Van Frank, 1957). In contrast, in the m2 of *Gyrinodon* the ento-hypoconulid and meta-entoconid folds are well defined (Hopwood, 1928). The m2 and m3 have a lingual enamel band between the anterior fold and the hypoconulid, as in all Toxodontinae (Forasiepi et al., 2015). The m3 has meta-entoconid and ento-hypoconulid folds, both absent in *Calchaquitherium* (Nasif et al., 2000). The ento-hypoconulid fold is present, but open, similar to *Mixotoxodon* and *Gyrinodon*. An open ento-hypoconulid fold is correlated with increasing mesiodistal crown length, a feature that appears as the tooth grows and is worn away (Madden, 1997).

TABLE 6. Dental measurements of *Falcontoxodon* (in mm). An asterisk (*) indicates tooth crown incomplete; double asterisk (**) indicates specimen measured at the alveolus.

Taxon	Specimen	Feature	Side	Measurement	Value
Falcontoxodon aguilerai	AMU-CURS 765	I1	Left	Maximum length	16
				Maximum width	25
		I2	Left	Maximum length	24
				Maximum width	35
		C	Left	Maximum length**	7
				Maximum width**	6
			Right	Maximum length**	7
				Maximum width**	6
		P1	Left	Maximum length**	13
				Maximum width**	16
		P2	Left	Maximum length	19
				Maximum width	19
			Right	Maximum length	19
				Maximum width	19
		P3	Left	Maximum length	22
				Maximum width	24
			Right	Maximum length	22
				Maximum width	25
		P4	Left	Maximum length	30
				Maximum width	29
			Right	Maximum length	29
				Maximum width	30
		M1	Left	Ectoloph length	45
				Maximum length	55
			Right	Ectoloph length	49
				Maximum length	36
		M2	Left	Ectoloph length	50
				Maximum width	44
			Right	Ectoloph length	51
				Maximum width	45
		M3	Left	Ectoloph length	63
				Maximum width	41
			Right	Ectoloph length	64
				Maximum width	41
		Diastema I2–C	Left	Length	51
			Right	Length	51
		Upper molar row	Left	Length	150
		i1	Left	Length	21
				Width	17
		i3	Left	Length	39
				Width	25

TABLE 6. (*Continued*)

Taxon	Specimen	Feature	Side	Measurement	Value
			Right	Length	40
				Width	24
		p1	Left	Length**	14
				Width**	9
		p2	Left	Length**	19
				Width**	22
		p3	Left	Length	22
				Width	16
			Right	Length	22
				Width	16
		m1	Left	Length	42
				Talonid width	17
			Right	Length	43
				Talonid width	21
		m2	Left	Length	42
				Trigonid width	18
				Talonid width	15
			Right	Length	41
				Trigonid width	18
				Talonid width	15
		m3	Left	Length	59
				Trigonid width	17
				Talonid width	11
			Right	Length	59
				Trigonid width	17
				Talonid width	12
		Lower molar row	Left	Length	14.6
			Right	Length	14.5
	AMU-CURS 70	m3	Left	Length	49.9
				Trigonid width	13.4
				Talonid width	9.2
Falcontoxodon aff. *F. aguilerai*	AMU-CURS 585	C	Right	Maximum length	21.6
				Maximum width	15.6
		P2	Left	Maximum length	14.9
				Maximum width	16.7
		P3	Left	Maximum length	16.3
				Maximum width	18.0
		P4	Left	Maximum length	26.0
				Maximum width	21.5
		M1	Left	Ectoloph length	44.4
				Maximum width	23.5

TABLE 6. (*Continued*)

Taxon	Specimen	Feature	Side	Measurement	Value
		M2	Left	Ectoloph length	47.2
				Maximum width	22.6
		M3	Left	Ectoloph length	54.6
				Maximum width	25.1
		Diastema	Right	Length	88.0
		Upper molar row	Left	Length	115.9
Falcontoxodon sp.	AMU-CURS 69	m1	Left	Length*	34.4
				Talonid width	12.0
		m2	Left	Length	36.1
				Trigonid width	13.3
				Talonid width	11.4
		m3	Left	Length	48.3
				Trigonid width	12.7
				Talonid width*	9.3
		Lower molar row	Left	Length	119.0
	AMU-CURS 270	m3	Left	Length	44.5
				Trigonid width	13.0
				Talonid width	8.7

Falcontoxodon aff. *F. aguilerai*

Referred Material. AMU-CURS 585, maxilla with left M3–P2 and right I2.

Locality and Horizon. Norte Casa Chiguaje, Vergel Member, San Gregorio Formation, Urumaco, Falcón State, Venezuela. 11°17′52.5″N 070°14′11.1″W (Figure 4a,b).

Description In AMU-CURS 585 the skull is pyriform in ventral view and the infraorbital foramen is separated from the zygomatic arch (Figure 17a,b), as in *F. aguilerai*. Only the zygomatic process of the maxilla is preserved, which is dorsal to the M3. The I3 and C are absent, as in *Hoffstetterius*, *Posnanskytherium*, *Paratrigodon*, and some specimens of *Toxodon* (Forasiepi et al., 2015). In *F. aguilerai* the I3 is absent and the C is greatly reduced. The P1 is absent, unlike in *F. aguilerai*, and as in *Hoffstetterius*, *Trigodon*, and *Paratrigodon* (Saint-André, 1993; Forasiepi et al., 2015). There is a large diastema between the I2 and P2 (Figure 17b). The P2 is nearly square in cross section, it does not have a lingual fold or fossette, and it shows enamel bands on the labial and mesiolingual sides (Figure 17c,d).

In AMU-CURS 585 the lingual enamel fold is absent in P3 but present in P4, and there are labial and mesiolingual enamel bands in P3 and P4. These features are also seen in the P3–P4 of *F. aguilerai*. In addition, the upper molars of AMU-CURS 585 have a simple lingual fold, and the protoloph supports a lingual column only in M3, as in *F. aguilerai*. However, AMU-CURS 585 differs from *F. aguilerai* in the absence of C and P1. These characters suggest that AMU-CURS 585 represents a closely related but different taxon from *F. aguilerai*. However, in the absence of more complete material, we prefer to refer AMU-CURS 585 to *Falcontoxodon* aff. *F. aguilerai*, following the recommendations for open nomenclature of Bengtson (1988).

Falcontoxodon sp.

Referred Material. AMU-CURS 69, partial left mandible with m1–m3 (cast PIMUZ A/V 5285). AMU-CURS 77, upper right I2, right P2, right P3 and unidentified left upper tooth. AMU-CURS 270, partial right mandible with m3 (cast PIMUZ A/V 4786). AMU-CURS 542, right astragalus, metatarsals III–IV, and two phalanges (cast PIMUZ A/V 5287). AMU-CURS 544, mandibular symphysis and four isolated lower teeth fragments. AMU-CURS 548, left M1/M2. AMU-CURS 562, left metatarsal IV and metatarsals II–III. AMU-CURS 563, distal portion of humerus. AMU-CURS 570, upper right I2 fragment, two unidentified upper premolars and seven

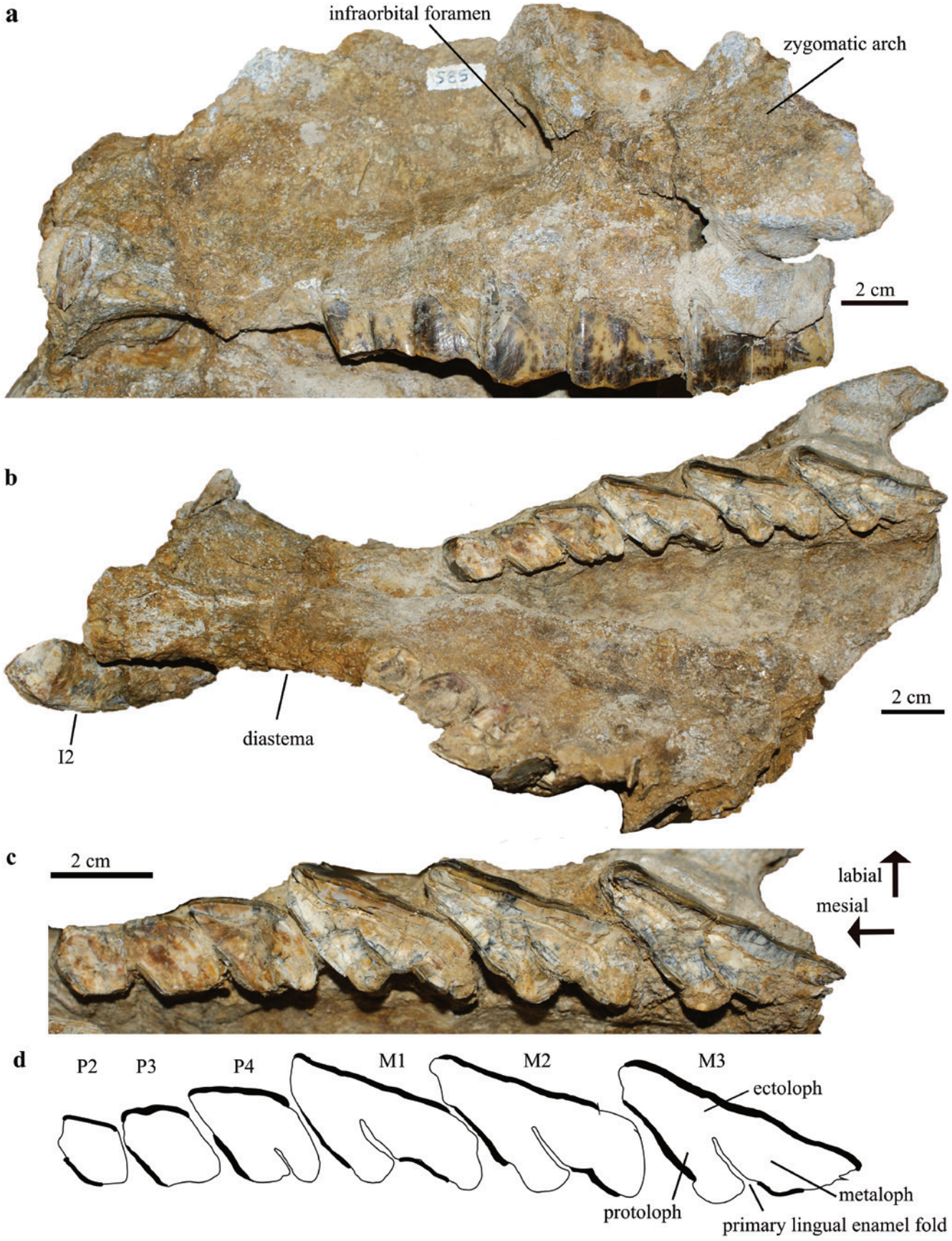

FIGURE 17. Partial skull of *Falcontoxodon* aff. *F. aguilerai* (AMU-CURS 585): (a) left lateral view; (b) ventral view; (c) detail of the upper left dentition in occlusal view; (d) schematic drawing of dentition: distribution of enamel is shown by thick lines.

teeth fragments. AMU-CURS 738, left calcaneus and three phalanges. AMU-CURS 739, partial m1/m2. AMU-CURS 741, right upper I2.

Locality and Horizon. Norte Casa Chiguaje, Vergel Member, San Gregorio Formation, Urumaco, Falcón State, Venezuela. 11°17′52.5″N 070°14′11.1″W (Figure 4a,b).

Description. In AMU-CURS 69 the m1 is not complete, but it shows lingual enamel extending mesially, reaching the meta-entoconid fold, as seen in *F. aguilerai* and in contrast to *Mixotoxodon,* where the lingual enamel does not extend mesially beyond the meta-entoconid fold. The lingual enamel of m2 does not extend distally to the hypoconulid, as in most Toxodontinae (Forasiepi et al., 2015). The m2 has a marked ento-hypoconulid fold and shallow meta-entoconid fold (Figure 18b), as in *Mixotoxodon* (Van Frank, 1957; Laurito, 1993; Rincón, 2011) and *F. aguilerai*. The m2 of AMU-CURS 69 differs from that of *F. aguilerai*, *Gyrinodon*, and *Mixotoxodon* in the presence of a mesial fossettid and distal fossettids (Figure 17b).

The m3 of AMU-CURS 69 and 270 have lingual enamel between the mesial fold and the hypoconulid. They show an open ento-hypoconulid fold, similar to the condition in *F. aguilerai*, *Gyrinodon* (Hopwood, 1928), and *Mixotoxodon* (Van Frank, 1957; Laurito, 1993; Rincón, 2011). The m3 of AMU-CURS 270 shows mesial, accessory, and distal fossettids (Figure 18g). Madden (1997) noted that during life the lower molar enamel folds can become isolated, forming fossettids, and eventually obliterate in individuals with advanced wear. In *Pericotoxodon* the ento-hypoconulid fold first becomes isolated and eventually wears away completely, and in an even more advanced stage the meta-entoconid fold becomes isolated as a fossettid.

Several isolated foot bones were recovered in the San Gregorio Formation. Among toxodontids, foot anatomy is best known for the Santacrucian *Nesodon imbricatus* (Figure 19) and *Adinotherium ovinum* (Scott, 1912), and for the Pleistocene *Toxodon platensis* (Owen, 1840). The right astragalus (AMU-CURS 542) from San Gregorio is comparable in size to that of *Nesodon,* larger than in *Adinotherium*, and smaller than in *Toxodon* (Table 7). AMU-CURS 542 has a shallow trochlear groove (Figure 20a), which is deeper in *Nesodon* (Figure 20c), and shallower in *Toxodon* (Figure 20e). The neck is very short (Figure 20a), similar to *Toxodon* (Figure 20e), and somewhat less defined than in *Nesodon* (Figure 20c). The medial tibial facet is expanded medially, forming a tuberosity (Figure 20a), which is absent in *Nesodon* (Figure 20c) and less developed in *Toxodon* (Figure 20e). In plantar view, the sustentacular and navicular facets are connected (Figure 20b), whereas in *Nesodon* and *Toxodon* they are separate (Figure 20d, f). The navicular facet is larger than the sustentacular facet, as in other toxodontids. In *Nesodon,* the navicular facet reaches the distal plane and it can be observed in dorsal view (Figure 20c), whereas in AMU-CURS 542 and *Toxodon*, it is restricted to the plantar plane. The ectal facet is concave and elongate. The PCA of toxodontid astragalar measurements (Table 7) roughly differentiates the four taxa, *Adinotherium*, *Nesodon*, *Toxodon*, and *Falcontoxodon* (Figure 21a). They are mainly separated along the PC1, which correlates with size, with the smaller *Adinotherium* toward the negative values, the larger *Toxodon* toward the positive values, and *Nesodon* and *Falcontoxodon* in between.

The left calcaneus of *Falcontoxodon* (AMU-CURS 738) is of comparable length but wider, and somewhat more robust, than the calcanei of *Nesodon*. It is smaller than the calcaneus of *Toxodon* (Table 8; Figure 22a–h). In *Falcontoxodon* the cuboid facet is wider than in *Nesodon*. The ectal facet is approximately perpendicular to the fibular facet, and the sustentacular facet is inclined anteromedially (Figure 22a). AMU-CURS 542 and 562 include tarsals consisting of a fragment of metatarsal II, and complete metatarsals III (Figure 22i–k) and metatarsal IV (Figure 22 l–n). Overall, they are comparable in length and width to those of *Nesodon*, and much smaller than in *Toxodon* (Table 8).

Toxodontinae indet.

Referred Material. MUN-STRI 13103, lower molar fragment. MUN-STRI 13118, upper molar fragment. MUN-STRI 34153, upper molar fragment. MUN-STRI 34168, lower molar fragment. MUN-STRI 34178, molar fragments. MUN-STRI 34184, molar fragments. MUN-STRI 34189, lower molar fragment. MUN-STRI 34353, lower incisor fragment. MUN-STRI 37507, lower molar fragment; MUN-STRI 37561, lower molar fragment; MUN-STRI 44459, partial palate with I3.

Locality and Horizon Ware Formation, Police Station. MUN-STRI 13103 and MUN-STRI 13118 come from STRI locality 390020; MUN-STRI 34153 and MUN-STRI 34168 come from STRI locality 470061; MUN-STRI 34178, MUN-STRI 34184, MUN-STRI 34189, MUN-STRI 34353 and MUN-STRI 44459 come from STRI locality 470060; MUN-STRI 37507 comes from STRI locality 470062; MUN-STRI 37561 comes from STRI locality 470059; (Figure 3).

Description. The isolated teeth are upper molars (Figure 23). The enamel is not well preserved (Figure 23b). They have a simple primary lingual enamel fold, which separates the protoloph from the metaloph (Figure 23a), as in *Falcontoxodon,* some specimens of *Pericotoxodon* with an advanced stage of dental wear (Madden, 1997), *Andinotoxodon* (Madden, 1990), *Mixotoxodon* (Laurito, 1993), *Piauhytherium* (Guérin and Faure, 2013), and *Gyrinodon* (Figure 15d). The protoloph does not support a lingual column (Figure 23a); the metaloph is broad and does not taper distally, as in *Falcontoxodon* and most specimens of *Pericotoxodon* (Madden, 1997).

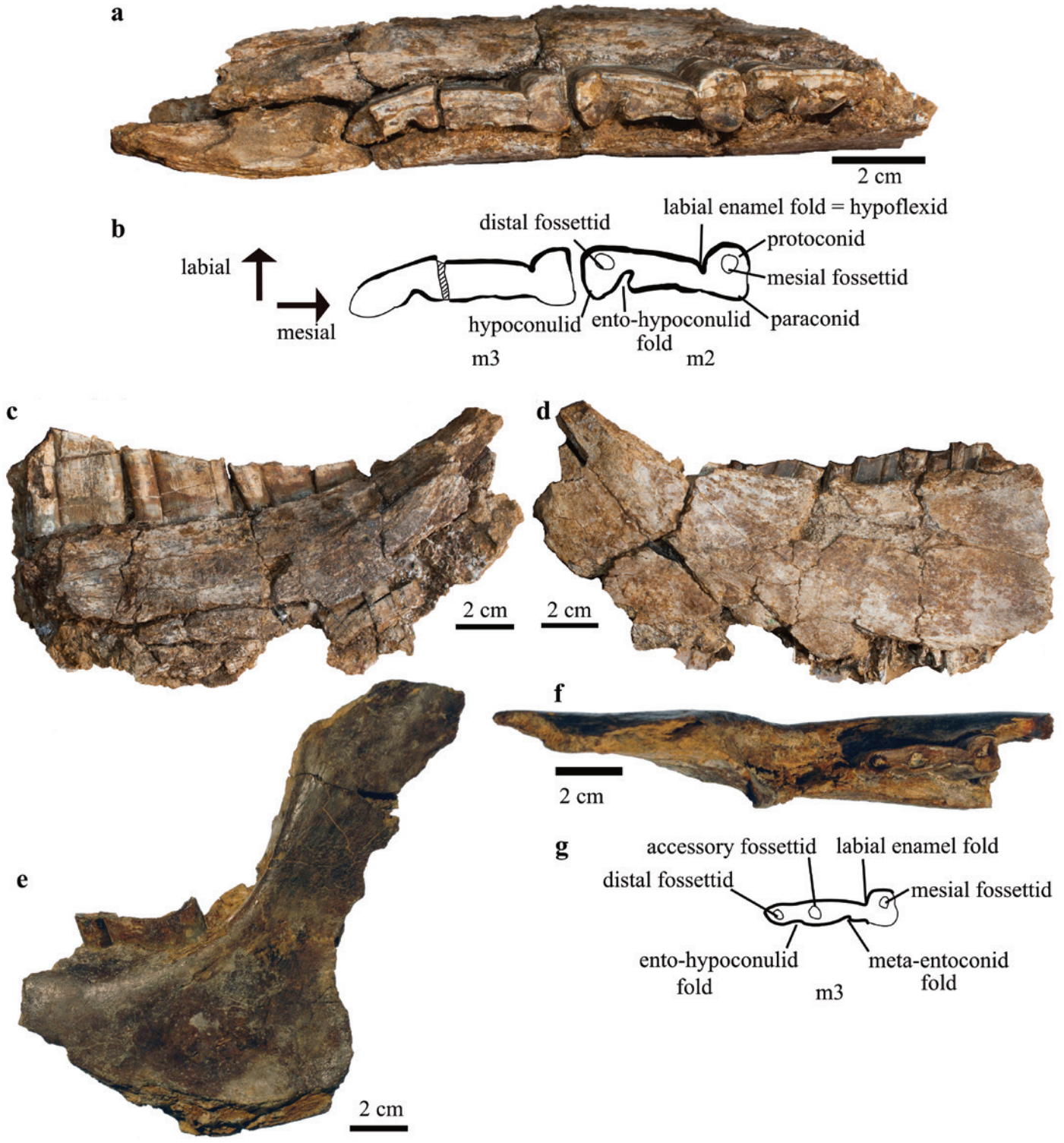

FIGURE 18. Partial mandibles of *Falcontoxodon* sp.: (a) left mandible (AMU-CURS 69), in occlusal view; (b) schematic drawing of m2 and m3 of AMU-CURS 69: distribution of enamel is shown by thick lines; (c) AMU-CURS 69 in lateral view; (d) AMU-CURS 69 in medial view; (e) left partial mandible (AMU-CURS 270) in lateral view; (f) AMU-CURS 270 in occlusal view; (g) schematic drawing of the m3 of AMU-CURS 270: distribution of enamel is shown by thick lines.

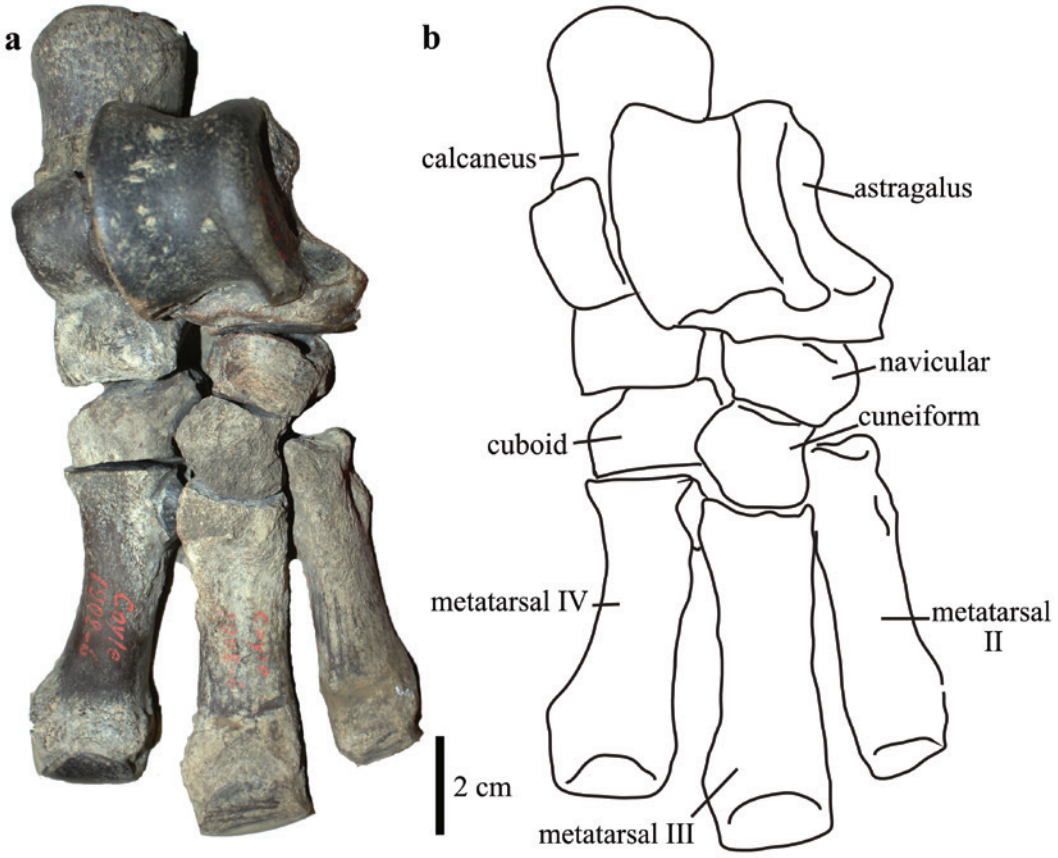

FIGURE 19. Right foot (without phalanges) of *Nesodon imbricatus* (Toxodontidae) (MNHN F SCZ 212) from the Santa Cruz Formation (Santacrucian SALMA) in Argentina: (a) articulated right foot in dorsal view; (b) schematic drawing of foot.

TABLE 7. Astragalar measurements (mm) of toxodontids. Measurements follow those of Tsubamoto (2014: fig. 1). Li1 = transverse width of the tibial trochlea; Li2 = proximodistal length of the lateral trochlear ridge of the tibial trochlea; Li3 = proximodistal length of the medial trochlear ridge of the tibial trochlea; Li4 = transverse width of the astragalus; Li5 = proximodistal length of the astragalus; Li6 = proximodistal length of the central part of the tibial trochlea; Li7 = transverse width between the medial and lateral trochlear ridges of the tibial trochlea; Li8 = dorsoventral thickness of the lateral part of the astragalus; Li9 = dorsoventral thickness of the medial part of the astragalus. Measurements are shown in Figure 21b.

Taxon	Specimen	Li1	Li2	Li3	Li4	Li5	Li6	Li7	Li8	Li9
Adinotherium sp.	MLP 67-XII-8-1	18.0	21.6	20.9	24.2	27.0	17.0	14.7	14.6	21.3
	MLP 67-XII-8-2	23.8	33.6	29.7	32.8	34.4	24.8	20.3	24.2	34.4
Nesodon imbricatus	MNHN SCZ 1902-6	34.08	45.1	43.81	54.13	56.79	35.27	27.69	33.5	43.08
	MNHN SCZ 30	35.62	42.31	43.25	47.1	48.25	32.07	26.19	30.08	35.17
	NHM UK M 96594	32	41.3	41.5	48.9	48.8	35.1	25	28.3	42.4
	NHM UK M5475	31.9	41.9	41.6	49.3	48.2	34.5	27.9	22.7	37.7
Toxodon platensis	MNHN PAM 284	58.33	67.22	60.72	83.68	66.55	48.3	53.01	36.44	59.03
	NHM UK M 5486	63	69.4	58.1	86.6	67.2	50.4	56	36	56.1
Falcontoxodon sp.	AMU-CURS 542	40.3	45.2	44.1	60.9	51.3	36.7	34	31.2	38.1

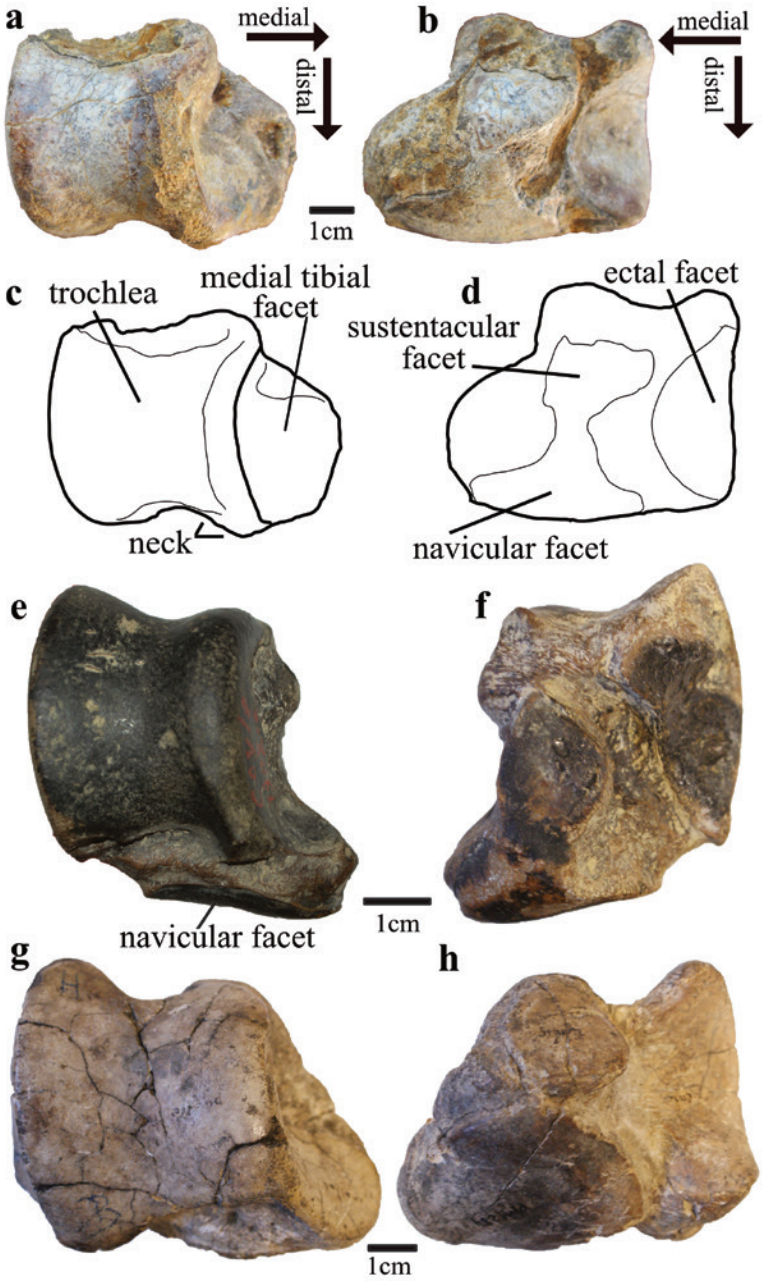

FIGURE 20. Toxodontid astragali: (a) *Falcontoxodon* sp. (gen. nov.), right astragalus (AMU-CURS 542) in dorsal view; (b) AMU-CURS 542 in plantar view; (c) schematic drawing of AMU-CURS 542 in dorsal view; (d) schematic drawing of AMU-CURS 542 in plantar view; (e) *Nesodon imbricatus,* right astragalus (MNHN F SCZ 212) in dorsal and (f) plantar view; (g) *Toxodon platensis,* right astragalus (MNHN PAM 284) in dorsal and (h) plantar view.

Body Mass Estimation

The different craniodental measurements (Table 9) yielded body mass estimates for *F. aguilerai* that range from 616 to 1075 kg (Table 10). The arithmetic mean is 796 kg. The mean minimum estimate, taking into account the percentage of error, is 735 kg, and the maximum is 946 kg.

Phylogenetic Analysis of Toxodontidae

The parsimony analysis with extended implied weighting resulted in nine most parsimonious trees of 268 steps, with a consistency index of 0.507 and retention index of 0.641. In the strict consensus (Figure 24a), the clade Toxodontidae has a bootstrap value of 0.62 and is supported by two unambiguous

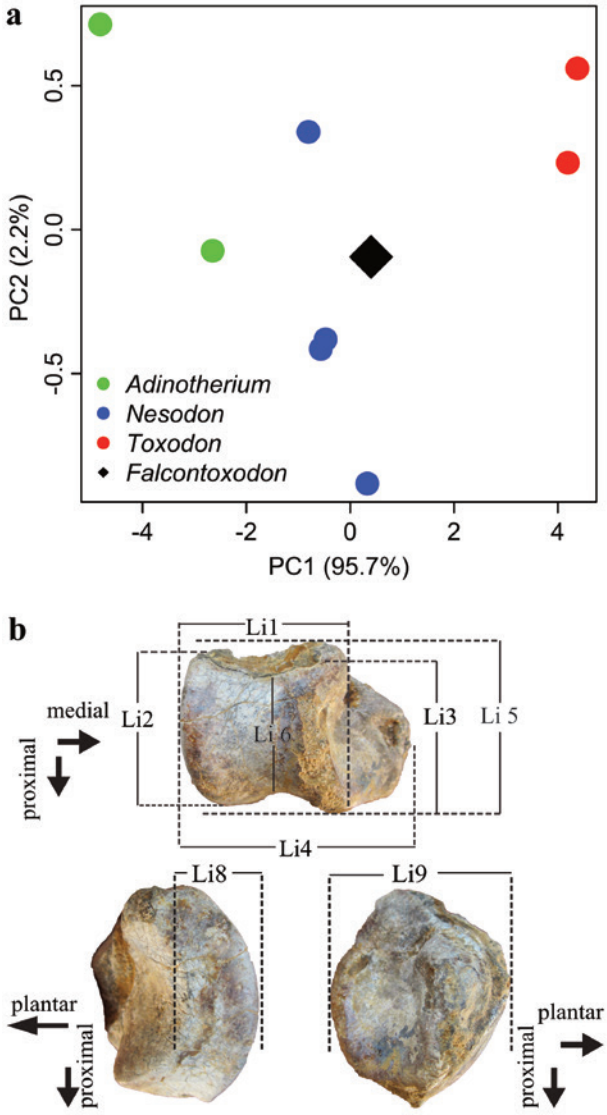

FIGURE 21. Astragalar morphospace in selected toxodontids: (a) bivariate plot of the first two principal components of the PCA; (b) linear measurements follow Tsubamoto (2014).

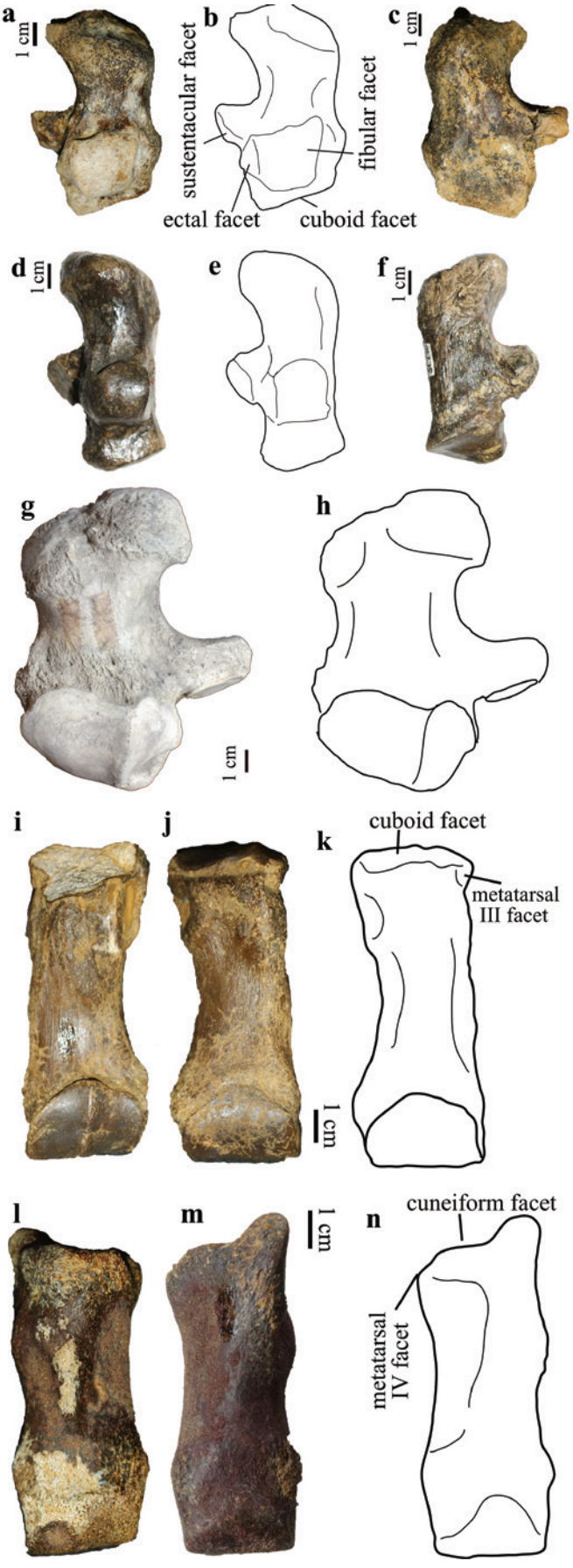

FIGURE 22. Toxodontid calcanei and metatarsals. Left calcaneus of *Falcontoxodon* sp. (gen. nov.) (AMU-CURS 738): (a) photograph and (b) schematic drawing in dorsal view; (c) plantar view. Left calcaneus of *Nesodon imbricatus* (MNHN SCZ 30): (d) photograph and (e) schematic drawing in dorsal view; (f) plantar view. Right calcaneus of *Toxodon platensis* (MHMUK PV M 5486): (g) photograph and (h) schematic drawing in dorsal view. Metatarsals of *Falcontoxodon* sp. (gen. nov.) (AMU-CURS 542). Left metatarsal III: (i) plantar view; (j) photograph and (k) schematic drawing in dorsal view. Left metatarsal IV: (l) plantar view; (m) photograph and (n) schematic drawing in dorsal view.

TABLE 8. Measurements (in mm) of the calcaneus and metatarsals of toxodontids. Mt = Metatarsal. A dash (-) indicates data not available.

Taxon	Specimen	Element	Length	Distal width	Proximal width
Falcontoxodon sp.	AMU-CURS 542	Mt IV	93	39	39.5
		Mt III	70.6	29.7	27.6
	AMU-CURS 562	Mt IV	91.4	46.8	39.8
		Mt III	-	42.7	-
		Mt II	-	32	-
	AMU-CURS 738	Calcaneus	88.8	46.7	46.4
Nesodon imbricatus	MNHN SCZ 30	Mt IV	77.3	28.8	32
		Mt III	82.8	29.9	29.7
		Calcaneus	87.9	34.3	40
	MNHN SCZ 212	Mt IV	78.9	27	31.7
		Mt III	83.7	28.9	25
		Calcaneus	82.7	31	35.3
	NHM UK M96586	Calcaneus	88.2	33.6	38
	NHM UK M96585	Calcaneus	87.9	32.3	43.2
Toxodon platensis	NHM UK M 5487	Mt III	160	78.8	72.7
	NHM UK M 5486	Calcaneus	133	67.2	73.9

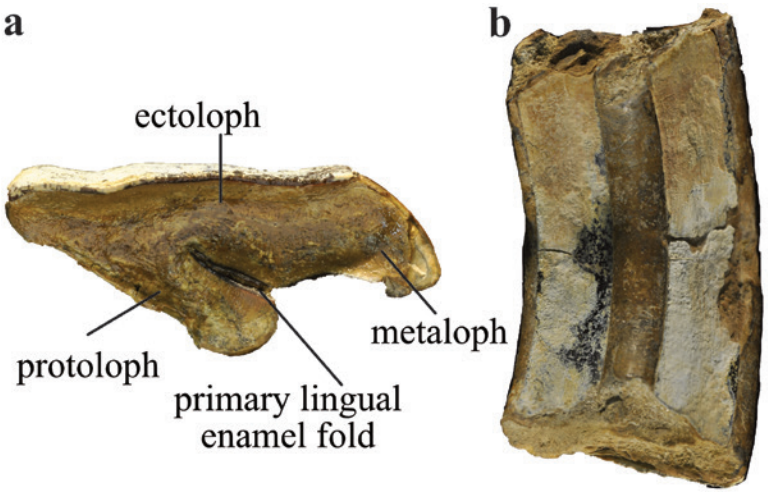

FIGURE 23. Toxodontinae indet. left M1 or M2 from Ware Formation. (a) Occlusal and (b) lingual view.

synapomorphies: i1 that is triangular in cross section (36[1]) and lingual enamel of i3 that is narrower than the labial enamel (40[3]). *Proadinotherium* is hypothesized as being the sister taxon of all the other toxodontids (Figure 24a). The Nesodontinae comprises *Adinotherium* and *Nesodon* (Figure 24a), and is supported by one unambiguous synapomorphy, the symphysis without a well-differentiated chin angle (16[0]). The clade Toxodontinae has a bootstrap value of 0.96 (Figure 24a) and is supported by ten unambiguous synapomorphies: short sagittal crest (4[1]), hypselodont cheek teeth (19[2]), molars without fossettes (29[1]), M1–M2 with distal groove/fossette smooth or absent (31[1]), M3 with groove smooth or absent (32[1]), lingual enamel extending distally to the posterior groove (33[1]), the mesial fold of m1–m2 at the same level as the labial fold (49[1]), m1 with lingual enamel between the anterior fold and the hypoconulid (55[1]), lingual enamel of m2 restricted between the mesial fold and the hypoconulid (56[1]), and lingual enamel of m3 reaching the level of the hypoconulid (57[1]).

TABLE 9. Cranial and mandibular measurements (mm) of *Falcontoxodon aguilerai* sp. nov. (holotype, AMU-CURS 765).

Variable	Acronym	Definition	Value	Reference
Lower premolar row length	LPRL	Measured along the base of the teeth	96	Janis (1990)
Lower molar row length	LMRL	Measured along the base of the teeth	148	Janis (1990)
Anterior jaw length	AJL	Measured from the boundary between p4 and m1 to the base of i1	164	Janis (1990)
Posterior jaw length	PJL	Measured as the horizontal distance from the back of the condyle to distal border of m3	150	Janis (1990)
Depth of mandibular angle	DMA	Measured from the top of the condyle to the deepest point of the mandibular angle	344	Janis (1990)
Maximum width of mandibular angle	WMA	Measured from the junction of the distal part of m3 with the dentary to the most distant point on the mandibular angle	199	Janis (1990)
Length of coronoid process	JD	Measured as the vertical distance from the base of the condyle to the tip of the coronoid process	35	Mendoza et al. (2006)
Length of ridge for masseteric attachment	MFL	Measured from the posterior portion of the glenoid to the most anterior extent of the scar for the origin of the masseter muscle	190	Janis (1990)
Posterior skull length	PSL	Measured from the occipital condyle to the distal edge of M3	240	Janis (1990)
Depth of face under orbit	SD	Measured from the boundary between premolar and molar tooth rows to the nearest point of the orbit	125	Mendoza et al. (2006)
Muzzle width	MZW	Measured between the most lateral points between the maxilla and premaxilla contact	100	Janis (1990)
Basicranial length	BCL	Measured from the ventral edge of the foramen magnum to the point of the basicranium where a change in angulation occurs between the basicranium and the palate	235	Janis (1990)
Total jaw length	TJL	TJL = PJL + LMRL + AJL	462	Janis (1990)
Total skull length	TSL	TSL = PSL + LMRL + AJL	552	Janis (1990)

TABLE 10. Body mass (BM) estimates (kg) for *Falcontoxodon aguilerai* sp. nov. (holotype, AMU-CURS 765) using the multivariate regression functions from Mendoza et al. (2006). RPE = range of PE; PE = Percent of error. See Table 9 for definitions of acronyms used in the equations.

Algorithm or statistic	Equation	Adj. R^2	% RPE	mid % PE	BM	BM + mid PE	BM – mid PE
2.1	ln BM = –1.602 * ln(LMRL) + 2,791 * ln(SLML) + 0.576 * ln(JLB) + 1.005 * ln(JMA) + 2.402	0.99	13.5–15	14.25	616	704	607
2.2	ln BM = –1.352 * ln(LMRL) + 2.434 * ln(SLML) + 0.587 * ln(JLB) + 0.866 * ln(JMA) + 0.263 * ln(JMC) + 1.890	0.99	13.5–15	14.25	674	770	578
2.3	ln BM = –1.366 * ln(LMRL) + 2.421 * ln(SLML) + 0.542 * ln(JLB) + 1.017 * ln(JMA) + 0.716 * ln(JMC) – 0.509 * ln(JMB) + 2.006	0.99	13.5–15	14.25	608	695	521
3.1	ln BM = 1.119 * ln(LMRL) + 0.210 * ln(LPRL) + 0.730 * ln(JMA) + 0.637 * ln(JMC) + 0.181 * ln(JD) + 0.619	0.98	21–25	23	1,075	1,322	1,018
3.2	ln BM = 1.0 * ln(LMRL) + 0.176 * ln(LPRL) + 0.823 * ln(JMA) + 0.968 * ln(JMC) + 0.167 * ln(JD) – 0.331 * ln(JMB) + 0.573	0.98	21–25	23	1,006	1,237	952
Mean					796	946	735

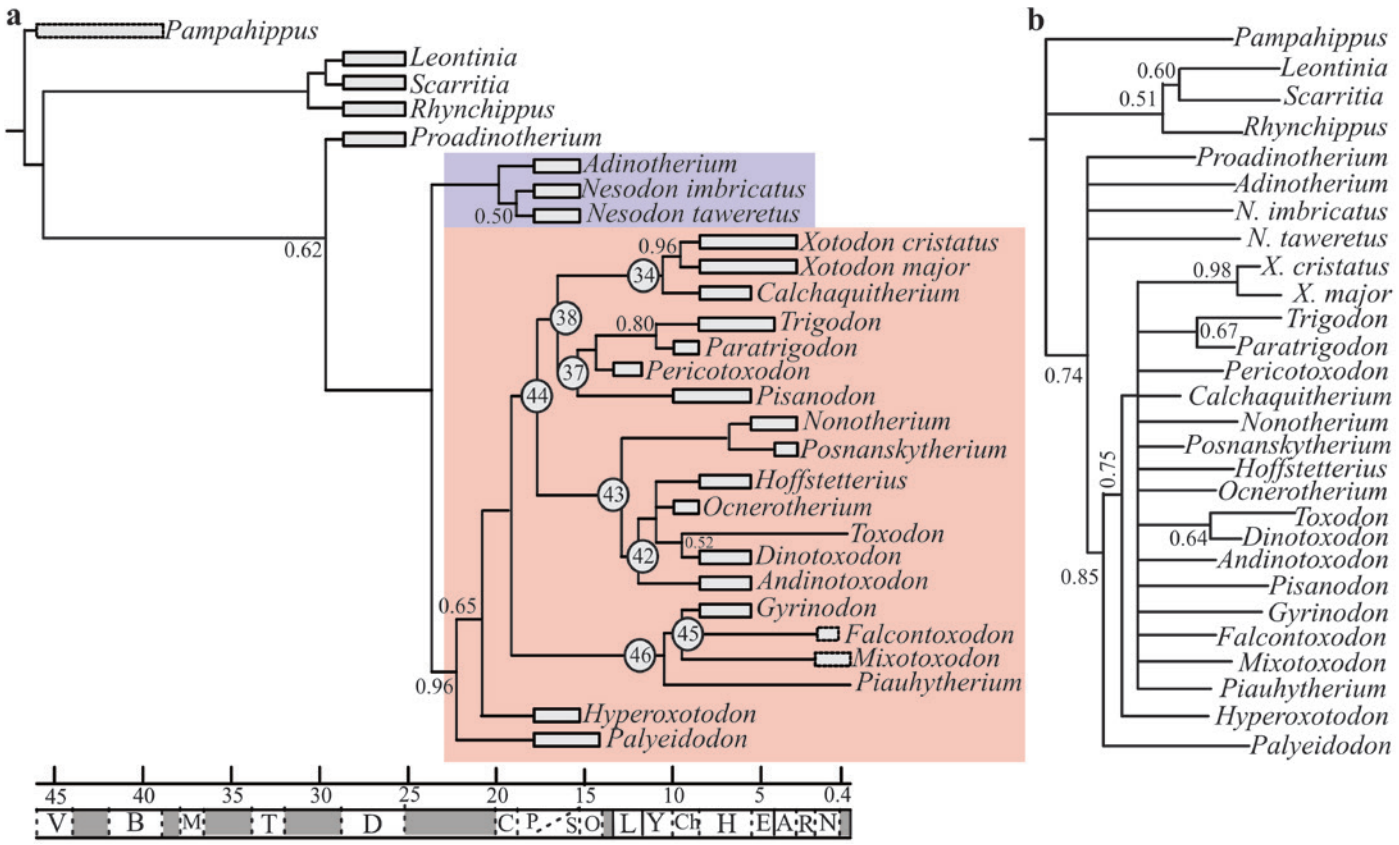

FIGURE 24. Hypothesis of phylogenetic relationships within Toxodontidae. (a) Time calibrated topology of the most parsimonious tree resulting from an analysis with PAUP using implied weighting (k = 3). Bootstrap values higher than 0.50 are indicated for several nodes. Numbers within circles designate nodes discussed in the text. Blue shading = Nesodontinae, red shading = Toxodontinae. Letters below time line (MYA) denote SALMAs (from left to right): V = Vacan; B = Barrancan; M = Mustersan; T = Tinguirican; D = Deseadan; C = Colhuehuapian; P = "Pinturan"; S = Santacrucian; O = Colloncuran; L = Laventan; Y = Mayoan; Ch = Chasicoan; H = Huayquerian; E = Montehermosan; A = Chapadmalalan; R = Marplatan; N = Ensenadan. (b) Strict consensus of the 12 most parsimonious trees resulting from the analysis of the same data matrix but without using character weighting. Bootstrap values higher than 0.50 are indicated for several nodes.

Palyeidodon is the first taxon to diverge within Toxodontinae, followed by *Hyperoxotodon* (Figure 24a). The remaining Toxodontinae are divided into two main clades: nodes 44 and 46. Node 44 is supported unambiguously by a P2 without groove or fossette (25[1]). It comprises two clades: nodes 38 and 43 (Figure 24a). Node 38 comprises two groups: one (node 34) consists of (*Calchaquitherium* [*Xotodon major*, *Xotodon cristatus*]) and it is supported unambiguously by a mandibular symphysis with a median ventral keel (15[1]), upraised mandibular symphysis and lower incisors (18[2]), smooth or absent labial groove in p2–m4 (45[1]), and a smooth or absent entohypoconulid fold in m3 (53[1]). The second group (node 37) consists of (*Pisanodon* [*Pericotoxodon* (*Paratrigodon*, *Trigodon*)]), and is supported unambiguously by the presence of I3 (22[0]), the absence of enamel in P1 (24[1]) and upper molars with median crista and an incipient median valley (30[1]). Node 43 comprises two groups (Figure 24a). One includes *Nonotherium* and *Posnanskytherium* and it is supported by a very concave ectoloph (34[1]). The second group (node 42) consists of (*Andinotoxodon* [*Hoffstetterius*, *Ocnerotherium*, (*Toxodon*, *Dinotoxodon*)]), and is supported by a straight alveolar border of the symphysis (14[1]).

Within Toxodontinae, node 46 (Figure 24a) groups the clade (*Piauhytherium* [*Mixotoxodon*, *Falcontoxodon*, *Gyrinodon*]), which is supported by a rounded posteroventral border of the vertical mandibular ramus (12[0]), mandibular symphysis without a well-differentiated angle (16[0]), absence of lower canines (41[1]) and absence of lingual enamel in p2–p4 (44[2]).

The Venezuelan toxodontids form a clade (node 45; Figure 24a) supported by a smooth or absent ento-hypoconulid fold in m3 (53[1]) and the presence of a deep and narrow labial groove in the molars (54[2]).

The analysis using equal weights yielded 193 most parsimonious trees of 264 steps, with a consistency index of 0.515 and retention index of 0.652. In the strict consensus (Figure 24b), Toxodontinae has a bootstrap value of 0.85, and is supported by the following unambiguous synapomorphies: short sagittal crest (4[1]), mandibular symphysis with smooth chin angle (16[1]), euhypsodont cheek teeth (19[2]), molars without fossettes (29[1]), upper molars without a groove, or if present being smooth (31[1] and 32[1]), lingual enamel in M3 extending distally to the distal groove (33[1]), the mesial fold in m1–m2 at the same level as labial fold (49[1]), the lingual enamel of m1 (55[1]) and m2 (56[1]) between the mesial fold and the hypoconulid, and the lingual enamel of m3 reaching the level of the hypoconulid (57[1]). In this analysis Nesodontinae was not recovered as monophyletic (Figure 24b). Within Toxodontinae, *Palyeidodon* is the first taxon to diverge, followed by *Hyperoxotodon*. The remaining taxa form a clade which is not well resolved. It includes the clades (*Xotodon cristatus, Xotodon major*), (*Toxodon*, *Dinotoxodon*) and (*Trigodon*, *Paratrigodon*) in a polytomy with the other toxodontinaes (Figure 24b).

Litopterna (Ameghino, 1889)

Proterotheriidae (Ameghino, 1887)

Lambdaconus (Ameghino, 1897)

Type Species. *Lambdaconus suinus* (Ameghino, 1897).

Lambdaconus cf. *L. colombianus* (Hoffstetter and Soria, 1986) comb. nov.

=*Neodolodus colombianus* (Hoffstetter and Soria, 1986) by original designation.

=*Prothoatherium colombianus* (Cifelli and Guerrero, 1989) comb. nov.

Referred Material. MUN-STRI 16716, a left dentary with the alveolus of p3 and m2, and the p4, m1 and m3 (cast PIMUZ A/V 5291).

Locality and Horizon. Makaraipao, Castilletes Formation. STRI locality 930093; 11.9089°N, 71.3401°W (Figure 3).

Description. The partial mandible preserves part of the alveolus of p3, the p4, m1, the alveolus of m2, and a fragment of m3 (Figure 25a–d). The teeth are brachyodont, bicrescentic, and very low crowned (Figure 25a), as in *Lambdaconus colombianus* (Hoffstetter and Soria, 1986; Cifelli and Guerrero, 1989). The cheek teeth have four roots (Figure 25b,d). The lophs are not well defined (Figure 25b) due to the low crown height and wear, as in *L. colombianus* (Cifelli and Guerrero, 1989).

Lambdaconus colombianus was described by Hoffstetter and Soria (1989) on the basis of a partial mandible with worn lower dentition. These authors considered that the taxon represented a new genus and species (*Neodolodus colombianus*), and referred it to Didolodontidae. Cifelli and Guerrero (1989) transferred the taxon to *Prothoatherium* (Proterotheriidae, Litopterna) and assigned the new combination of *Prothoatherium colombianus*. *Prothoatherium* was named by Ameghino (1902), who recognized two species and later added a third one (Ameghino, 1904). Soria (2001) did not recognize *Prothoatherium* as valid, and transferred one species to *Lambdaconus* (*L. lacerum*) and established the other two as synonyms of *Paramacrauchenia scammata* (=*Prothoatherium scammatum* [partim] and *Prothoatherium plicatum*) and *Paramacrauchenia inexpectata* (=*Prothoatherium scammatum* [partim]). Soria died in 1989, and his dissertation (published posthumously in 2001) made no mention of *Lambdaconus (=Prothoatherium) colombianus*.

Based on the descriptions of Hoffstetter and Soria (1986) and Cifelli and Guerrero (1989), we consider that *L. colombianus* belongs to *Lambdaconus* and not to *Paramacrauchenia*. *L. colombianus* shows some diagnostic characters of *Lambdaconus* as revised by Soria (2001), including the following: m1–m3 without paraconid and with entoconid (Hoffstetter and Soria, 1986; Cifelli and Guerrero, 1989), P4–M3 with metaconule, and M3 with a reduced hypocone (Cifelli and Guerrero, 1989). In contrast, in *Paramacrauchenia* the P4 does not have a metaconule, in the M1–M2 the metaconule is reduced and associated with the hypocone, and the M3 does not have a hypocone (Soria, 2001).

In *Lambdaconus* cf. *L. colombianus* (MUN-STRI 16716), the p4 is molariform and narrows mesially in occlusal view (Figure 25d). It measures 12.4 mm in mesiodistal length and 8.5 mm in labiolingual width. The ectoflexid is shallow and the paraconid is reduced (Figure 25d). There is no evidence of labial or lingual cingula (Figure 25a,c), which are present in *L. colombianus* and poorly developed or absent in *L. lacerum* (Cifelli and Guerrero, 1989; Soria, 2001; Kramarz and Bond, 2005). The p4 has a hypoconulid, unlike in *Megadolodus* where it is absent (Cifelli and Villarroel, 1997). The p4 and m1 have a well-developed hypoconid, and the metaflexid and entoflexid are present (Figure 25d).

The m1 measures 13.5 mm in mesiodistal length and 9.8 mm in labiolingual width. The protoconid and metaconid are well developed, as in *L. colombianus* (Hoffstetter and Soria, 1986). The paraconid is present, unlike in *Prolicaphrium* and *Megadolodus* (Cifelli and Guerrero, 1997; Cifelli and Villarroel, 1997). The ectoflexid is deep and the hypoconid is well

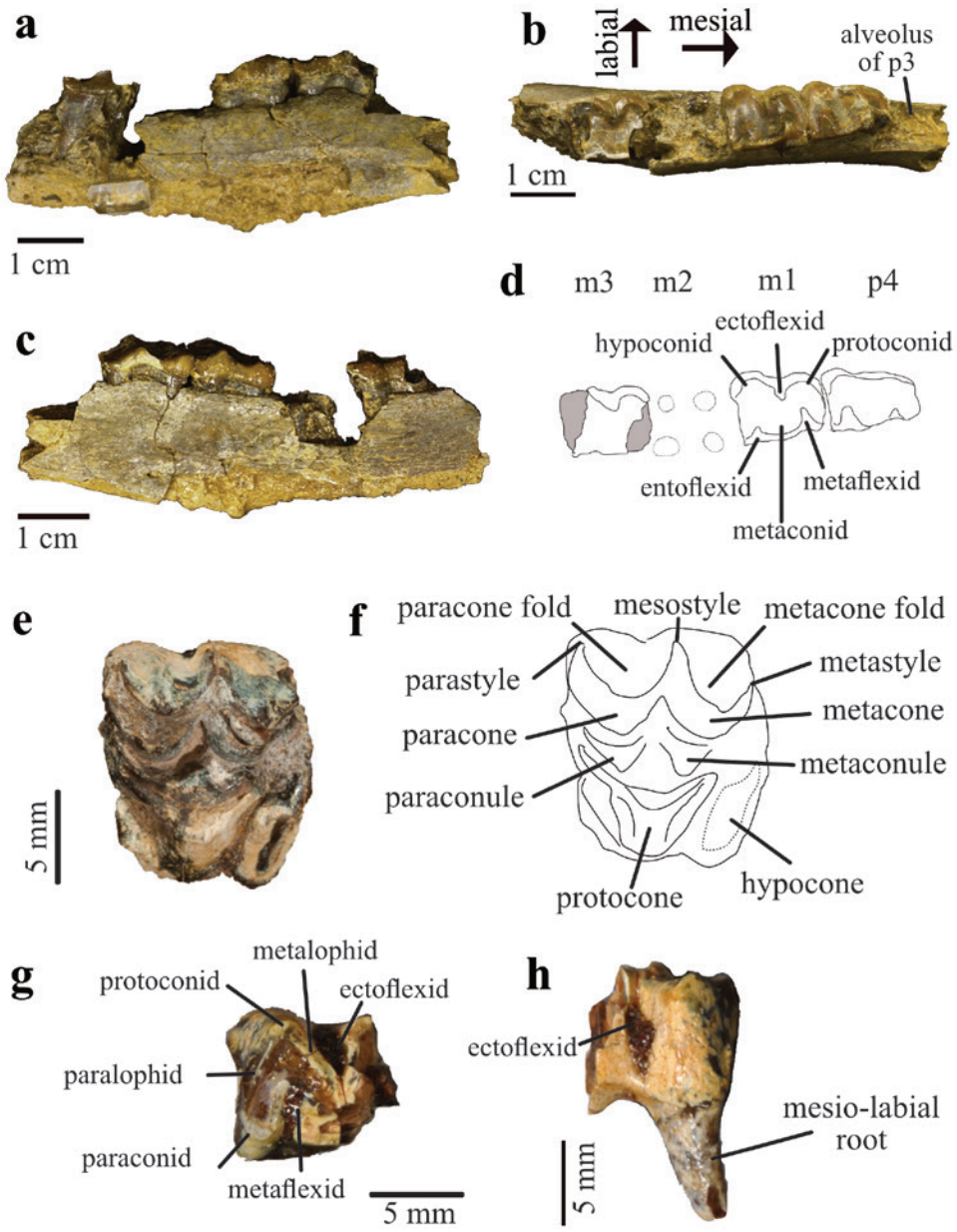

FIGURE 25. Proterotheriidae (Litopterna) from the Cocinetas Basin. *Lambdaconus* cf. *L. colombianus*, left dentary (MUN-STRI 16716) from the Castilletes Formation: (a) lingual, (b) occlusal, and (c) labial views; (d) schematic drawing of dentition in occlusal view. Proterotheriidae indet. from the Ware Formation. Left M1 or M2 (MUN-STRI 34170) in occlusal view: (e) photograph and (f) schematic drawing. Fragment of right lower molar (MUN-STRI 16289) in (g) occlusal and (h) labial views.

developed, with a marked crescent shape, as in *L. colombianus* (Hoffstetter and Soria, 1986). The entoconid and hypoconulid are undifferentiated, due to wear (Figure 25d). The alveolus of the m2 accommodates four roots (Figure 25b,d). The crown of the m3 is broken, missing distal and mesiolingual portions (Figure 25d). It measures 97 mm in labiolingual width, and it has a deep ectoflexid. MUN-STRI 16716 differs from *Megadolodus* (McKenna, 1956; Cifelli and Villarroel, 1997) in having less bunodont and more rectangular molars, having a paraconid, and lacking cingula.

PROTEROTHERIIDAE INDET.

REFERRED MATERIAL. MUN-STRI 13119, diaphysis and distal epiphysis of left humerus. MUN-STRI 13120, right ulna. MUN-STRI 13121, left metacarpal III. MUN-STRI 16289, fragment of lower molar. MUN-STRI 19544, right calcaneus. MUN-STRI 34170, M1/M2. MUN-STRI 34185, partial mandible with fragment of left m2. MUN-STRI 34348, distal fragment of metapodial. MUN-STRI 34372, diaphysis and distal epiphysis of left humerus. MUN-STRI 34641, left M2. MUN-STRI 37753,

metapodial. AMU-CURS 745, epiphysis of metacarpal III. AMU-CURS 746, left metacarpal III.

Locality and Horizon. Police Station, Ware Formation; 11.8487°N, 71.3243°W. MUN-STRI 13119, 13120, 13121 come from STRI locality 390020. MUN-STRI 19544 comes from STRI locality 390018. MUN-STRI 16289 comes from STRI locality 430052. MUN-STRI 34170, MUN-STRI 34185, MUN-STRI 34348 and MUN-STRI 34641 come from STRI locality 470060. MUN-STRI 34372 comes from STRI locality 470061. MUN-STRI 37753 comes from STRI locality 470062. AMU-CURS 745 and 746 come from the Algodones Member, Codore Formation, 11°17′39.8″N, 70°14′15.6″W.

Description. The upper molar (MUN-STRI 34170) is brachyodont and quadrangular in occlusal view, suggesting that it represents an M1 or M2 (or a molarized P4). The M3 in proterotheriids has a distinctive outline in occlusal view; for example, in *Brachytherium* it is trapezoidal (Schmidt, 2015), and in *Villarroelia* it is more triangular (Cifelli and Guerrero, 1997). It has a mesiodistal length of 10.4 mm and a labiolingual width of 10.6 mm (Figure 25e). MUN-STRI 34170 is referred to a Proterotheriidae indet. based on its size, the bunoselenodont (Janis, 2000: fig. 7.2) condition and the position of the hypocone posterior to the paracone (Schmidt, 2013).

MUN-STRI 34170 differs from the megadolodine *Bounodus enigmaticus* (Carlini et al., 2006b) in having a more developed protocone, and the paracone positioned less mesially. The mesiolingual border of the crown is broken, and the presence of the mesiolingual cingulum cannot be evaluated. The protocone is the largest cusp (Figure 25f), as in *Brachytherium* (Schmidt, 2015). The hypocone is broken, but it appears to have been separated from the protocone by a distolingual groove, as in *Brachytherium*, *Proterotherium*, and *Prothoatherium* (Cifelli and Guerrero, 1989; Schmidt, 2015). The paraconule is not connected with the protocone by a loph, as it is in the Proterotheriinae (Schmidt, 2013). The metaconule is also an isolated cusp, as in *Prothoatherium* (Cifelli and Guerrero, 1989), and it is not reduced as in *Neolicaphrium* (Ubilla et al., 2011), or connected to the protocone, as in *Prolicaphrium* (Cifelli and Guerrero, 1997). The metaconule is located distal to the paraconule and mesiolingual to the hypocone (Figure 25f). MUN-STRI 34170 has three labial styles (Figure 25f), as in the Protherotheriinae (Schmidt, 2013). The mesostyle is well developed, as in *Villarroelia* (Cifelli and Guerrero, 1997), and as opposed to the reduced condition seen in *Neobrachytherium* (Schmidt, 2015). The paracone and metacone labial folds are well developed as in *Brachytherium* and *Proterotherium*, and unlike *Neobrachytherium* and *Thoatheriopsis* (Villafañe et al., 2012; Schmidt, 2015).

The lower molar fragment (MUN-STRI 16289) measures 8.2 mm in labiolingual width and 8.9 mm in crown height on the labial side. It preserves the mesial portion of the crown, with well-defined paralophid and metalophid (Figure 25g). The protoconid and paraconid are well developed, and the metaflexid and ectoflexid are deep (Figure 25g,h). This lower molar fragment preserves only the mesio-labial root, which is long and narrow (Figure 25h).

The proterotheriid humerus (MUN-STRI 34372) preserves part of the diaphysis and the distal epiphysis (Figure 26a–c). The capitulum is rounded and projects less distally than the trochlea (Figure 26a). The medial and lateral epicondyles are weakly developed. There is a supratrochlear foramen. The olecranon fossa is a fenestra (Figure 26c), as in *Prothoatherium* and *Proterotherium* (Cifelli and Guerrero, 1989). The diaphysis is mediolaterally compressed, as in other proterotheriids (Cifelli and Guerrero, 1989). The proximal portion of the diaphysis (at the level of the deltoid tuberosity) has the greatest anteroposterior depth, which decreases distally (Figure 26b) (Table 11).

The ulna (MUN-STRI 13120) is fairly complete, missing only a portion of the olecranon and a distal portion (Figure 26d–f; Table 11). The diaphysis is narrow and nearly straight. The anconeal process is not well developed, but projects laterally (Figure 26d). The coronoid process is small and projects distomedially (Figure 26d). The preserved portion of the olecranon is in the same plane as the shaft (Figure 26d,f).

The calcaneus (MUN-STRI 19544) has an elongate shape, with the distal portion broader than the body (Figure 26g,h). The body is not lateromedially compressed, as in *Neolicaphrium* (Scherer et al., 2009). The ectal facet is oval and located in the midline of the body (Figure 26g), as in *Neolicaphrium*. The sustentacular facet is also oval and elongated posteroventrally (Figure 26g), as in *Neolicaphrium* (Scherer et al., 2009). The metatarsals III from the Ware (MUN-STRI 13121; Figure 26i,j) and Codore (AMU-CURS 746; Figure 26k,l) Formations are very similar. The diaphysis is straight and long (Table 11). The distal epiphysis has a well-defined median keel.

Artiodactyla (Owen, 1848)

Camelidae (Gray, 1821)

cf. Camelidae indet.

Referred Material. MUN-STRI 34380 (cast PIMUZ A/V 5289), right m1 or m2.

Locality and Horizon. Police Station, Ware Formation. STRI locality 470060. 11.8487°N, 71.3243°W (Figure 3).

Description. The tooth measures 15.2 mm in mesiodistal length and 8.9 mm in labiolingual width. The crown height at the labial side is 10.4 mm, yielding a hypsodonty index of 0.7; this is a minimum value because the tooth is worn. The molar is bicrescentic and the talonid is approximately the same size as the trigonid (Figure 27a). The trigonid and talonid fossae are deep, semilunar, and elongated mesiodistally (Figure 27b), as in *Hemiauchenia* (Scherer et al., 2007). The protoconid and hypoconid are well developed, the labial lophids are V-shaped, but the labial edge is not as defined as in *Palaeolama* (Scherer et al., 2007). The

FIGURE 26. Proterotheriidae (Litopterna) postcrania from Ware and Codore Formations. Left humerus (MUN-STRI 34372): (a) anterior, (b) medial, and (c) posterior view. Right ulna (MUN-STRI 13120): (d) anterior, (e) medial, and (f) posterior view. Right calcaneus (MUN-STRI 19544): (g) dorsal and (h) plantar view. Left metacarpal III (MUN-STRI 13121): (i) anterior and (j) posterior view. Left metacarpal III (AMU-CURS 746): (k) anterior and (l) posterior view.

TABLE 11. Postcranial measurements (mm) of the Proterotheriidae indet. specimens of the Ware Formation; width = mediolateral; thickness = anteroposterior; a dash (–) indicates measurement could not be taken in the specimen.

	Humerus	Ulna	Calcaneus	Metacarpal III	
Measurement	**MUN-STRI 13119**	**MUN-STRI 13120**	**MUN-STRI 19544**	**MUN-STRI 13121**	**AMU-CURS 746**
Diaphysis width	12.6	10.1	–	9.8	15.9
Diaphysis thickness	18.3	12.0	–	–	–
Distal width	29.0 (Epiphysis) 20.6 (Trochlea)	–	–	11.8	21.2
Lateral epicondyle thickness	16.7	–	–	–	–
Medial epicondyle thickness	18.2	–	–	–	–
Sigmoid cavity height	–	18.2	–	–	–
Olecranon thickness	–	14.0	–	–	–
Olecranon width	–	8.7	–	–	–
Total length	–	–	53.9	70.1	89.3
Maximum width	–	–	19.2	–	–
Maximum thickness	–	–	14.8	–	–
Proximal width	–	–	–	12.6	19.9
Proximal thickness	–	–	–	11.1	–

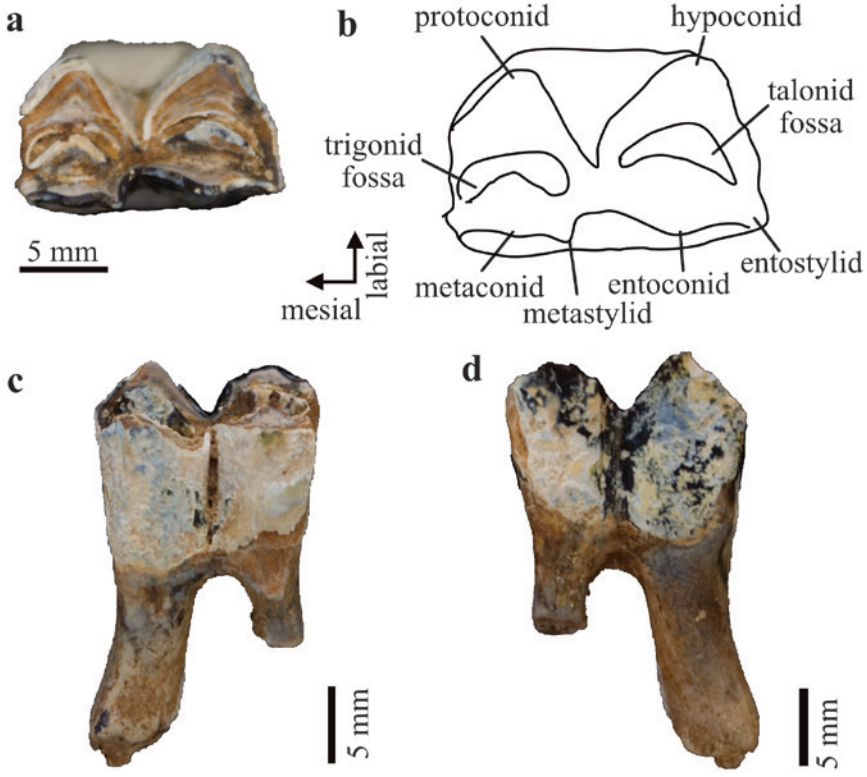

FIGURE 27. cf. Camelidae indet. (Artiodactyla) from the Ware Formation. Right m1 or m2 (MUN-STRI 34380): (a) photograph and (b) schematic drawing in occlusal view; (c) labial and (d) lingual views.

most mesial portion of the crown is broken and the presence of the proto- and parastylid ("llama buttress") cannot be evaluated (Figure 27a). South American camelids are thought to belong to the clade Lamini (Scherer, 2013), and the presence of a "llama buttress" has been proposed as a synapomorphy of the clade (Harrison, 1985; Webb and Meachen, 2004). However, Scherer (2013) noticed that the development of proto- and parastylid is highly variable in South American camelids. Despite being in an advanced wear stage, MUN-STRI 34380 differs from the lower molars of cervoids in being more hypsodont, and it differs from derived protoceratids (Synthetoceratines) in having a more developed metastylid. Finally, the Camelinae (sensu Webb and Meachen, 2004) is in need of systematic revision, and diagnostic characters for different taxa must be reevaluated on the basis of genomic and morphological data recovered from fossil taxa (Heintzman et al., 2015).

Chronostratigraphy of the Falcón Basin

The Falcón Basin is divided between a western and an eastern sector. For each of the sectors, author L. Quiroz did an extensive stratigraphic study and described several stratigraphic sequences to produce a composite sequence of both regions (Quiroz and Jaramillo, 2010) (Figures 28, 29). Seven sections were measured and described in western Urumaco, producing a composite sequence that is 8.75 km thick (Figure 28), and in eastern Urumaco three sections were measured and described, producing a composite sequence that is 2.25 km thick (Figure 29).

We provide a detailed description of each section, including its geographic position, in appendix 1 of the supplementary materials (Carrillo et al., 2018b). The biostratigraphic record of foraminifera in the Urumaco region (both western and eastern) has been extensively studied, and correlated to Bolli's biostratigraphic schemes from Trinidad (Renz, 1948; Bermudez and Bolli, 1969; Blow, 1969; Díaz de Gamero 1977a,b, 1985a,b, 1989, 1996; Díaz de Gamero et al., 1988; Díaz de Gamero and Linares, 1989; Wozniak and Wozniak, 1987; Guerra and Mederos, 1988; Rey, 1990; Hambalek, 1993; Bolli et al., 1994; Pérez et al., 2016). For a detailed description of the key studies, see appendix 2 in supplementary materials (Carrillo et al., 2018b). The age of the Querales Formation is further supported by nannoplankton (Pérez et al., 2016). The foraminiferal ages of the Urumaco Formation are also supported by vertebrates (Linares, 2004; Sánchez-Villagra, 2006; Sánchez-Villagra and Aguilera, 2006). A sample from the lower member of the Urumaco Formation (Urumaco West section, Figure 28) was analyzed for nannoplankton and yielded a flora that includes *Coccolithus pelagicus*, *Discoaster deflandrei*, *Sphenolithus abies*, and *Sphenolithus moriformis*. This association corresponds to Nannoplankton Zone NN7, which is equivalent to Planktonic Zone N14, early Tortonian (Figure 28). Herrera (2008) studied the magnetic stratigraphy of the Urumaco Formation at the same locality of our Urumaco West section. Herrera identified the top of Chron C4 Ar2r within the Urumaco Formation at meter 6693 of our section (Figure 28). Overall, the top boundaries of the formations in the Urumaco region, both East and West, are well dated and summarized in Table 12 and Figures 28 and 29.

To estimate the age of the stratigraphic horizons where the fossil mammals are recorded in the Falcón and Cocinetas Basins, we used the age model presented by Hendy et al. (2015) for the Jimol and Castilletes Formations in the Cocinetas Basin. We followed the chronostratigraphic framework described above for the Codore and San Gregorio Formations in the Falcón Basin. The stratigraphic occurrence and age of each specimen are summarized in Table 13.

DISCUSSION

Astrapotheriidae

The clade Uruguaytheriinae is registered in low and middle latitudes (<23°S; Goillot et al., 2011; Vallejo-Pareja et al., 2015; Croft et al., 2016), with the exception of *Uruguaytherium*, the most basal Uruguaytheriinae, whose precise provenance and age are unknown. The oldest record of Uruguaytheriinae comes from the bank of Río Beu, near the Santa Rosa locality in Peru, and it is interpreted to be late Oligocene in age (Antoine et al., 2016). The time-calibrated tree (Figure 12) is also consistent with the origin of Uruguaytheriinae in the late Oligocene. Given the current evidence, it is unclear whether the clade's origin took place in low or high latitudes, and more complete material from the late Oligocene deposits should help to clarify this issue. In any event, the middle Miocene (Laventan) uruguaytheriine taxa are the last occurring astrapotheres (Johnson and Madden, 1997; Goillot et al., 2011) (Figure 12).

The interrelationships of northern Uruguaytheriinae are not well resolved (Figure 12). *Hilarcotherium* is known only from Colombia, and its biochron extends from the upper Burdigalian–Langhian (Santacrucian/Colloncuran; 16.7–14.2 mya; Moreno et al., 2015) to the Serravallian (?Laventan; Vallejo-Pareja et al., 2015). *Granastrapotherium* is a monospecific genus and *Xenastrapotherium* includes five species; some were described from fragmentary remains without associated upper and lower dentition, and more complete specimens are needed to evaluate their validity.

Postcranial elements of Uruguaytheriinae are rare, and their intra- and interspecific variation has not been studied. Isolated postcranial elements are common in the Castilletes fauna. They are not associated with dental remains and we tentatively refer them to *Hilarcotherium* cf. *H. miyou*, as this is the only astrapotherid taxon recognized for the Castilletes Formation. All the postcranial elements are large, and given the size of *H. miyou*, it is plausible that they belong to this taxon. The material described

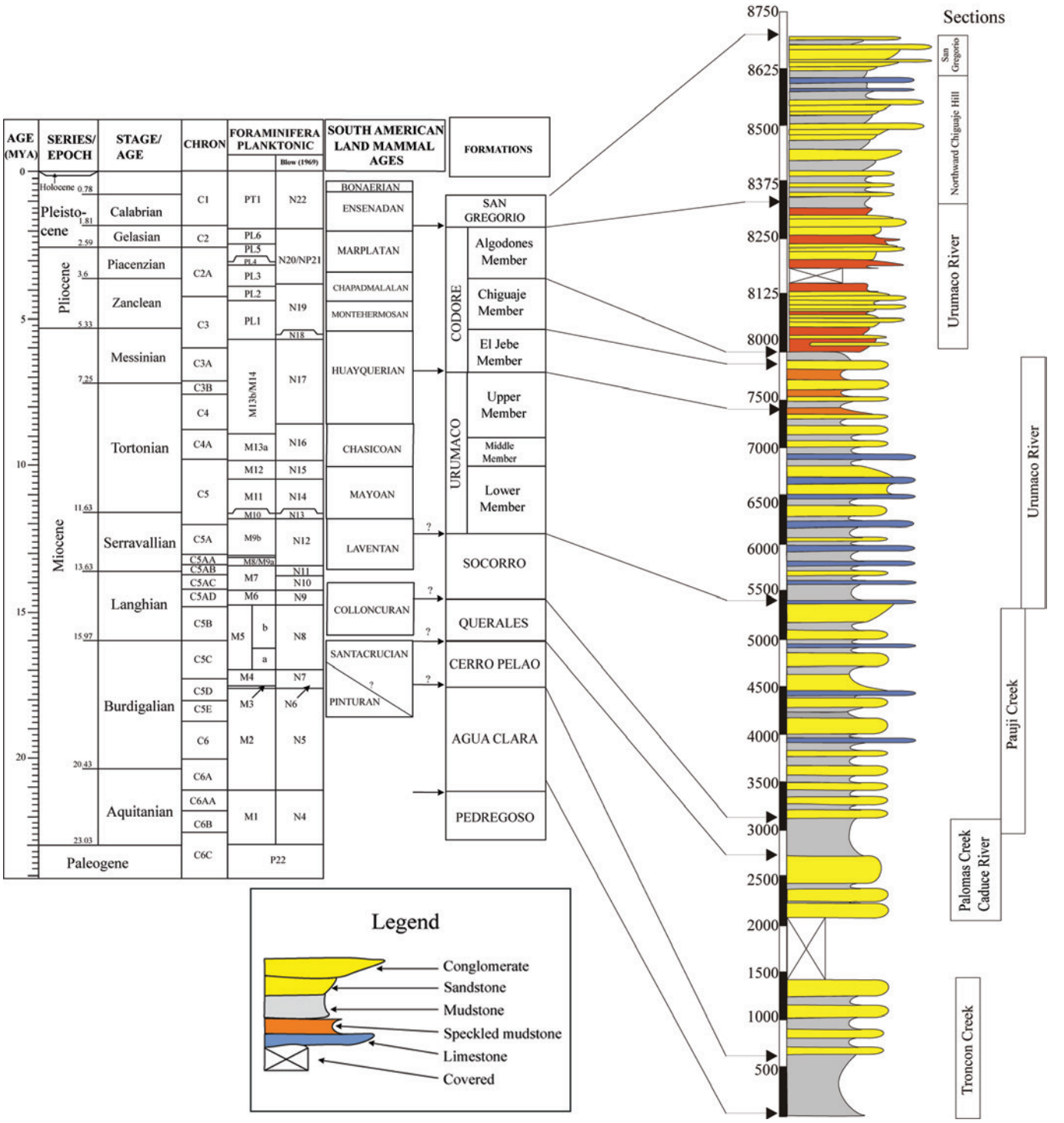

FIGURE 28. Urumaco western sequence chronostratigraphy. Composite section corresponds to several outcrop sections measured in western Urumaco, Venezuela, and described in Quiroz and Jaramillo (2010); scale bar values are total thickness (m). A detailed description of each individual section and its geographic position is given in supplementary materials by Carrillo et al. (2018b: appdx. 1). The ages (MYA) are derived from multiple foraminiferal, nannoplankton, and magnetic stratigraphic studies (Renz, 1948; Bermudez and Bolli, 1969; Blow, 1969; Díaz de Gamero 1977a,b, 1985a,b, 1989, 1996; Díaz de Gamero et al., 1988; Díaz de Gamero and Linares, 1989; Wozniak and Wozniak, 1987; Guerra and Mederos, 1988; Rey, 1990; Hambalek, 1993; Bolli et al., 1994; Pérez et al., 2016).

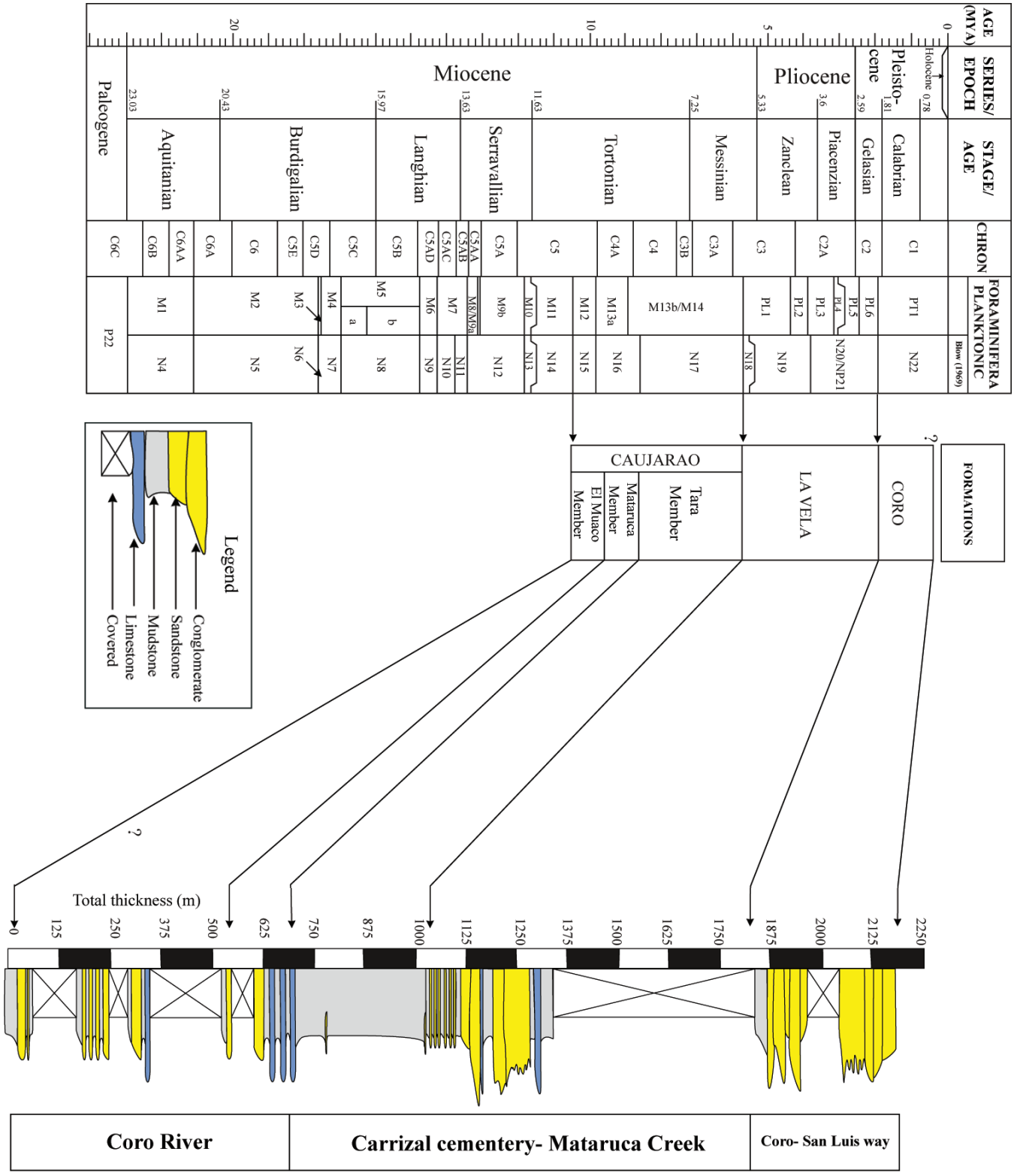

FIGURE 29. Chronostratigraphy of Falcón State east of Urumaco town. Composite section corresponds to several outcrop sections measured in eastern Urumaco. Formation ages are derived from multiple foraminiferal, nannoplankton, and magnetic stratigraphic studies (see text and Figure 28 for references).

TABLE 12. Chronostratigraphic data for composite Urumaco East and West sections. Numerical ages follow Gradstein et al. (2012). Reported ages (MYA) are for the top of each section.

Datum (event top)	Composite section (M)	Age (MYA)
Codore Algodones	8,285	1.81
Codore Chiguaje	7,935	3.6
Codore Jebe	7,886	5.33
Urumaco	7,403	6.8
Top C4 Ar2r	6,693.6	8.1
Socorro	5,338	12.4
Querales	3,130	14.5
Cerro Pelado	2,704	16
Agua Clara	631	17.5
Coro	2,185	0.4
La Vela	1,838	1.81
Caujarao Tara	1,025	5.6
Caujarao Mataruca	710	8.6
Caujarao Muaco	538	9.6

here will serve as a basis to compare the postcranial morphology of uruguaytheriine and non-uruguaytheriine astrapotheres in order to assess possible paleobiological differences or phylogenetically informative characters.

The dental measurements and associated body mass estimates of *H. miyou* (Figure 8; Tables 3, 5) indicate that it is one of the largest astrapotheres, comparable in size to *G. snorki*, *Parastrapotherium martiale* (Deseadan–Colhuehuapian SALMAs), and *Parastrapotherium herculeum*? (Colhuehuapian; Kramarz and Bond, 2008, 2010, 2011). Few studies have addressed the estimation of body mass in astrapotheres, and the congruence between estimates from dental and postcranial measurements has not been studied. Previously reported body mass estimations in astrapotheres used only dental and craniomandibular measurements. The m2 length yields an estimate of ~6,456.6 kg for *H. miyou*, notably larger than *H. castanedaii* (~1,303 kg; Vallejo-Pareja et al., 2015) and *X. kraglievichi* (~1,238.7–1,324.7 kg; Johnson and Madden, 1997; Kramarz and Bond, 2011). It is possible that the dental measurements overestimate the body mass of astrapotheres (Kramarz and Bond, 2011). The best known astrapotheriid is *Astrapotherium magnum* from the Santa Cruz Formation (Santacrucian SALMA) in Patagonia, which is known by almost complete skeletons with skulls and associated postcranial remains (Scott, 1928, 1937). The mean body mass estimate for *A. magnum* using bivariate and multivariate regression equations from craniomandibular measurements is ~921.3 kg (Cassini et al., 2012), much smaller than the mean estimate of ~1,824.5 kg using the m1–m3 length (Kramarz and Bond, 2011). Similarly, the mean estimate for *G. snorki* using craniomandibular measurements reported by Johnson and Madden (1997; table 22.8) is ~1,126.1 kg, whereas the estimate using the m1–m3 length is ~3,141.9 kg.

Proximal limb bones are considered better estimators of body mass because they are weight-bearing elements and subject to greater biomechanical constraints (Scott, 1990). Body mass estimates using the humeral length (Table 5) yield similar values to the estimates from dental measurements in *H. castanedaii* (~1,306.5 kg; Vallejo-Pareja et al., 2015), but this was not the case in *G. snorki* (~4,501.1 kg) and *A. magnum* (~2,096.5 kg), where the humeral estimates were larger than estimates from craniodental measurements. The estimate for the *Hilarcotherium* cf. *H. miyou* humerus from Castilletes (MUN-STRI 16777) was approximatedly 4,985.0 kg, 23% smaller than the estimate for *H. miyou* using the m2 length (Table 5). It is worth mentioning that the humerus of the former was associated with a radius that indicated the individual was a juvenile. These results emphasize the need for a comparative study on the relative proportions and scaling of teeth and limb bones in astrapotheres to choose an adequate living analog to estimate body mass in this group.

TOXODONTIDAE

The obtained phylogenetic hypothesis for Toxodontidae differs from the ones presented by Forasiepi et al. (2015: fig. 11) and Bonini et al. (2017a: fig. 6) mainly in the position of several taxa within Toxodontinae. The clades (*Paratrigodon*, *Trigodon*) and (*Toxodon*, *Dinotoxodon*) are recovered also in Forasiepi

TABLE 13. Biochronology of the Cocinetas and Falcón Basins. For Cocinetas, the age model of Hendy et al. (2015) used a linear regression of the stratigraphic position and the $^{87}Sr/^{86}Sr$ isotopes ages for the upper part of the Jimol and the Castilletes Formations. The regression function is $y = -0.0058x + 16.722$, where y is the age in MYA and x is the stratigraphic meter. The original equation cannot be applied for the Ware Formation due to an unconformity between the Castilletes and Ware Formations (Moreno et al., 2015). For the Ware Formation, a mean age of 3.2 MYA was estimated for the shell bed at the top of the formation (Hendy et al., 2015; Moreno et al., 2015). This shell bed is 17–20 m above the stratigraphic horizons where the vertebrates were recovered. Assuming the same sedimentation rate for the Jimol, Castilletes, and Ware Formations, we used the regression equation presented by Hendy et al. (2015) to estimate the age of the horizons of fossil vertebrates from the Ware Formation. Using the age of 3.2 MYA obtained for the horizon at stratigraphic meter 22, we calculated that 3.2 = –0.0058 * 22 + intercept, and we obtained a regression function for the Ware formation of $y = -0.0058x + 3.0724$. Abbreviations: SM = Stratigraphic meter; Lat = latitude; Lon = longitude.

Basin	Clade	Subclade	Taxon	Specimen ID	Formation	Locality	Section ID	Lat.	Long.	SM	SM composite section	Age (MYA)
Falcón	Notoungulata	Toxodontidae	*Falcontoxodon aguilerai*	AMU-CURS 765	Codore	Codore Algodones	NA	11.29	–70.24	2,530	8,257	1.96
				AMU-CURS 70	Codore	Codore Algodones	NA	11.29	–70.24	2,530	8,257	1.96
	Litopterna	Proterotheriidae	Proterotheriidae indet.	AMU-CURS 745	Codore	Codore Algodones	NA	11.29	–70.24	2,530	8,257	1.96
				AMU-CURS 746	Codore	Codore Algodones	NA	11.29	–70.24	2,530	8,257	1.96
	Xenarthra	Glyptodontidae	*Boreostemma pliocena*	AMU-CURS 158	Codore	Road to Tío Gregorio	NA	11.26	–70.29	2,530	8,257	1.96
	Notoungulata	Toxodontidae	*Falcontoxodon* aff. *F. aguilerai*	AMU-CURS 585	San Gregorio	Norte Casa Chiguaje	NA	11.29	–70.24	4	8,291	1.78
			Falcontoxodon sp.	AMU-CURS 69	San Gregorio	Norte Casa Chiguaje	NA	11.29	–70.24	7	8,294	1.79
				AMU-CURS 77	San Gregorio	Norte Casa Chiguaje	NA	11.29	–70.24	7	8,294	1.79
				AMU-CURS 270	San Gregorio	Norte Casa Chiguaje	NA	11.29	–70.24	7	8,294	1.79
				AMU-CURS 542	San Gregorio	Norte Casa Chiguaje	NA	11.29	–70.24	7	8,294	1.79
				AMU-CURS 544	San Gregorio	Norte Casa Chiguaje	NA	11.29	–70.24	7	8,294	1.79
				AMU-CURS 548	San Gregorio	Norte Casa Chiguaje	NA	11.29	–70.24	7	8,294	1.79
				AMU-CURS 562	San Gregorio	Norte Casa Chiguaje	NA	11.29	–70.24	7	8,294	1.79
				AMU-CURS 563	San Gregorio	Norte Casa Chiguaje	NA	11.29	–70.24	7	8,294	1.79
				AMU-CURS 570	San Gregorio	Norte Casa Chiguaje	NA	11.29	–70.24	7	8,294	1.79
				AMU-CURS 738	San Gregorio	Norte Casa Chiguaje	NA	11.29	–70.24	7	8,294	1.79
				AMU-CURS 739	San Gregorio	Norte Casa Chiguaje	NA	11.29	–70.24	7	8,294	1.79
				AMU-CURS 741	San Gregorio	Norte Casa Chiguaje	NA	11.29	–70.24	7	8,294	1.79
	Carnivora	Procyonidae	*Cyonasua* sp.	AMU-CURS 224	San Gregorio	Norte Casa Chiguaje	NA	11.29	–70.23	5	8,292	1.78
	Rodentia	Caviomorpha	cf. *Caviodon*	UNEFM-VF-53	San Gregorio	Norte Casa Chiguaje	NA	11.29	–70.24	5	8,292	1.78
			Hydrochoeropsis? wayuu	UNEFM-VF-50	San Gregorio	Norte Casa Chiguaje	NA	11.29	–70.24	5	8,292	1.78

(*Continued*)

TABLE 13. (*Continued*)

Basin	Clade	Subclade	Taxon	Specimen ID	Formation	Locality	Section ID	Lat.	Long.	SM	SM composite section	Age (MYA)
				UNEFM-VF-51	San Gregorio	Norte Casa Chiguaje	NA	11.29	–70.24	5	8,292	1.78
				UNEFM-VF-52	San Gregorio	Norte Casa Chiguaje	NA	11.29	–70.24	5	8,292	1.78
			Marisela gregoriana	UNEFM-VF-55	San Gregorio	Norte Casa Chiguaje	NA	11.29	–70.24	5	8,292	1.78
			Neoepiblema sp.	UNEFM-VF-54	San Gregorio	Norte Casa Chiguaje	NA	11.29	–70.24	5	8,292	1.78
	Xenarthra	Dasypodidae	*Pliodasypus vergelianus*	AMU-CURS 192	San Gregorio	Norte Casa Chiguaje	NA	11.28	–70.24	5	8,292	1.78
Cocinetas	Sparassodonta	Borhyaenoidea	*Lycopsis padillai*	MUN-STRI 34113	Castilletes	STRI 390093	170514	11.91	–71.34	128	280	15.1
	Xenarthra	Megatheroidea	*Hyperleptus*?	MUN-STRI 37413	Castilletes	STRI 130024	430103	11.93	–71.33	80	80	16.3
	Astrapotheria	Uruguaytheriinae	*Hilarcotherium miyou*	IGMp 881327	Castilletes	STRI 470058	430103	11.95	–71.32	28	28	16.6
				MUN-STRI 34216	Castilletes	STRI 470058	430103	11.95	–71.32	28	28	16.6
			Hilarcotherium cf. *H. miyou*	MUN-STRI 16778	Castilletes	STRI 390094	430103	11.95	–71.33	46	46	16.5
				MUN-STRI 34229	Castilletes	STRI 390094	430103	11.95	–71.33	46	46	16.5
				MUN-STRI 34223	Castilletes	STRI 390094	430103	11.95	–71.33	46	46	16.5
				MUN-STRI 34222	Castilletes	STRI 390094	430103	11.95	–71.33	46	46	16.5
				MUN-STRI 34221	Castilletes	STRI 390094	430103	11.95	–71.33	46	46	16.5
				MUN-STRI 34217	Castilletes	STRI 390094	430103	11.95	–71.33	46	46	16.5
				MUN-STRI 16777	Castilletes	STRI 390094	430103	11.95	–71.33	46	46	16.5
				MUN-STRI 34212	Castilletes	STRI 290632	430103	11.95	–71.33	28	28	16.6
				MUN-STRI 37384	Castilletes	STRI 390094	430103	11.95	–71.33	46	46	16.5
				MUN-STRI 37765	Castilletes	STRI 130024	430103	11.93	–71.33	80	80	16.3
				MUN-STRI 34225	Castilletes	STRI 390094	430103	11.95	–71.33	46	46	16.5
				MUN-STRI 34310	Castilletes	STRI 390094	430103	11.95	–71.33	46	46	16.5
				MUN-STRI 36644	Castilletes	STRI 390094	430103	11.95	–71.33	46	46	16.5
				MUN-STRI 37390	Castilletes	STRI 390094	430103	11.95	–71.33	46	46	16.5
				MUN-STRI 34292	Castilletes	STRI 390093	170514	11.91	–71.34	128	280	15.1
				MUN-STRI 16779	Castilletes	STRI 390094	430103	11.95	–71.33	46	46	16.5
				MUN-STRI 16785	Castilletes	STRI 390094	430103	11.95	–71.33	46	46	16.5

TABLE 13. (*Continued*)

Basin	Clade	Subclade	Taxon	Specimen ID	Formation	Locality	Section ID	Lat.	Long.	SM	SM composite section	Age (MYA)
	Notoungulata	Leontinidae	cf. *Huilatherium*	MUN-STRI 34312	Castilletes	STRI 390094	430103	11.95	−71.33	46	46	16.5
	Litopterna	Proterotheriidae	*Lambdaconus* cf. *L. colombianus*	MUN-STRI 16716	Castilletes	STRI 390093	170514	11.91	−71.34	128	280	15.1
	Xenarthra	Lestodontini	Lestodontini gen. et sp. nov.	MUN-STRI 36643	Ware	STRI 470060	430052	11.85	−71.32	4	NA	3.05
				MUN-STRI 20424	Ware	STRI 390023	430052	11.85	−71.32	3.5	NA	3.05
				MUN-STRI 34353	Ware	STRI 470060	430052	11.85	−71.32	4	NA	3.05
		Scelidotheriinae	Scelidotheriinae gen. et sp. indet.	MUN-STRI 16535	Ware	STRI 390025	430052	11.85	−71.32	4.5	NA	3.05
		Megalonychidae	Megalonychidae gen. et sp. nov.	MUN-STRI 16601	Ware	STRI 390077	430052	11.85	−71.32	1.7	NA	3.06
				MUN-STRI 34226	Ware	STRI 470060	430052	11.85	−71.32	4	NA	3.05
		Megatheriinae	*Pliomegatherium lelongi*	MUN-STRI 36685	Ware	STRI 390024	430052	11.85	−71.32	4.5	NA	3.05
				MUN-STRI 19747	Ware	STRI 390017	430052	11.85	−71.33	5	NA	3.04
				MUN-STRI 20446	Ware	STRI 390026	430052	11.85	−71.33	5	NA	3.04
		Nothrotheriinae	cf. *Nothrotherium*	MUN-STRI 12924	Ware	STRI 390024	430052	11.85	−71.32	4.5	NA	3.05
	Rodentia	Caviomorpha	*Hydrochoeropsis*? *wayuu*	MUN-STRI 12846	Ware	STRI 390017	430052	11.85	−71.33	5	NA	3.04
				MUN-STRI 37602	Ware	STRI 470062	430052	11.85	−71.32	5	NA	3.04
				MUN-STRI 16233	Ware	STRI 430052	430052	11.85	−71.32	5	NA	3.04
				MUN-STRI 16438	Ware	STRI 430052	430052	11.85	−71.32	5	NA	3.04
				MUN-STRI 34315	Ware	STRI 470062	430052	11.85	−71.32	5	NA	3.04
	Notoungulata	Toxodontidae	Toxodontidae indet.	MUN-STRI 37507	Ware	STRI 470062	430052	11.85	−71.32	5	NA	3.04
				MUN-STRI 37561	Ware	STRI 470059	430052	11.85	−71.32	2	NA	3.06
	Artiodactyla	Camelidae	Camelidae indet.	MUN-STRI 34380	Ware	STRI 470060	430052	11.85	−71.32	4	NA	3.05
	Carnivora	Procyonidae	*Chapalmalania* sp.	MUN-STRI 34114	Ware	STRI 470061	430052	11.85	−71.32	4.3	NA	3.05
	Litopterna	Proterotheriidae	Proterotheriidae indet.	MUN-STRI 34170	Ware	STRI 470060	430052	11.85	−71.32	4	NA	3.05
				MUN-STRI 13378	Ware	STRI 390023	430052	11.85	−71.32	3.5	NA	3.05
				MUN-STRI 13121	Ware	STRI 390020	430052	11.85	−71.32	5	NA	3.04
				MUN-STRI 19544	Ware	STRI 390018	430052	11.85	−71.32	4.5	NA	3.05
				MUN-STRI 13119	Ware	STRI 390020	430052	11.85	−71.32	5	NA	3.04
				MUN-STRI 13120	Ware	STRI 390020	430052	11.85	−71.32	5	NA	3.04
				MUN-STRI 16289	Ware	STRI 430052	430052	11.85	−71.32	5	NA	3.04

et al. (2015) and Bonini et al. (2017a) topologies but their positions are different in the cladograms. Concerning the toxodontinaes from northern South America, the main difference in our result is that the toxodontids recorded in Venezuela (*Mixotoxodon*, *Gyrinodon*, and *Falcontoxodon*) form a monophyletic group (node 45) and belong to a clade that also includes *Piauhytherium* (node 46; Figure 24a).

Bond et al. (2006) described a specimen of Toxodontinae (UNEFM-CIAAP 616) from the middle member of the Urumaco Formation consisting of a partial mandibular ramus with m1–m3. The specimen UNEFM-CIAAP 616 shows unique characters not seen in combination in other toxodontids. Some of these characters are also seen in *Falcontoxodon*: a broad trigonid with a lingual enamel-less contour, a weakly developed meta-entoconid fold in m2, and an open labial enamel fold. The morphology of the lower molar folds can be affected by wear, as noticed in *Pericotoxodon* (Madden, 1997). The UNEFM-CIAAP 616 differs from *Falcontoxodon* in having a weakly developed meta-entoconid fold in m1, and a better developed ento-hypoconulid fold in m2 than in m1. The fragmentary nature of UNEFM-CIAAP 616 impedes the precise assessment of its phylogenetic affinities (Bond et al., 2006). More complete toxodontid material from the Urumaco Formation may confirm or refute whether the clade that includes *Gyrinodon*, *Falcontoxodon* and *Mixotoxodon* was present in the region since the late Miocene.

The type of *Gyrinodon quassus* (NHMUK PV M13158) was collected in La Puerta Formation (middle to late Miocene) (Gonzalez de Juana et al., 1980), western Buchivacoa, Falcón, Venezuela. Additional material from Acre, Brazil, has been referred to this taxon (Bond et al., 2006; Sánchez-Villagra et al., 2010). *Mixotoxodon larensis* is recorded in late Pleistocene sediments of tropical localities of South and Central America (between 15°S and 18°N) (Rincón, 2011). *Mixotoxodon* is the only toxodontid that migrated to Central and North America during the GABI (Webb and Perrigo, 1984; Laurito, 1993; Lucas et al., 1997; Cisneros, 2005; Lucas, 2008, 2014; Lundelius et al., 2013).

The estimated body mass of approximately 796 kg for *Falcontoxodon aguilerai* is comparable to that of *Pericotoxodon platignathus* (~798 kg, Madden, 1997), larger than estimates for *Nesodon taweretus* (~550 kg, Forasiepi et al., 2015), *Nesodon imbricatus* (~637 kg, Cassini et al., 2012; ~250–300 kg, Croft, 2016), and *Xotodon* sp. (mean = 626 kg, standard deviation [sd] = 59 kg; Elissamburu, 2012), and smaller than *Toxodon platensis* (mean = 1,642 kg, geometric mean = 1,187 kg, Fariña et al., 1998), *Trigodon* (mean = 1,809 kg, sd = 508 kg) and *Mixotoxodon larensis* (mean = 3,797 kg, sd = 1,296 kg, Elissamburu, 2012). With a sample size of six taxa, Elissamburu (2012) estimated a body mass range for toxodontids of 104–3,797 kg. *Falcontoxodon* shows an intermediate body mass among Toxodontinae, and did not reach the large sizes of the Pleistocene taxa.

Miocene Fauna

Of the seven mammalian taxa currently recognized for the assemblage of the Castilletes Formation in the Cocinetas Basin (Table 1), three are SANUs. The taxa previously described for this assemblage are the sparassodont *Lycopsis padillai* (Suarez et al., 2016) and the megatherioid sloth *Hyperleptus*? (Amson et al., 2016). Althought the taxonomic status of *Hyperleptus*? needs to be confirmed with more complete material, the current evidence suggests that these two taxa belong to genera that show a wide latitudinal range and are also recorded at higher latitudes in the Santacrucian fauna (Kay et al., 2012). The SANUs from the Castilletes Formation (*Lambdaconus* cf. *L. colombianus, H. miyou*, and cf. *Huilatherium*) have affinities with taxa also recorded in the Laventan fauna of the Magdalena valley in Colombia (Cifelli and Guerrero, 1989; Villarroel and Colwell Danis, 1997; Vallejo-Pareja et al., 2015). The records of these taxa in Castilletes expand their temporal and geographical distribution.

With the referral of *Lambdaconus (=Prothoatherium) colombianus* to *Lambdaconus*, the biochron of this genus now spans from the Deseadan to the Laventan SALMAs (Soria, 2001; Cifelli and Guerrero, 1989). In low latitudes, *Lambdaconus* is recorded in middle Miocene deposits (Santacrucian and Laventan SALMAs), whereas in high latitudes it is represented by three species recorded in Oligocene and early middle Miocene deposits of the Sarmiento and Pinturas Formations (Deseadan, Colhuehuapian SALMAs, and "Pinturan") (Soria, 2001; Kramarz and Bond, 2005). *L. colombianus* and *Megadolodus molariformes* are two small proterotheriids recorded in La Venta and originally referred to Didolodontidae (McKenna, 1956; Hoffstetter and Soria, 1986). However, additional material was used to hypothesize assignation to Proterotheriidae (Cifelli and Guerrero, 1989; Cifelli and Villarroel, 1997). The distinctiveness of *Megadolodus* warranted the recognition of a distinct clade within Proterotheriidae, the Megadolodinae (Cifelli and Villarroel, 1997). This clade also includes *Bounodus enigmaticus* from the Urumaco Formation (Carlini et al., 2006b). A systematic revision of Proterotheriidae including the middle Miocene taxa from low latitudes is necessary to clarify the phylogenetic relationships and paleobiogeography of tropical proterotheriids.

The deposition of the Castilletes Formation represents a shallow marine to fluvio-deltaic environment with transgressive sequences (Hendy et al., 2015; Moreno et al., 2015). The localities where the mammal remains were collected show a strong fluvial influence (Moreno et al., 2015), as indicated by the diverse assemblage of crocodiles (Moreno-Bernal et al., 2016) and turtles (Cadena and Jaramillo, 2015a). The mammal record is in agreement with this paleoenvironmental reconstruction (Figures 30, 31). The astrapothere remains from the Castilletes Formation were collected from muddy sediments and were often associated with freshwater "invertebrates"

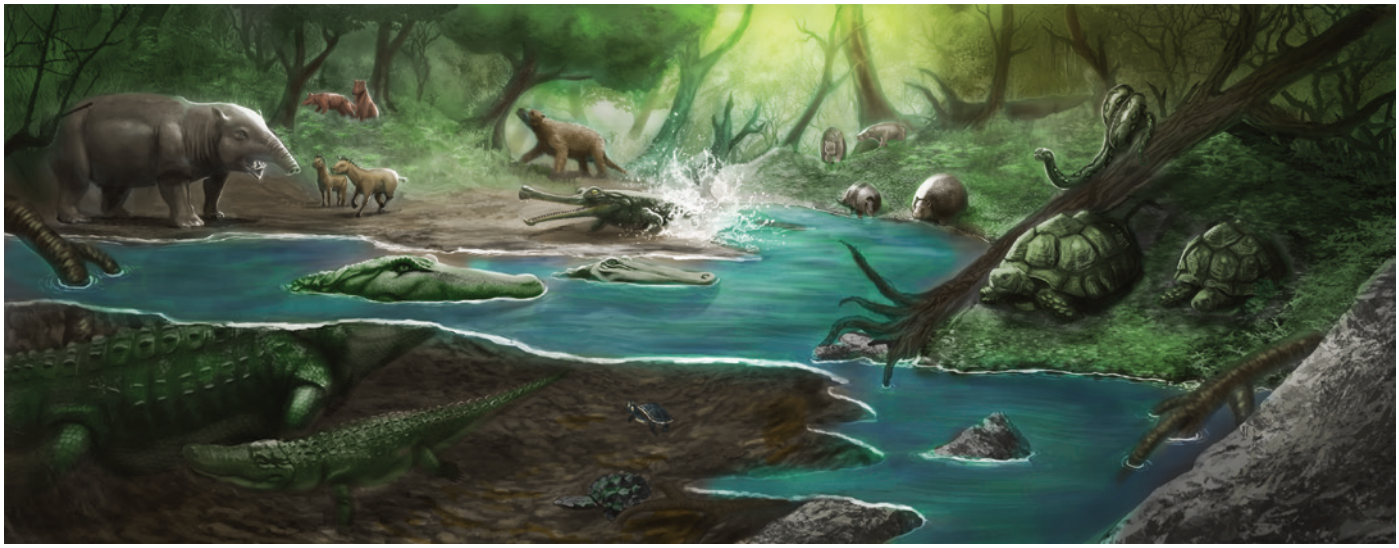

FIGURE 30. Life reconstruction of the Castilletes Formation faunal assemblage, Cocinetas Basin, Colombia. Artist: Stjepan Lukac.

FIGURE 31. Key of the reconstruction shown in Figure 30. 1. *Hilarcotherium miyou* n. sp. (Astrapotheriidae). 2. *Lycopsis padillai* (Borhyaenoidea). 3. *Hyperleptus*? (Megatherioidea). 4. cf. *Huilatherium* (Leontiniidae). 5. Boidae indet. (Squamata). 6. *Lambdaconus* cf. *L. colombianus* (Proterotheriidae). 7. Gavialoidea indet. (Crocodilia). 8. Pampatheriidae indet. 9. Glyptodontidae indet. 10. *Mourasuchus* sp. (Crocodilia). 11. *Chelonoidis* sp. (Testudines). 12. *Purussaurus* sp. (Crocodilia). 13. Podocnemidae (Testudines). 14. *Chelus colombiana* (Testudines).

(Moreno et al., 2015). Astrapotheres are commonly reported to occur in sediments representing stream channels (Riggs, 1935; Scott, 1937; Marshall et al., 1990), and in association with aquatic fauna (Sánchez-Villagra et al., 2004). The bone microstructure (studied in *Parastrapotherium*) is similar to that of graviportal taxa, and it is possible that astrapotheres were specialized for graviportality and semiaquatic habits (Houssaye et al., 2016). Based on the body mass and skeletal adaptations of *L. colombianus*, Cifelli and Guerrero (1989) inferred cursorial and forest-dwelling habits for this species.

Pliocene/Pleistocene Faunas

The toxodontid and proterotheriid material from the Codore Formation comes from the upper part of the Algodones Member (Figure 4b), 30 stratigraphic meters below the contact with the San Gregorio Formation. At the moment, the mammal fauna of the Codore Formation includes four taxa (Table 2). The glyptodont *Boreostemma pliocena* is recorded in the lower member (El Jebe) of the Codore Formation (Carlini et al., 2008b). When compared with the better known underlying Urumaco Formation (Sánchez-Villagra and Aguilera, 2006) and even the San Gregorio Formation (Table 2), the mammal diversity of Codore is modest. This is due to undersampling, and further efforts will increase the diversity of this unit (Carlini, 2010).

The San Gregorio fauna includes macro and micro mammals (e.g., rodents; Table 2). Small vertebrates have not been recovered in the Urumaco Formation, the fauna of which is mostly characterized by large crocodiles, turtles, and xenarthrans. However, in San Gregorio the lithology favors the preservation of small vertebrates, and it promises for the late Pliocene/early Pleistocene to offer a more complete picture of the faunal assemblage in the Falcón Basin (Figures 32, 33). The age of San Gregorio overlaps with two GABI migration pulses (GABI 2 and 3; Figure 1) (Woodburne, 2010). Paleontological and molecular evidence shows that GABI significantly increased during the early Pleistocene (Woodburne, 2010; Bacon et al., 2015; Carrillo et al., 2015). However, in San Gregorio so far only one of the ten described mammalian taxa is an immigrant from North America, the procyonid *Cyonasua* (Forasiepi et al., 2014). The age of San Gregorio corresponds to the Ensenadan SALMA (Figure 28), of which the type locality is located in La Plata county (~34° S) in Argentina (Cione et al., 2015). In southern South America, this time interval is characterized by the presence of several clades of Holarctic origin (e.g., Cervidae, Ursidae, Tapiridae, Felidae, and Gomphotheriidae; Cione et al., 2015), which contrasts with the pattern observed in the Falcón Basin.

A similar pattern is observed in the mammalian fauna of the Ware Formation, in the Cocinetas Basin, which is slightly older than San Gregorio and close to the first GABI migration pulse (GABI 1; Figure 1) (Woodburne, 2010; Moreno et al., 2015). Despite its close proximity to the Isthmus of Panama, of the 13 taxa recorded for the Ware fauna (Table 1), only two are migrants from North America, the procyonid *Chapalmalania* (Forasiepi et al., 2014) and a camelid. The latter is arguably the oldest well-dated record of Camelidae in South America, although the record of *Hemiauchenia* reported by Gasparini et al. (2017) from Chapadmalalan deposits in Argentina could be older, as it comes from a locality assignable to the Gauss Chron (3.55–2.59 mya). Hendy et al. (2015) reported a mean age of 3.2 mya (range from 3.40 to 2.78 mya) calculated from $^{87}Sr/^{86}Sr$ ratios for the shell bed at the top of the formation (Figure 3), which is 16 stratigraphic meters above where the camelid was collected. Macroinvertebrate biostratigraphy also yielded a Piacenzian age for the Ware Formation (Hendy et al., 2015; Moreno et al., 2015).

The oldest record of Camelidae in South America has been a problematic point in the understanding of the paleobiogeography of this group during GABI (Scherer, 2013; Gasparini et al., 2017). The most recent evidence suggests that the putative oldest camelid record in the continent is Chapadmalalan (Gasparini et al., 2017). The Chapadmalalan record is from the Buenos Aires province in Argentina (~36°S; Gasparini et al., 2017), more than 5,000 km south from the Isthmus of Panama. The camelid record from Ware supports a minimum age of ca. 3.2 mya for the arrival of camelids in South America, as would be expected given its proximity to the Isthmus. Unfortunately, the material available does not permit us to evaluate whether it belongs to the Lamini, like the other South American camelids (Scherer, 2013; Gasparini et al., 2017), or to the group of camelids that inhabited the Central American tropics beginning in the early Miocene (Rincón et al., 2012).

The mammalian fauna of the Ware Formation is characterized by a high diversity of herbivores (Figures 34, 35), which includes at least five different taxa of sloths (Amson et al., 2016), as well as cingulates, caviomorph rodents (Moreno et al., 2015; Pérez et al., 2016), a toxodont, a proterotheriid, and a camelid (Table 1). The diversity and wide body mass range of herbivores from the Ware Formation suggest that they occupied different ecological niches, and that there was enough vegetation cover to sustain a complex herbivorous community. Other vertebrates from the assemblage, such as crocodiles, turtles, and freshwater fishes (Aguilera et al., 2013a,b; Moreno et al., 2015; Moreno-Bernal et al., 2016), are indicative of the fluvial influence in the region during the late Pliocene. A provenance study of the Ware Formation indicates that the sediments were derived mostly from local sources within the Guajira peninsula ranges and the water was probably derived by local precipitation (Pérez-Consuegra et al., 2018). Today, the Guajira peninsula is dominated by a dry landscape with low rainfall (less than 500 mm of mean annual precipitation), high seasonality, xerophytic vegetation, and lack of large rivers (Pabón-Caicedo et al., 2001).

The Pliocene climate prior to the increase of the Northern Hemisphere glaciations was characterized by warmer mean annual temperatures than the preindustrial conditions, higher levels of CO_2 (>400 ppm), and reduced meridional and vertical ocean temperature gradients than today (Pagani et al., 2010). We hypothesize that the change in the landscape in the Cocinetas and Falcón Basins relates to the increase of the Northern Hemisphere

FIGURE 32. (*Top*) Life reconstruction of the San Gregorio Formation faunal assemblage, Falcón Basin, Venezuela. Artist: Stjepan Lukac.

FIGURE 33. (*Bottom*) Key of the reconstruction shown in Figure 32. 1. *Cyonasua* (Procyonidae). 2. *Tupinambis* sp. (Squamata). 3. *Boreostemma?* sp. (Glyptodontidae). 4. *Neoepiblema* (Neoepiblemidae). 5. *Hydrochoeropsis? wayuu* (Caviidae). 6. *Pliodasypus vergelianus* (Dasypodidae). 7. Pampatheriidae. 8. aff. *Proeremotherium* (Megatheriinae). 9. *Marisela gregoriana* (Octodontoidea). 10. *Falcontoxodon* sp. (Toxodontidae). 11. cf. *Caviodon* (Caviidae). 12. Characiformes indet. 13. Loricariidae indet. (Siluriformes). 14. *Crocodylus falconensis* (Crocodilia). 15. Potamotrygonidae indet. (Myliobatiformes). 16, Doradidae indet. (Siluriformes). 17, Podocnemidae indet. (Testudines).

FIGURE 34. (*Top*) Life reconstruction of the Ware Formation faunal assemblage, Cocinetas Basin, Colombia. Artist: Stjepan Lukac.

FIGURE 35. (*Bottom*) Key of the reconstruction shown in Figure 34. 1. *Pliomegatherium lelongi* (Megatheriinae). 2. cf. *Nothrotherium* (Nothrotheriinae). 3. Camelidae indet. 4. Proterotheriidae indet. 5. *Hydrochoeropsis? wayuu* (Caviidae). 6. Podocnemidae indet. (Testudines). 7. *Crocodylus* (Crocodylidae). 8. *Chapalmalania* sp. (Procyonidae). 9. Toxodontinae indet. 10. Lestodontini gen. et sp. nov. 11. Pampatheriidae indet. 12. Glyptodontidae indet. 13. Erethizontidae indet. 14. Megalonychidae gen. et sp. nov. 15. Scelidotheriinae gen. et sp. indet.

glaciations in the Pliocene (ca. 2.7 MYA), which was mainly controlled by a decrease of the atmospheric CO_2 (Lunt et al., 2008). During the early Pliocene (ca. 4–5 MYA) the CO_2 concentration ranged from ~390 to 280 ppm, and CO_2 atmospheric levels progressively decreased from 5 to 0.5 MYA (Pagani et al., 2010). Global rainfall is higher at the Intertropical Convergence Zone (ITCZ), a tropical belt of clouds. The ITCZ migrates seasonally between the boreal and austral summers toward the warmer hemisphere, and its position is linked to the atmospheric energy transport (Schneider et al., 2014). The increase of ice cover in the Northern Hemisphere during the Pliocene could have caused the ITCZ to migrate toward a more southern position. For example, Holocene sediments from the Cariaco Basin (coast of north central Venezuela) indicate a southward ITCZ migration during time intervals when the high northern latitudes cooled (Schneider et al., 2014: fig. 6). A southward migration of the ITCZ would have reduced the amount of rainfall in northwestern South America, producing the landscape change observed in the Cocinetas and Falcón Basins.

CONCLUSION

We describe new material of SANUs from the Neogene deposits of the Cocinetas and Falcón Basins, in northern South America, a region less represented in the fossil record than the southern portion of the continent. The middle Miocene deposits of the Castilletes Formation in the Cocinetas Basin are characterized by the presence of a large uruguaytheriine astrapothere (*Hilarcotherium miyou* sp. nov.), the leontiniid cf. *Huilatherium*, and the proterotheriid *Lambdaconus* cf. *L. colombianus*. All of the above have affinities with taxa that are otherwise recorded in the Laventan fauna of the Magdalena valley, Colombia. *Lambdaconus* cf. *L. colombianus* and other members of the mammalian fauna (the sparassodont *Lycopsis padillai* and the sloth *Hyperleptus?*), belong to groups with a wide latitudinal distribution across the continent, whereas *Hilarcotherium* and *Huilatherium* are restricted to low latitudes. *Hilarcotherium miyou* is one of the largest astrapotheres, with an estimated body mass of about 6,456.6 kg, although estimations based on dental measurements in astrapotheres should be taken with caution. Astrapothere postcranial elements are common in the Castilletes Formation and found in association with freshwater "invertebrates."

We describe a new species of Toxodontinae (*Falcontoxodon aguilerai* gen. et sp. nov.), the holotype of which was found in the Codore Formation, and we refer some dental and postcranial remains from the San Gregorio Formation to the same genus. *F. aguilerai* shows an intermediate body mass among Toxodontinae, with an estimate of ~796 kg. The new material allows us to recognize a tropical clade within Toxodontinae that includes the Venezuelan toxodonts recorded from the Miocene (*Gyrinodon*) to the Pleistocene (*Falcontoxodon* and *Mixotoxodon*). *Mixotoxodon* is the only toxodont that migrated to Central and North America as part of the GABI. The Pliocene/Pleistocene faunas of Codore and San Gregorio Formations in the Falcón Basin and Ware Formation in the Cocinetas Basin are characterized by a predominance of South American native taxa in spite of their age and proximity to the Isthmus of Panama. This suggests that biotic interactions and biogeography influenced the timing and distribution of migrations in northern South America during the interchange.

The North American immigrants include procyonids and the putative oldest record of Camelidae in South America, which was recovered in the Ware Formation and has a minimum age of ca. 3.2 MYA, based on $^{87}Sr/^{86}Sr$ ratios and macroinvertebrate biostratigraphy.

ACKNOWLEDGMENTS

Our gratitude goes to all the other members of the different field efforts in the Cocinetas and Falcón Basins. In particular, J. D. Carrillo-Briceño, T. M. Scheyer, A. Wegmann, G. Aguirre-Fernández (PIMUZ), A. A. Carlini (MLP), A. Hendy (Natural History Museum of Los Angeles County), A. Reyes, D. Gutiérrez, and the students from the University of Zurich for the 2013 field projects in Falcón. The González family kindly provided access to collect in their land. We thank the authorities at the Instituto del Patrimonio Cultural of the República Bolivariana de Venezuela and the Alcaldía Municipio de Urumaco for their generous support.

For fieldwork in Cocinetas, we are grateful to J. W. Moreno-Bernal, C. Montes, and J. Escobar (Universidad del Norte, Colombia); M. C. Vallejo (Sam Houston State University); F. Moreno (Univesity of Rochester); C. Martinez (Cornell University); A. Hendy (NHMLA); J. D. Carrillo-Briceño (PIMUZ); J. Luque (University of Alberta, Canada); C. Suarez and K. Jimenez (MLP); E. Cadena (Yachay Tech University, Ecuador); G. Ballén (University of Sao Paulo, Brazil); A. Cárdenas (Universidad Eafit, Colombia); and N. Pérez-Consuegra (Syracuse University). The constant help of L. Londoño (STRI) is also acknowledged.

We thank Carlos Rosero for managing all the logistics in the field in Colombia. We also extend thanks to the communities of Warpana, Patajau, Aulechit, Nazareth, Wososopo, Sillamana, Paraguachon, La Flor de la Guajira, and Ipapura, as well as to the Colombian National Police (Castilletes base) and the Colombian Army. We express special thanks to our drivers, Grillo, Lalo, and Medardo.

We thank M. L. Parra and the Centro de Investigaciones Paleontológicas in Villa de Leyva for the preparation of the specimens from the Cocinetas Basin. We thank J. E. Arenas, M. Pardo-Jaramillo (Servicio Geológico Colombiano), J. Escobar (Universidad del Norte), L. Costeur (NMB), G. Billet (MNHN), P. Brewer (NHMUK), A. Kramarz, S. Alvarez (MACN), M. Reguero, A. Scarano (MLP), G. Ojeda (UNEFM-CIAAP), and H. Moreno (Museo de Ciencias, Caracas) for allowing access to the collections under their care.

We are grateful to J. D. Carrillo-Briceño, T. M. Scheyer (PIMUZ), C. Pimiento (Museum für Naturkunde, Germany), A. A. Carlini (MLP), A. Forasiepi (Instituto Argentino de Nivología, Glaciología y Ciencias Ambientales [IANIGLA], CCT-CONICET, Argentina), R. Salas-Gismondi, J. W. Moreno-Bernal (Universidad del Norte), G. Billet (MNHN), R. J. Asher (University of Cambridge), M. Pardo (Servicio Geológico Colombiano), and the Evolutionary Morphology and Palaeobiology of Vertebrates group in Zurich for valuable advice.

Graphic reconstructions of the faunas (Figures 30–35) were made by S. Lukac. C. Ziegler shot the photo in Figure 3d; L. Goodayle took the photos shown in Figure 15, which were provided by the NHMUK; G. Billet (MNHN) provided pictures from the YPM collections (Figure 10c,d,l,m); and L. Costeur (NMB) provided pictures of *X. christi* in Figure 7a,b,c.

Our research was supported by Swiss National Fund P1ZHP3_165068 to J. D. Carrillo and by SNF 31003A-149605 and 31003A-169395 to M. R. Sánchez-Villagra. E. Amson was granted a short-term postdoctoral fellowship by STRI and was subsequently funded by the Alexander von Humboldt Foundation. The Swiss National Science Foundation, the Smithsonian Institution, the National Geographic Society, the Anders Foundation, Gregory D. and Jennifer Walston Johnson, Universidad del Norte, and the National Science Foundation (Grant EAR 0957679) also helped to support this work.

We thank D. Croft and an anonymous reviewer for their comments that improved the manuscript, as well as G. Minkiewicz, C. Doran, and M. McQuoid-Greason for editorial assistance.

References

Aguilera, O. A., J. Lundberg, J. Birindelli, M. Sabaj Pérez, C. Jaramillo, and M. R. Sánchez-Villagra. 2013a. Palaeontological Evidence for the Last Temporal Occurrence of the Ancient Western Amazonian River Outflow into the Caribbean. *PLoS ONE*, 8(9):e76202. https://doi.org/10.1371/journal.pone.0076202.

Aguilera, O. A., H. Moraes-Santos, S. Costa, F. Ohe, C. Jaramillo, and A. Nogueira. 2013b. Ariid Sea Catfishes from the Coeval Pirabas (Northeastern Brazil), Cantaure, Castillo (Northwestern Venezuela) and Castilletes (North Colombia) Formations (Early Miocene), with Description of Three New Species. *Swiss Journal of Palaeontology*, 132(1):45–68. https://doi.org/10.1007/s13358-013-0052-4.

Aguirre-Fernández, G., J. D. Carrillo-Briceño, R. Sánchez, E. Amson, and M. R. Sánchez-Villagra. 2017a. Fossil Cetaceans (Mammalia, Cetacea) from the Neogene of Colombia and Venezuela. *Journal of Mammalian Evolution,* 24(1):71–90. https://doi.org/10.1007/s10914-016-9353-x.

Aguirre-Fernández, G., B. Mennecart, M. R. Sánchez-Villagra, R. Sánchez, and L. Costeur. 2017b. A Dolphin Fossil Ear Bone from the Northern Neotropics—Insights into Habitat Transitions in Iniid Evolution. *Journal of Vertebrate Paleontology*, e1315817. https://doi.org/10.1080/02724634.2017.1315817.

Ameghino, F. 1887. Enumeración sistemática de las especies de mamíferos fósiles coleccionados por Carlos Ameghino en los terrenos eocenos de la Patagonia austral y depositados en el Museo La Plata. *Boletín del Museo de La Plata,* 1:1–26.

Ameghino, F. 1889. Contribución al conocimiento de los mamíferos fósiles de la República Argentina. *Actas Academia Nacional Ciencias Córdoba*, 6:1–1027.

Ameghino, F. 1895. Première contribution à la connaissance de la faune mammalogique des couches à *Pyrotherium*. *Boletín Del Instituto Geográfico Argentino,* 15:603–660.

Ameghino, F. 1897. Mammifères crétacés de l'Argentine. Deuxième contribution à la connaissance de la faune mammalogique des couches à *Pyrotherium*. *Boletín Del Instituto Geográfico Argentino*, 18:405–521.

Ameghino, F. 1902. Première contribution à la connaissance de la faune mammalogique des couches a *Colpodon*. *Boletín de La Academia Nacional de Ciencias de Córdoba,* 17:71–138.

Ameghino, F. 1904. Rechérches de morphologie phylogénétique sur les molaires supérieures des ongulés. *Anales Del Museo Nacional de Buenos Aires,* III:1689–1699.

Amson, E., J. D. Carrillo, and C. Jaramillo. 2016. Neogene Sloth Assemblages (Mammalia, Pilosa) of the Cocinetas Basin (La Guajira, Colombia): Implications for the Great American Biotic Interchange. *Palaeontology*, 59(4): 563–582. https://doi.org/10.1111/pala.12244

Antoine, P.-O., L. Marivaux, D. A. Croft, G. Billet, M. Ganerød, C. Jaramillo, T. Martin, M. J. Orliac, J. Tejada, A. J. Altamirano, F. Duranthon, G. Fanjat, S. Rousse, and R. Salas-Gismondi. 2012. Middle Eocene Rodents from Peruvian Amazonia Reveal the Pattern and Timing of Caviomorph Origins and Biogeography. *Proceedings of the Royal Society B: Biological Sciences*, 279:1319–1326. https://doi.org/10.1098/rspb.2011.1732

Antoine, P.-O., R. Salas-Gismondi, F. Pujos, M. Ganerød, and L. Marivaux. 2016. Western Amazonia as a Hotspot of Mammalian Biodiversity throughout the Cenozoic. *Journal of Mammalian Evolution,* 24(1):5–17. https://doi.org/10.1007/s10914-016-9333-1

Bacon, C. D., P. Molnar, A. Antonelli, A. J. Crawford, C. Montes, and M. C. Vallejo-Pareja. 2016. Quaternary Glaciation and the Great American Biotic Interchange. *Geology*, 44:375–378. https://doi.org/10.1130/g37624.1

Bacon, C. D., D. Silvestro, C. Jaramillo, B. T. Smith, P. Chakrabarty, and A. Antonelli. 2015. Biological Evidence Supports an Early and Complex Emergence of the Isthmus of Panama. *Proceedings of the National Academy of Sciences of the United States of America*, 112(19):6110–6115. https://doi.org/10.1073/pnas.1423853112

Barnosky, A. D., and E. L. Lindsey. 2010. Timing of Quaternary Megafaunal Extinction in South America in Relation to Human Arrival and Climate Change. *Quaternary International,* 217(1–2):10–29. https://doi.org/10.1016/j.quaint.2009.11.017

Bengtson, P. 1988. Open Nomenclature. *Palaeontology*, 31(1):223–227.

Bermudez, P. J., and H. M. Bolli. 1969. Consideraciones sobre los sedimentos del Mioceno medio al reciente de las costas central y oriental de Venezuela. Tercera parte: Los foraminíferos planctónicos. *Boletín de Geología, Ministerio de Minas e Hidrocarburos*, 10/20:137–223.

Billet, G. 2010. New Observations on the Skull of *Pyrotherium* (Pyrotheria, Mammalia) and New Phylogenetic Hypotheses on South American Ungulates. *Journal of Mammalian Evolution*, 17(1):21–59. https://doi.org/10.1007/s10914-009-9123-0

Billet, G. 2011. Phylogeny of the Notoungulata (Mammalia) Based on Cranial and Dental Characters. *Journal of Systematic Palaeontology*, 9(4):481–497. https://doi.org/10.1080/14772019.2010.528456

Billet, G., and T. Martin. 2011. No Evidence for an Afrotherian-like Delayed Dental Eruption in South American Notoungulates. *Naturwissenschaften*, 98(6):509–517. https://doi.org/10.1007/s00114-011-0795-y

Blow, W. H. 1969. Late Middle Eocene to Recent Planktonic Foraminiferal Biostratigraphy. *Proceedings of the First International Conference on Planktonic Microfossils, Geneva, 1967*, 1:199–421.

Bolli, H. M., J. P. Beckmann, and J. B. Saunders. 1994. *Benthic Foraminiferal Biostratigraphy of the South Caribbean Region*. London: Cambridge University Press.

Bond, M. 2016. "Ungulados nativos de Sudamérica. Una corta síntesis." In *Historia evolutiva y paleobiogeográfica de los vertebrados de América del Sur*, ed. F. L. Agnolin, G. L. Lio, F. Brissón Egli, N. R. Chimento, and F. E. Novas, pp. 293–301. Buenos Aires: Contribuciones del MACN.

Bond, M., and J. N. Gelfo. 2010. "The South American Native Ungulates of the Urumaco Formation." In *Urumaco and Venezuelan Paleontology: The Fossil Record of the Northern Neotropics*, ed. M. R. Sánchez-Villagra, O. A. Aguilera, and A. A. Carlini, pp. 256–268. Bloomington: Indiana University Press.

Bond, M., and G. López. 1995. Los mamíferos de la Formación Casa Grande (Eoceno) de la Provincia de Jujuy, Argentina. *Ameghiniana*, 32:310–309.

Bond, M., R. H. Madden, and A. A. Carlini. 2006. A New Specimen of Toxodontidae (Notoungulata) from the Urumaco Formation (Upper Miocene) of Venezuela. *Journal of Systematic Palaeontology,* 4(3):285–291. https://doi.org/10.1017/S1477201906001854

Bond, M., D. Perea, M. Ubilla, and A. Tauber. 2001. *Neolicaphrium recens* Frenguelli, 1921, the Only Surviving Proterotheriidae (Litopterna, Mammalia) into the South American Pleistocene. *Palaeovertebrata,* 30(1–2):37–50.

Bond, M., M. F. Tejedor, K. E. Campbell, L. Chornogubsky, N. Novo, and F. Goin. 2015. Eocene Primates of South America and the African Origins of New World Monkeys. *Nature,* 520:538–541. https://doi.org/10.1038/nature14120.

Bonini, R. A., G. I. Schmidt, M. A. Reguero, E. Cerdeño, A. M. Candela, and N. Solís. 2017a. First Record of Toxodontidae (Mammalia, Notoungulata) from the Late Miocene–Early Pliocene of the Southern Central Andes, NW Argentina. *Journal of Paleontology*, 91(3): 566-576. https://doi.org/10.1017/jpa.2016.160.

Bonini, R. A., G. I. Schmidt, M. A. Reguero, E. Cerdeño, A. M. Candela, and N. Solís. 2017b. Data from: First Record of Toxodontidae (Mammalia, Notoungulata) from the Late Miocene–Early Pliocene of the Southern Central Andes, NW Argentina. *Dryad Digital Repository*. https://doi.org/10.5061/dryad.3111m.

Buckley, M. 2015. Ancient Collagen Reveals Evolutionary History of the Endemic South American "Ungulates." *Proceedings of the Royal Society B: Biological Sciences*, 282(1806):20142671. https://doi.org/10.1098/rspb.2014.2671.

Cabrera, A. 1929. Un astrapoterido de Colombia. *Comunicaciones de La Sociedad Argentina de Ciencias Naturales*, 9:436–443.

Cadena, E., and C. Jaramillo. 2015a. Early to Middle Miocene Turtles from the Northernmost tip of South America: Giant Testudinids, Chelids, and Podocnemidids from the Castilletes Formation, Colombia. *Ameghiniana*, 52:188–203. https://doi.org/10.5710/AMGH.10.11.2014.2835.

Cadena, E. A., and C. A. Jaramillo. 2015b. The First Fossil Skull of *Chelus* (Pleurodira: Chelidae, Matamata turtle) from the Early Miocene of Colombia. *Paleontologia Electronica*, 18.2.32A:1–10.

Captain, D. M., and L. B. Captain. 2005. *Diccionario Basico Ilustrado: Wayuunaiki–Espanol, Espanol–Wayuunaiki*. Bogotá: Editorial Buena Semilla.

Carlini, A. A. 2010. Fossil Xenarthran Mammals from Venezuela—Taxonomy, Patterns of Evolution and Associated Faunas. Ph.D. diss., University of Zurich, Switzerland.

Carlini, A. A., D. Brandoni, and R. Sánchez. 2006a. First Megatheriines (Xenarthra, Phyllophaga, Megatheriidae) from the Urumaco (Late Miocene) and Codore (Pliocene) Formations, Estado Falcón, Venezuela. *Journal of Systematic Palaeontology*, 4(3):269–278. https://doi.org/10.1017/S1477201906001878.

Carlini, A. A., D. Brandoni, and R. Sánchez. 2008a. Additions to the Knowledge of *Urumaquia robusta* (Xenarthra, Phyllophaga, Megatheriidae) from the Urumaco Formation (Late Miocene), Estado Falcón, Venezuela. *Paläontologische Zeitschrift*, 82(2):153–162. https://doi.org/10.1007/BF02988406.

Carlini, A. A., J. N. Gelfo, and R. Sánchez. 2006b. A New Megadolodinae (Mammalia, Litopterna, Protherotheriidae) from the Urumaco Formation (Late Miocene) of Venezuela. *Journal of Systematic Palaeontology,* 4(3):279–284. https://doi.org/10.1017/S1477201906001830

Carlini, A. A., G. J. Scillato-Yané, and R. Sánchez. 2006c. New Mylodontoidea (Xenarthra, Phyllophaga) from the Middle Miocene–Pliocene of Venezuela. *Journal of Systematic Palaeontology*, 4(3):255–267. https://doi.org/10.1017/s147720190600191x.

Carlini, A. A., A. E. Zurita, G. J. Scillato-Yané, R. Sánchez, and O. A. Aguilera. 2008b. New Glyptodont from the Codore Formation (Pliocene), Falcón State, Venezuela, its Relationship with the *Asterostemma* Problem, and the Paleobiogeography of the Glyptodontinae. *Paläontologische Zeitschrift*, 82(2):139–152. https://doi.org/10.1007/BF02988405.

Carrillo, J. D., E. Amson, C. Jaramillo, R. Sánchez, L. Quiroz, C. Cuartas, A. F. Rincón, M. R. Sánchez-Villagra. 2018a. 3D Models Related to the Publication: The Neogene Record of Northern South American Native Ungulates. *MorphoMuseuM*, 4:e61. https://doi.org/10.18563/journal.m3.61.

Carrillo, J. D., E. Amson, C. Jaramillo, R. Sánchez, L. Quiroz, C. Cuartas, A. F. Rincón, M. R. Sánchez-Villagra. 2018b. Data from: The Neogene Record of Northern South American Native Ungulates. *Dryad Digital Repository*. https://doi.org/10.5061/dryad.m1n44.

Carrillo, J. D., and R. J. Asher. 2017. An Exceptionally Well-Preserved Skeleton of *Thomashuxleya externa* (Mammalia, Notoungulata), from the Eocene of Patagonia, Argentina. *Paleontologia Electronica*, 20.2.35A:1–33.

Carrillo, J. D., A. Forasiepi, C. Jaramillo, and M. R. Sánchez-Villagra. 2015. Neotropical Mammal Diversity and the Great American Biotic Interchange: Spatial and Temporal Variation in South America's Fossil Record. *Frontiers in Genetics*, 5:451. https://doi.org/10.3389/fgene.2014.00451.

Carrillo, J. D., and M. R. Sánchez-Villagra. 2015. Giant Rodents from the Neotropics: Diversity and Dental Variation of Late Miocene Neoepiblemid Remains from Urumaco, Venezuela. *Paläontologische Zeitschrift*, 89(4):1057–1071. https://doi.org/10.1007/s12542-015-0267-3.

Cassini, G. H., E. Cerdeño, A. L. Villafañe, and N. A. Muñoz. 2012. "Paleobiology of Santacrucian Native Ungulates (Meridungulata: Astrapotheria, Litopterna and Notoungulata)." In *Early Miocene Paleobiology in Patagonia: High Latitude Paleocommunities of the Santa Cruz Formation*, ed. S. F. Vizcaíno, R. F. Kay, and M. S. Bargo, pp. 243–286. Cambridge, UK: Cambridge University Press.

Castro, M. C., A. A. Carlini, R. Sánchez, and M. R. Sánchez-Villagra. 2014. A New Dasypodini Armadillo (Xenarthra: Cingulata) from San Gregorio Formation, Pliocene of Venezuela: Affinities and Biogeographic Interpretations. *Naturwissenschaften*, 101(2):77–86. https://doi.org/10.1007/s00114-013-1131-5.

Cerdeño, E., and B. Vera. 2015. A New Leontiniidae (Notoungulata) from the Late Oligocene Beds of Mendoza Province, Argentina. *Journal of Systematic Palaeontology*, 13(11):943–962. https://doi.org/10.1080/14772019.2014.982727.

Cifelli, R. L. 1983. The Origin and Affinities of the South American Condylarthra and Early Tertiary Litopterna (Mammalia). *American Museum Novitates*, 2772:1–49.

Cifelli, R. L. 1993. "The Phylogeny of the Native South American Ungulates." In *Mammal Phylogeny, Placentals*, ed. F. S. Szalay, M. J. Novacek, and M. C. McKenna, pp. 195–214. New York: Springer-Verlag.

Cifelli, R. L., and J. Guerrero. 1989. New Remains of *Prothoatherium colombianus* (Litopterna, Mammalia) from the Miocene of Colombia. *Journal of Vertebrate Paleontology,* 9(2):222–231.

Cifelli, R. L., and J. Guerrero. 1997. "Litopterns." In *Vertebrate Paleontology in the Neotropics: The Miocene Fauna of La Venta, Colombia,* ed. R. F. Kay, R. H. Madden, R. L. Cifelli, and J. J. Flynn, pp. 289–302. Washington, D.C.: Smithsonian Institution Press.

Cifelli, R. L., and C. Villarroel. 1997. "Paleobiology and Affinities of *Megadolodus*." In *Vertebrate Paleontology in the Neotropics: The Miocene Fauna of La Venta, Colombia,* ed. R. F. Kay, R. H. Madden, R. L. Cifelli, and J. J. Flynn, pp. 265–288. Washington, D.C.: Smithsonian Institution Press.

Cione, A. L., G. M. Gasparini, E. Soibelzon, L. H. Soibelzon, and E. P. Tonni. 2015. "The GABI in Southern South America." In *The Great American*

Biotic Interchange: A South American Perspective, ed. A. L. Cione, G. M. Gasparini, E. Soibelzon, L. H. Soibelzon, and E. P. Tonni, pp. 71–96. Dordrecht: Springer Netherlands.

Cione, A. L., and E. P. Tonni. 1999. Biostratigraphy and Chronological Scale of Uppermost Cenozoic in Pampean Area. *Quaternary of South America and Antarctic Peninsula*, 3:23–51.

Cione, A. L., and E. P. Tonni. 2001. Correlation of Pliocene to Holocene Southern South American and European Vertebrate-Bearing Units. *Bollettino della Società Paleontologica Italiana*, 40:167–173.

Cione, A. L., E. P. Tonni, and E. Soibelzon. 2003. The Broken Zig-Zag: Late Cenozoic Large Mammal and Tortoise Extinction in South America. *Revista Del Museo Argentino de Ciencias Naturales*, 51:1–19.

Cisneros, J. C. 2005. New Pleistocene Vertebrate Fauna from El Salvador. *Revista Brasileira de Paleontologia*, 8:239–255.

Cody, S., J. E. Richardson, V. Rull, C. Ellis, and R. T. Pennington. 2010. The Great American Biotic Interchange Revisited. *Ecography,* 33(2):326–332. https://doi.org/10.1111/j.1600-0587.2010.06327.x.

Croft, D. A. 1999. "Placentals: Endemic South American Ungulates." In *Encyclopedia of Paleontology*, Volume 2, ed. R. Singer, pp. 890–906. Chicago: Fitzroy Dearborn Publishers.

Croft, D. A. 2012. "Punctuated isolation. The Making and Mixing of South America's Mammals." In *Bones, Clones, and Biomes: The History and Geography of Recent Neotropical Mammals,* ed. B. D. Patterson and L. P. Costa, pp. 9–19. Chicago: University of Chicago Press.

Croft, D. A. 2016. *Horned Armadillos and Rafting Monkeys: The Fascinating Fossil Mammals of South America*. Bloomington: Indiana University Press.

Croft, D. A., A. A. Carlini, M. R. Ciancio, D. Brandoni, N. E. Drew, R. K. Engelman, and F. Anaya. 2016. New Mammal Faunal Data from Cerdas, Bolivia, a Middle-Latitude Neotropical Site that Chronicles the End of the Middle Miocene Climatic Optimum in South America. *Journal of Vertebrate Paleontology*, 36(5):e1163574. https://doi.org/10.1080/02724634.2016.1163574.

Croft, D. A., and D. Weinstein. 2008. The First Application of the Mesowear Method to Endemic South American Ungulates (Notoungulata). *Palaeogeography, Palaeoclimatology, Palaeoecology*, 269(1–2):103–114. https://doi.org/10.1016/j.palaeo.2008.08.007.

Damuth, J. 1990. "Problems in Estimating Body Masses of Archaic Ungulates Using Dental Measurements." In *Body Size in Mammalian Paleobiology: Estimation and Biological Implications,* ed. J. Damuth and B. J. MacFadden, pp. 229–253. Cambridge, UK: Cambridge University Press.

Dentzien-Dias, P., J. D. Carrillo-Briceño, H. Francischini, R. Sánchez. 2018. Paleoecological and Taphonomical Aspects of the Late Miocene Vertebrate Coprolites (Urumaco Formation) of Venezuela. *Palaeogeography, Palaeoclimatology, Palaeoecology*, 490:590–603. https://doi.org/10.1016/J.PALAEO.2017.11.048.

Díaz de Gamero, M. L. 1977a. Estratigrafía y micropaleontología del Oligoceno y Mioceno inferior del centro de la cuenca de Falcón, Venezuela. *GEOS*, 22:2–50.

Díaz de Gamero, M. L. 1977b. "Revisión de las unidades litoestratigráficas en Falcón central en base a su contenido de foraminíferos planctónicos." In *Memorias V Congreso Geológico de Venezuela*, Volume 1, pp. 81–86. Caracas: Sociedad Venezolana de Geólogos.

Díaz de Gamero, M. L. 1985a. "Estratigrafía de Falcón Nororiental." In *Memorias VI Congreso Geológico de Venezuela*, Volume 1, pp. 454–502. Caracas: Sociedad Venezolana de Geólogos.

Díaz de Gamero, M. L. 1985b. "Micropaleontología de la Formación Agua Salada, Falcón Nororiental." In *Memorias VI Congreso Geológico de Venezuela*, Volume 1, pp. 384–453. Caracas: Sociedad Venezolana de Geólogos.

Díaz de Gamero, M. L. 1989. El Mioceno Temprano y Medio de Falcón septentrional. *GEOS*, 29:25–35.

Díaz de Gamero, M. L. 1996. The Changing Course of the Orinoco River during the Neogene: A Review. *Palaeogeography, Palaeoclimatology, Palaeoecology*, 123:385–402.

Díaz de Gamero, M. L., and O. J. Linares. 1989. "Estratigrafía y paleontología de la Formación Urumaco, del Mioceno tardío de Falcón noroccidental." In *Memorias VII Congreso Geológico de Venezuela*, Volume 1, pp. 419–439. Caracas: Sociedad Venezolana de Geólogos.

Díaz de Gamero, M. L., V. Mitacchione, and M. Ruiz. 1988. La Formación Querales en su área tipo, Falcón noroccidental, Venezuela. *Boletín Sociedad Venezolana de Geología*, 34:34–46.

Eizirik, E. 2012. "A Molecular View on the Evolutionary History and Biogeography of Neotropical Carnivores (Mammalia, Carnivora)." In *Bones, Clones, and Biomes: The History and Geography of Recent Neotropical Mammals,* ed. B. D. Patterson and L. P. Costa, pp. 123–142. Chicago: University of Chicago Press.

Elissamburu, A. 2012. Estimación de la masa corporal en géneros del Orden Notoungulata. *Estudios Geológicos*, 68:91–111.

Fariña, R. A., S. F. Vizcaíno, and M. S. Bargo. 1998. Body Mass Estimations in Lujanian (Late Pleistocene–Early Holocene of South America) Mammal Megafauna. *Matozoología Neotropical*, 5:87–108.

Flynn, J. J., and C. C. Swisher. 1995. Cenozoic South American Land Mammal Ages: Correlation to Global Geochronology. *Geochronology Time Scales and Global Stratigraphic Correlation, SEPM Special Publication*, 54:317–333.

Forasiepi, A. M., E. Cerdeño, M. Bond, G. I. Schmidt, M. Naipauer, F. R. Straehl, A. G. Martinelli, A. C. Garrido, M. D. Schmitz, and J. L. Crowley. 2015. New toxodontid (Notoungulata) from the Early Miocene of Mendoza, Argentina. *Paläontologische Zeitschrift*, 89(3):611–634. https://doi.org/10.1007/s12542-014-0233-5.

Forasiepi, A.M., R. D. E. MacPhee, S. Hernández del Pino, G. I. Schmidt, E. Amson, and C. Grohe. 2016. Exceptional Skull of *Huaqueriana* (Mammalia, Litopterna, Macraucheniidae) from the Late Miocene of Argentina: Anatomy, Systematics, and Paleobiological Implications. *Bulletin of the American Museum of Natural History*, 404:1–76. https://doi.org/10.5531/sd.sp.23.

Forasiepi, A. M., L. H. Soibelzon, C. Suarez-Gomez, R. Sánchez, L. I. Quiroz, C. Jaramillo, and M. R. Sánchez-Villagra. 2014. Carnivorans at the Great American Biotic Interchange: New Discoveries from the Northern Neotropics. *Naturwissenschaften*, 101(11):965–974. https://doi.org/10.1007/s00114-014-1237-4.

Gasparini, G. M., M. De los Reyes, A. Francia, C. S. Scherer, D. G. Poiré. 2017. The Oldest Record of *Hemiauchenia* Gervais and Ameghino (Mammalia, Cetartiodactyla) in South America: Comments about its Paleobiogeographic and Stratigraphic Implications. *Geobios*, 50(2):141–351. https://doi.org/10.1016/j.geobios.2016.12.003.

Geiger, M., L. A. B. Wilson, L. Costeur, R. Sánchez, M. R. Sánchez-Villagra. 2013. Diversity and Growth in Giant Caviomorphs from the Northern Neotropics: A Study of Femoral Variation in *Phoberomys* (Rodentia). *Journal of Vertebrate Paleontology*, 33(6):1449–1456. https://doi.org/10.1080/02724634.2013.780952.

Gelfo, J. N., F. J. Goin, M. O. Woodburne, and C. de Muizon. 2009. Biochronological Relationships of the Earliest South American Paleogene Mammalian Faunas. *Palaeontology*, 52(1):251–269. https://doi.org/10.1111/j.1475-4983.2008.00835.x.

Gervais, H. 1847. Observations sur les mammifères fossiles du midi de la France. *Annales de Sciences Naturelles, Zoologie*, 3:203–224.

Giannini, N., and D. García-López. 2014. Ecomorphology of Mammalian Fossil Lineages: Identifying Morphotypes in a Case Study of Endemic South American Ungulates. *Journal of Mammalian Evolution*, 21(2):195–212. https://doi.org/10.1007/s10914-013-9233-6.

Goillot, C., P.-O. Antoine, J. Tejada, F. Pujos, and R. Salas-Gismondi. 2011. Middle Miocene Uruguaytheriinae (Mammalia, Astrapotheria) from Peruvian Amazonia and a Review of the Astrapotheriid Fossil Record in Northern South America. *Geodiversitas*, 33(2):331–345. https://doi.org/10.5252/g2011n2a8.

Goloboff, P. A. 2014. Extended Implied Weighting. *Cladistics*, 30(3):260–272. https://doi.org/10.1111/cla.12047.

Goloboff, P. A., J. M. Carpenter, J. S. Arias, and D. R. M. Esquivel. 2008. Weighting Against Homoplasy Improves Phylogenetic Analysis of Morphological Datasets. *Cladistics*, 24:758–773. https://doi.org/10.1111/j.1096-0031.2008.00209.x.

Gomes-Rodrigues, H., A. Herrel, and G. Billet. 2017. Ontogenetic and Life History Trait Changes Associated with Convergent Ecological Specializations in Extinct Ungulate Mammals. *Proceedings of the National Academy of Sciences*,114(5):1069–1074. https://doi.org/10.1073/pnas.1614029114.

Gonzalez de Juana, C., J. M. Iturralde de Arozena, and X. Picard Cadillat. 1980. *Geología de Venezuela y sus cuencas petrolíferas*. Caracas: FONINVES.

Gradstein, F. M., J. G. Ogg, M. D. Schmitz, and G. M. Ogg. 2012. *The Geological Time Scale 2012*. Volume 2. Amsterdam: Elsevier.

Grand, A., A. Corvez, L. M. Duque-Velez, and M. Laurin. 2013. Phylogenetic Inference Using Discrete Characters: Performance of Ordered and Unordered Parsimony and of Three-Item Statements. *Biological Journal of the Linnean Society*, 110(4):914–930. https://doi.org/10.1111/bij.12159.

Gray, J. E. 1821. On the natural arrangement of vertebrate animals. *London Medical Repository*, 15:296–310.

Guérin, C., and M. Faure. 2013. Un nouveau Toxodontidae (Mammalia, Notoungulata) du Pléistocène supérieur du Nordeste du Brésil. *Geodiversitas*, 35(1):155–205. https://doi.org/10.5252/g2013n1a7.

Guerra, A., and S. Mederos. 1988. Estudio sedimentológico y bioestratigráfico de una zona ubicada entre las poblaciones de Urumaco y Sabaneta, estado Falcón. Undergraduate diss., Universidad Central de Venezuela, Caracas.

Hambalek, N. 1993. Palinoestratigrafia del Mioceno-Plioceno de la región de Urumaco, Falcón Noroccidental. Undergraduate diss., Universidad Central de Venezuela.

Harrison, J. A. 1985. *Giant Camels from the Cenozoic of North America*. Smithsonian Contributions to Paleobiology, No. 57. Washington, D.C.: Smithsonian Institution Press.

Heintzman, P. D., G. D. Zazula, J. A. Cahill, A. V. Reyes, R. D. E. MacPhee, and B. Shapiro. 2015. Genomic Data from Extinct North American *Camelops* Revise Camel Evolutionary History. *Molecular Biology and Evolution*, 32(9):2433–240. https://doi.org/10.1093/molbev/msv128.

Hendy, A. J. W., D. S. Jones, F. Moreno, V. Zapata, and C. Jaramillo. 2015. Neogene Molluscs, Shallow Marine Paleoenvironments, and Chronostratigraphy of the Guajira Peninsula, Colombia. *Swiss Journal of Palaeontology*, 134(1):45–75. https://doi.org/10.1007/s13358-015-0074-1.

Herrera, C. 2008. Estratigrafía de la Formación Urumaco y geología estructural entre el Domo de Agua Blanca y Hato Viejo (Edo. Falcón). Master's diss., Universidad Simón Bolivar, Caracas, Venezuela.

Hoffstetter, R., and M. F. Soria. 1986. *Neodolodus colombianus* gen. et sp. nov., un nouveau Condylarthre (Mammalia) dans le Miocène de Colombie. *Comptes Rendus de l'Académie Des Sciences, Paris*, series II, 3 03(17):1619–1622.

Hopwood, A. T. 1928. *Gyrinodon quassus*, a new Genus and Species of Toxodont from Western Buchivacoa (Venezuela). *Quarterly Journal of the Geological Society of London*, 84:573–583.

Horovitz, I. 2004. Eutherian Mammal Systematics and the Origins of South American Ungulates as Based on Postcranial Osteology. *Bulletin of Carnegie Museum of Natural History*, 36:63–79. https://doi.org/10.2992/0145-9058(2004)36[63:emsato]2.0.co;2.

Horovitz, I., M. R. Sánchez-Villagra, T. Martin, and O. A. Aguilera. 2006. The Fossil Record of *Phoberomys pattersoni* Mones 1980 (Mammalia, Rodentia) from Urumaco (Late Miocene, Venezuela), with an Analysis of its Phylogenetic Relationships. *Journal of Systematic Palaeontology*, 4(3):293–306. https://doi.org/10.1017/S1477201906001908.

Horovitz, I., M. R. Sánchez-Villagra, M. G. Vucetich, and O. A. Aguilera. 2010. "Fossil Rodents from the Late Miocene Urumaco and Middle Miocene Cumaca Formations, Venezuela." In *Urumaco and Venezuelan Paleontology: The Fossil Record of the Northern Neotropics,* ed. M. R. Sánchez-Villagra, O. A. Aguilera, and A. A. Carlini, pp. 214–232. Bloomington: Indiana University Press.

Houssaye, A., V. Fernandez, and G. Billet. 2016. Hyperspecialization in Some South American Endemic Ungulates Revealed by Long Bone Microstructure. *Journal of Mammalian Evolution*, 23(3):221–235. https://doi.org/10.1007/s10914-015-9312-y.

Janis, C. M. 1990. "Correlation of Cranial and Dental Variables with Body Size in Ungulates and Macropodoids." In *Body Size in Mammalian Palaeobiology: Estimation and Biological Implications*, ed. J. Damuth and B. J. MacFadden, pp. 255–299. Cambridge, UK: Cambridge University Press.

Janis, C. M. 2000. "Patterns in the Evolution of Herbivory in Large Terrestrial Mammals: The Paleogene of North America." In *Evolution of Herbivory in Terrestrial Vertebrates: Perspectives from the Fossil Record*, ed. H.-D. Sues, pp. 168–222. Cambridge, UK: Cambridge University Press.

Jaramillo, C., F. Moreno, A. J. W. Hendy, M. R. Sánchez-Villagra, and D. Marty. 2015. Preface: La Guajira, Colombia: A New Window into the Cenozoic Neotropical Biodiversity and the Great American Biotic Interchange. *Swiss Journal of Palaeontology*, 134(1):1–4. https://doi.org/10.1007/s13358-015-0075-0.

Jaramillo, C. 2018. "Evolution of the Isthmus of Panama: Biological, Paleoceanographic and Paleoclimatological Implications." In *Mountains, Climate and Biodiversity*, ed. C. Hoorn, A. Perrigo, and A. Antonelli, pp. 323–338. Oxford, UK: Wiley-Blackwell Publishing.

Johnson, S. C. 1984. Astrapotheres from the Miocene of Colombia, South America. Ph.D. diss., University of California, Berkeley.

Johnson, S. C., and R. H. Madden. 1997. "Uruguaytheriine Astrapotheres of Tropical South America." In *Vertebrate Paleontology in the Neotropics: The Miocene Fauna of La Venta*, ed. R. F. Kay, R. H. Madden, R. L. Cifelli, and J. J. Flynn, pp. 355–381. Washington, D.C.: Smithsonian Institution Press.

Kay, R. F., S. F. Vizcaíno, and M. S. Bargo. 2012. "A Review of the Paleoenvironment and Paleoecology of the Miocene Santa Cruz Formation." In *Early Miocene Paleobiology in Patagonia: High Latitude Paleocommunities of the Santa Cruz Formation,* ed. S. F. Vizcaíno, R. F. Kay, and S. Bargo, pp. 331–365. Cambridge, UK: Cambridge University Press.

Koepfli, K. P., M. E. Gompper, E. Eizirik, C. C. Ho, L. Linden, J. E. Maldonado, and R. K. Wayne. 2007. Phylogeny of the Procyonidae (Mammalia: Carnivora): Molecules, Morphology and the Great American Interchange. *Molecular Phylogenetics and Evolution*, 43:1076–1095. https://doi.org/10.1016/j.ympev.2006.10.003.

Kraglievich, L. 1928. *Sobre el supuesto* Astrapotherium christi *Stehlin descubierto en Venezuela (*Xenastrapotherium *n. gen) y sus relaciones con* Astrapotherium magnum *y* Uruguaytherium beaulieui. Buenos Aires: La Editorial Franco.

Kramarz, A. G., and M. Bond. 2005. Los Litopterna (Mammalia) de la Formación Pinturas, Mioceno temprano-medio de Patagonia. *Ameghiniana*, 42:611–625.

Kramarz, A. G., and M. Bond. 2008. Revision of *Parastrapotherium* (Mammalia, Astrapotheria) and Other Deseadan Astrapotheres of Patagonia. *Ameghiniana*, 45:537–551.

Kramarz, A. G., and M. Bond. 2009. A New Oligocene Astrapothere (Mammalia, Meridiungulata) from Patagonia and a New Appraisal of Astrapothere Phylogeny. *Journal of Systematic Palaeontology*, 7(1):117–128. https://doi.org/10.1017/S147720190800268X.

Kramarz, A. G., and M. Bond. 2010. "Colhuehuapian Astrapotheriidae (Mammalia) from Gran Barranca south of Lake Colhue-Huapi." In *The Paleontology of Gran Barranca: Evolution and Environmental Change through the Middle Cenozoic of Patagonia,* ed. R. H. Madden, A. A. Carlini, M. G. Vucetich, R. F. Kay, pp. 182–192. Cambridge, UK: Cambridge University Press.

Kramarz, A., and M. Bond. 2011. A New Early Miocene Astrapotheriid (Mammalia, Astrapotheria) from Northern Patagonia, Argentina. *Neues Jahrbuch für Geologie und Paläontologie – Abhandlungen*, 260(3):277–287. https://doi.org/10.1127/0077-7749/2011/0132.

Kramarz, A., and M. Bond. 2013. On the Status of *Isolophodon* Roth, 1903 (Mammalia, Astrapotheria) and Other Little-Known Paleogene Astrapotheres from Central Patagonia. *Geobios*, 46(3):203–211. https://doi.org/10.1016/j.geobios.2012.10.015.

Kramarz, A., and M. Bond. 2014. Critical Revision of the Alleged Delayed Dental Eruption in South American "Ungulates." *Mammalian Biology*, 79(3):170–175. https://doi.org/10.1016/j.mambio.2013.11.001.

Kramarz, A. G., M. Bond, and A. M. Forasiepi. 2011. New Remains of *Astraponotus* (Mammalia, Astrapotheria) and Considerations on Astrapothere Cranial Evolution. *Paläontologische Zeitschrift*, 85:185–200. https://doi.org/10.1007/s12542-010-0087-4.

Kramarz, A., M. Bond, and G. W. Rougier. 2017. Re-Description of the Auditory Region of the Putative Basal Astrapothere (Mammalia) *Eoastrapostylops riolorense* Soria and Powell, 1981. Systematic and Phylogenetic Considerations. *Annals of Carnegie Museum*, 84(2):95–164. https://doi.org/10.2992/007.084.0204.

Kramarz, A. G., M. G. Vucetich, A. A. Carlini, M. R. Ciancio, M. A. Abello, C. M. Deschamps, and J. N. Gelfo. 2010. "A New Mammal Fauna at the Top of the Gran Barranca Sequence and its Biochronological Significance." In *The Paleontology of Gran Barranca: Evolution and Environmental Change through the Middle Cenozoic of Patagonia*, ed. R. H. Madden, A. A. Carlini, M. G. Vucetich, and R. F. Kay, pp. 264–277. Cambridge, UK: Cambridge University Press.

Laurito, C. A. 1993. Análisis topológico y sistemático del toxodonte de bajo de los Barrantes, Provincia de Alajuela, Costa Rica. *Revista Geológica de America Central*, 16:61–68.

Leigh, E. G., A. O'Dea, and G. J. Vermeij. 2014. Historical Biogeography of the Isthmus of Panama. *Biological Reviews*, 89(1):148–172. https://doi.org/10.1111/brv.12048.

Leite, R. N., S. O. Kolokotronis, F. C. Almeida, F. P. Werneck, D. S. Rogers, and M. Weksler. 2014. In the Wake of Invasion: Tracing the Historical Biogeography of the South American Cricetid Radiation (Rodentia, Sigmodontinae). *PloS ONE*, 9(6):e100687. https://doi.org/10.1371/journal.pone.0100687.

Linares, O. J. 2004. Bioestratigrafía de la fauna de mamíferos de las Formaciones Socorro, Urumaco y Codore (Mioceno Medio-Plioceno Temprano) de la región de Urumaco, Falcón, Venezuela. *Paleobiología Neotropical*, 1:1–26.

Loomis, F. B. 1914. *The Deseado Formation of Patagonia: Eighth Amherst Expedition.* Concord, N.H.: Rumford Press.

Lucas, S. G. 2008. Pleistocene Mammals from Yeroconte, Honduras. *New Mexico Museum of Natural History and Science Bulletin*, 44:403–408.

Lucas, S. G. 2014. Late Pleistocene mammals from El Hatillo, Panama. *Revista Geológica de América Central*, 50:139–151.

Lucas, S. G., G. E. Alvarado, and E. Vega. 1997. The Pleistocene Mammals of Costa Rica. *Journal of Vertebrate Paleontology*, 17:413–427.

Lundelius, E. L., V. M. Bryant, R. Mandel, K. J. Thies, and A. Thoms. 2013. The First Occurrence of a Toxodont (Mammalia, Notoungulata) in the United States. *Journal of Vertebrate Paleontology*, 33:1:229–232. https://doi.org/10.1080/02724634.2012.711405

Lunt, D., G. L. Foster, A. M. Haywood, and E. J. Stone. 2008. Late Pliocene Greenland Glaciation Controlled by a Decline in Atmospheric CO_2 Levels. *Nature*, 454(7208):1102–1105. https://doi.org/10.1038/nature07223

Lydekker, R. 1884. Contribution to the Knowledge of the Fossil Vertebrates of Argentina: A Study of Extinct Argentine Ungulates. *Anales Del Museo de La Plata*, 2:1–32.

MacFadden, B. J. 2005. Diet and Habitat of Toxodont Megaherbivores (Mammalia, Notoungulata) from the Late Quaternary of South and Central America. *Quaternary Research*, 64:113–124. https://doi.org/10.1016/j.yqres.2005.05.003

Madden, R. H. 1990. Miocene Toxodontidae (Notoungulata, Mammalia) from Colombia, Ecuador and Chile. Ph.D. diss., Duke University, Durham, North Carolina.

Madden, R. H. 1997. "A new Toxodontid Notoungulate." In *Vertebrate Paleontology in the Neotropics: The Miocene Fauna of La Venta,* ed. R. F. Kay, R. H. Madden, R. L. Cifelli, and J. J. Flynn, pp. 335–354. Washington, D.C.: Smithsonian Institution Press.

Madden, R. H. 2015. "Hypsodonty in the South American Fossil Record." In *Hypsodonty in Mammals: Evolution, Geomorphology and the Role of Earth Surface Processes*, pp. 12–59. Cambridge, UK: Cambridge University Press.

Madden, R. H., J. Guerrero, R. F. Kay, J. J. Flynn, C. C. Swisher III, and A. Watson. 1997. "The Laventan Stage and Age." In *Vertebrate Paleontology in the Neotropics: The Miocene Fauna of La Venta*, ed. R. F. Kay, R. H. Madden, R. L. Cifelli, and J. J. Flynn, pp. 499–519. Washington, D.C.: Smithsonian Institution Press.

Marshall, L. G., P. Salinas, and M. Suarez. 1990. *Astrapotherium* sp. (Mammalia, Astrapotheriidae) from Miocene Strata along the Quepuca River, Central Chile. *Revista Geologica de Chile*, 17:215–223.

Marshall, L. G., S. D. Webb, J. J. Sepkoski Jr., and D. M. Raup. 1982. Mammalian Evolution and the Great American Interchange. *Science*, 215:1351–1357. https://doi.org/10.1126/science.215.4538.1351.

McKenna, M. C. 1956. Survival of Primitive Notoungulates and Condylarths into the Miocene of Colombia. *American Journal of Science*, 254:736–743.

McKenna, M. C. 1975. "Towards a Phylogenetic Classification of the Mammalia." In *Phylogeny of Primates: A Multidisciplinary Approach,* ed. W. P. Luckett and F. S. Szalay, pp. 21–46. New York: Plenum Press.

McKenna, M. C., and S. K. Bell. 1997. *Classification of Mammals above the Species Level*. New York: Columbia University Press.

Mendoza, M., C. M. Janis, and P. Palmqvist. 2006. Estimating the Body Mass of Extinct Ungulates: A Study on the Use of Multiple Regression. *Journal of Zoology*, 270:90–101. https://doi.org/10.1111/j.1469-7998.2006.00094.x.

Mones, A. 1982. An Equivocal Nomenclature: What Means Hypsodonty? *Paläontologische Zeitschrift*, 56(1–2):107–111. https://doi.org/10.1007/BF02988789.

Moreno, F., A. J. W. Hendy, L. Quiroz, N. Hoyos, D. S. Jones, V. Zapata, S. Zapata, G. A. Ballen, E. Cadena, A. L. Cárdenas, J. D. Carrillo-Briceño, J. D. Carrillo, D. Delgado-Sierra, J. Escobar, J. I. Martínez, C. Martínez, C. Montes, J. Moreno, N. Pérez, R. Sánchez, C. Suárez, M. C. Vallejo-Pareja, and C. Jaramillo. 2015. Revised Stratigraphy of Neogene Strata in the Cocinetas Basin, La Guajira, Colombia. *Swiss Journal of Palaeontology*, 134(1):5–43. https://doi.org/10.1007/s13358-015-0071-4.

Moreno-Bernal, J. W., J. Head, and C. A. Jaramillo. 2016. Fossil Crocodilians from the High Guajira Peninsula of Colombia: Neogene Faunal Change in Northernmost South America. *Journal of Vertebrate Paleontology*, 36(3):e1110586. https://doi.org/10.1080/02724634.2016.1110586.

Muizon, C. de, and R. L. Cifelli. 2000. The "Condylarths" (Archaic Ungulata, Mammalia) from the Early Palaeocene of Tiupampa (Bolivia): Implications on the Origin of the South American Ungulates. *Geodiversitas*, 22(1):47–150.

Nasif, N. L., S. Musalem, and E. Cerdeño. 2000. A New Toxodont from the Late Miocene of Catamarca, Argentina, and a Phylogenetic Analysis of the Toxodontidae. *Journal of Vertebrate Paleontology*, 20(3):591–600. https://doi.org/10.1671/0272-4634(2000)020[0591:antftl]2.0.co;2.

O'Dea, A., H. A. Lessios, A. G. Coates, R. I. Eytan, S. A. Restrepo-Moreno, A. L. Cione, L. S. Collins, A. de Queiroz, D. W. Farris, R. D. Norris, R. F. Stallard, M. O. Woodburne, O. Aguilera, M.-P. Aubry, W. A. Berggren, A. F. Budd, M. A. Cozzuol, S. E. Coppard, H. Duque-Caro, S. Finnegan, G. M. Gasparini, E. L. Grossman, K. G. Johnson, L. D. Keigwin, N. Knowlton, E. G. Leigh, J. S. Leonard-Pingel, P. B. Marko, N. D. Pyenson, P. G. Rachello-Dolmen, E. Soibelzon, L. Soibelzon, J. A. Todd, G. J. Vermeij, and J. B. C. Jackson. 2016. Formation of the Isthmus of Panama. *Science Advances*, 2(8):e1600883. https://doi.org/10.1126/sciadv.1600883.

O'Leary, M. A., J. I. Bloch, J. J. Flynn, T. J. Gaudin, A. Giallombardo, N. P. Giannini, S. L. Goldberg, B. P. Kraatz, Z. Luo, J. Meng, X. Ni, M. J. Novacek, F. A. Perini, Z. S. Randall, G. W. Rougier, E. J. Sargis, M. T. Silcox, N. B. Simmons, M. Spaulding, P. M. Velazco, M. Weksler, J. R. Wible, and A. L. Cirranello. 2013. The Placental Mammal Ancestor and the Post-K-Pg Radiation of Placentals. *Science*, 339(6120):662–667. https://doi.org/10.1126/science.1229237.

Owen, P. 1853. Description of Some Species of the Extinct Genus *Nesodon*, with Remarks on the Primary Group (Toxodontia) of Hoofed Quadrupeds, to which that Genus is Referable. *Philosophical Transactions of the Royal Society of London*, 143:291–310.

Owen, R. 1840. "Fossil Mammalia." In *The Zoology of the H.M.S. Beagle, under the Command of Captain Fitzroy, R.N., during the years 1832–1836,* ed. C. Darwin. London: Smith Elder and Co.

Owen, R. 1848. Description of Teeth and Portions of Two Extinct Anthracothroid Quadrupeds (*Hyopotamus vectianus* and *H. bovinus*) Discovered by Marchioness of Hastings in the Eocene Deposits of the N.W. Coast of the Isle of Wight, with an Attempt to Develop Cuvier's Idea. *Quarterly Journal of the Geological Society of London*, 4:104–141.

Pabón-Caicedo, J. D., J. A. Eslava-Ramirez, R. E. Gómez-Torres. 2001. Generalidades de la distribución espacial y temporal de la temperatura del aire y de la precipitación en Colombia. *Meteorología Colombiana*, 4:47–59.

Pagani, M., Z. Liu, J. LaRiviere, and A. C. Ravelo. 2010. High Earth-System Climate Sensitivity Determined from Pliocene Carbon Dioxide Concentrations. *Nature Geoscience*, 3(1):27–30. https://doi.org/10.1038/ngeo724

Pardo-Jaramillo, M. 2010. Reporte de un nuevo ejemplar de *Granastrapotherium snorki* en el valle superior del Magdalena, Desierto de la Tatacoa, Huila, Tolima. *Revista de la Academia Colombiana de Ciencias*, 34(131):253–256.

Paula Couto, C. 1979. *Tratado de Paleonastozoologia*. Rio de Janeiro: Academia Brasileira de Ciencias.

Pérez, L. M., J. P. Pérez-Panera, O. A. Aguilera, D. I. Ronchi, R. Sánchez, M. O. Manceñido, and M. R. Sánchez-Villagra. 2016. Palaeontology, Sedimentology, and Biostratigraphy of a Fossiliferous Outcrop of the Early Miocene Querales Formation, Falcón Basin, Venezuela. *Swiss Journal of Palaeontology*, 135:187–203. https://doi.org/10.1007/s13358-015-0105-y.

Pérez, M. E., M. C. Vallejo-Pareja, J. D. Carrillo, and C. A. Jaramillo. 2017. A New Pliocene Capybara (Rodentia, Caviidae) from Northern South America (Guajira, Colombia), and its Implications for the Great American Biotic Interchange. *Journal of Mammalian Evolution*, 24(1):111–125. https://doi.org/10.1007/s10914-016-9356-7.

Pérez, M. E., and Vucetich, M. G. 2012. A Revision of the Fossil Genus *Phanomys* Ameghino, 1887 (Rodentia, Hystricognathi, Cavioidea) from the Early Miocene of Patagonia (Argentina) and the Acquisition of Euhypsodonty in Cavioidea sensu stricto. *Paläontologische Zeitschrift*, 86(2):187–204. https://doi.org/10.1007/s12542-011-0120-2.

Pérez-Consuegra, N. P., M. Parra, C. Jaramillo, D. Silvestro, S. Echeverri, C. Montes, J. M Jaramillo, J. Escobar. 2018. Provenance Analysis of the Pliocene Ware Formation in the Guajira Peninsula, Northern Colombia: Paleodrainage Implications. *Journal of South American Earth Sciences*, 81:66–77. https://doi.org/10.1016/j.jsames.2017.11.002.

Quiroz, L. I., and C. A. Jaramillo. 2010. "Stratigraphy and Sedimentary Environments of Miocene Shallow to Marginal Marine Deposits in the Urumaco Trough, Falcón Basin, Western Venezuela." In *Urumaco and Venezuelan Paleontology: The fossil record of the Northern Neotropics*, ed. M. R. Sánchez-Villagra, O. A. Aguilera, and A. A. Carlini, pp. 153–172. Bloomington: Indiana University Press.

Ré, G. H., S. E. Geuna, and J. F. Vilas. 2010. "Paleomagnetism and Magnetostratigraphy of Sarmiento Formation (Eocene-Miocene) at Gran Barranca, Chubut, Argentina." In *The Paleontology of Gran Barranca: Evolution and Environmental Change through the Middle Cenozoic of Patagonia*, ed.

R. H. Madden, A. A. Carlini, M. G. Vucetich, and R. F. Kay, pp. 32–58. Cambridge, UK: Cambridge University Press.

Renz, H. H. 1948. *Stratigraphy and Fauna of the Agua Salada Group, State of Falcón, Venezuela*. Boulder, Colorado: Geologic Society of America Memoir.

Rey, O. 1990. Análisis comparativo y correlación de las formaciones Codore y La Vela, estado Falcón. Master's diss., Universidad Central de Venezuela, Caracas.

Ribeiro, A. M., G. López, and M. Bond. 2010. "The Leontiniidae (Mammalia, Notoungulata) from the Sarmiento Formation at Gran Barranca, Chubut Province, Argentina." In *The Paleontology of Gran Barranca: Evolution and Environmental Change through the Middle Cenozoic of Patagonia*, Ed. R. H. Madden, A. A. Carlini, M. G. Vucetich, and R. F. Kay, pp. 170–181. Cambridge, UK: Cambridge University Press.

Riggs, E. S. 1935. A Skeleton of *Astrapotherium*. *Geological Series of Field Museum of Natural History*, 6:167–177.

Rincón, A. D. 2011. New Remains of *Mixotoxodon larensis* Van Frank 1957 (Mammalia: Notoungulata) from Mene de Inciarte tar pit, North-Western Venezuela. *Interciencia*, 36:894–899.

Rincón, A. D., H. G. McDonald, A. Solórzano, M. N. Flores, and D. Ruiz-Ramoni. 2015. A New Enigmatic Late Miocene Mylodontoid Sloth from Northern South America. *Royal Society Open Science*, 2:140256. https://doi.org/10.1098/rsos.140256

Rincón, A. F., J. I. Bloch, C. Suarez, B. J. MacFadden, and C. A. Jaramillo. 2012. New Floridatragulines (Mammalia, Camelidae) from the Early Miocene Las Cascadas Formation, Panama. *Journal of Vertebrate Paleontology*, 32:456–475. https://doi.org/10.1080/02724634.2012.635736.

Roth, S. 1903. Los ungulados sudamericanos. *Anales Del Museo de La Plata*, 5:1–36.

Saint-André, P.-A. 1993. *Hoffstetterius imperator* n.g., n. sp. Du Miocène supérieur de l'Altiplano bolivien et le statut des Dinotoxodontinés (Mammalia, Notoungulata). *Comptes Rendus de l'Académie Des Sciences. Série 2, Mécanique, Physique, Chimie, Sciences de L'univers, Sciences de La Terre*, 316:539–545.

Sánchez-Villagra, M. R. 2006. Vertebrate Fossils from the Neogene of Falcón State, Venezuela: Contributions on Neotropical Palaeontology. *Journal of Systematic Palaeontology*, 4(3):211. https://doi.org/10.1017/S1477201906001842.

Sánchez-Villagra, M. R. 2010. "A Short History of the Study of Venezuelan Vertebrate Fossils." In *Urumaco and Venezuelan Paleontology: The Fossil Record of the Northern Neotropics*, ed. M. R. Sánchez-Villagra, O. A. Aguilera, and A. A. Carlini, pp. 9–18. Bloomington: Indiana University Press.

Sánchez-Villagra, M. R., and O. A. Aguilera. 2006. Neogene Vertebrates from Urumaco, Falcón State, Venezuela: Diversity and Significance. *Journal of Systematic Palaeontology*, 4(3):213–220. https://doi.org/10.1017/S1477201906001829

Sánchez-Villagra, M. R., O. A. Aguilera, and I. Horovitz. 2003. The Anatomy of the World's Largest Extinct Rodent. *Science*, 301(5640):1708–1710. https://doi.org/10.1126/science.1089332

Sánchez-Villagra, M. R., O. A. Aguilera, R. Sánchez, and A. A. Carlini. 2010. "The Fossil Vertebrate Record of Venezuela of the Last 65 Million Years." In *Urumaco and Venezuelan Paleontology: The Fossil Record of the Northern Neotropics*, ed. M. R. Sánchez-Villagra, O. A. Aguilera, and A. A. Carlini, pp. 19–51. Bloomington: Indiana University Press.

Sánchez-Villagra, M. R., R. J. Asher, A. D. Rincón, A. A. Carlini, P. Meylan, and R. W. Purdy. 2004. New Faunal Reports from the Cerro La Cruz Locality (Lower Miocene), North-Western Venezuela. *Special Papers in Palaeontology*, 71:105–112.

Scherer, C. S. 2013. The Camelidae (Mammalia, Artiodactyla) from the Quaternary of South America: Cladistic and Biogeographic Hypotheses. *Journal of Mammalian Evolution*, 20(1):45–56. https://doi.org/10.1007/s10914-012-9203-4.

Scherer, C. S., J. Ferigolo, A. M. Ribeiro, and C. Cartelle. 2007. Contribution to the Knowledge of *Hemiauchenia paradoxa* (Artiodactyla, Camelidae) from the Pleistocene of Southern Brazil. *Revista Brasileira de Paleontologia*, 10:35–52.

Scherer, C. S., V. Pitana, and A. M. Ribeiro. 2009. Proterotheriidae and Macraucheniidae (Litopterna, Mammalia) from the Pleistocene of Rio Grande do Sul State, Brazil. *Revista Brasileira de Paleontologia*, 12:231–246.

Schmidt, G. I. 2011. Los Proterotheriidae (Litopterna) de Entre Ríos (Argentina): consideraciones nomenclaturales e implicancias sistemáticas. *Ameghiniana*, 48(3):605–620. https://doi.org/10.5710/AMGH.v48i2(291).

Schmidt, G. I. 2013. Litopterna y Notoungulata (Mammalia) de la Formación Ituzaingó (Mioceno tardío-Plioceno) de la Provincia de Entre Ríos: sistemática, bioestratigrafía y paleobiogeografía. Tomo [Volume] 1. Ph.D. diss., Universidad Nacional de La Plata, La Plata, Argentina.

Schmidt, G. I. 2015. Actualización sistemática y filogenia de los Proterotheriidae (Mammalia, Litopterna) del "Mesopotamiense" (Mioceno tardío) de Entre Ríos, Argentina. *Revista Brasileira de Paleontologia*, 18:521–546.

Schneider, T., T. Bischoff, and G. H. Haug. 2014. Migrations and Dynamics of the Intertropical Convergence Zone. *Nature,* 513(7516):45–53. https://doi.org/10.1038/nature13636.

Scott, K. M. 1990. "Postcranial Dimensions of Ungulates as Predictors of Body Mass." In *Body Size in Mammalian Paleobiology: Estimation and Biological Implications*, ed. J. Damuth and B. J. MacFadden, pp. 301–335. Cambridge, UK: Cambridge University Press.

Scott, W. B. 1912. "Mammalia of the Santa Cruz Beds. Paleontology III. Part II. Toxodonta." In *Reports of the Princeton University Expeditions to Patagonia, 1896–1899*, ed. W. B. Scott, pp. 111–300. Princeton, N.J., and Stuttgart: Princeton University; E. Schweizerbart'sche Verlagshandlung (E. Nägele), Stuttgart.

Scott, W. B. 1928. "Mammalia of the Santa Cruz Beds. Paleontology III. Part IV. Astrapotheria." In *Reports of the Princeton University Expeditions to Patagonia 1896–1899*, ed. W. B. Scott, pp. 301–351. Princeton, N.J., and Stuttgart: Princeton University; E. Schweizerbart'sche Verlagshandlung (E. Nägele), Stuttgart.

Scott, W. B. 1937. The Astrapotheria. *Proceedings of the American Philosophical Society*, 77:309–393.

Shockey, B. J., J. J. Flynn, D. A. Croft, P. Gans, and A. R. Wyss. 2012. New Leontiniid Notoungulata (Mammalia) from Chile and Argentina: Comparative Anatomy, Character Analysis, and Phylogenetic Hypotheses. *American Museum Novitates*, 3737:1–64.

Simpson, G. G. 1980. *Splendid Isolation: The Curious History of South American Mammals*. New Haven, Conn.: Yale University Press.

Smith, J. B., and P. Dodson. 2003. A Proposal for a Standard Terminology of Anatomical Notation and Orientation in Fossil Vertebrate Dentitions. *Journal of Vertebrate Paleontology*, 23:1–12. https://doi.org/10.1671/0272-4634(2003)23[1:apfast]2.0.co;2.

Soria, M. F. 1987. Estudios sobre los Astrapotheria (Mammalia) del Paleoceno y Eoceno. *Ameghiniana*, 24:21–34.

Soria, M. F. 2001. Los Proterotheriidae (Litopterna, Mammalia), sistemática, origen y filogenia. *Monografías Del Museo Argentino de Ciencias Naturales*, 1:1–167.

Soria, M. F., and J. E. Powell. 1981. Un primitivo Astrapotheria (Mammalia) y la edad de la Formación Río Loro, Provincia de Tucumán, República Argentina. *Ameghiniana*, 18:155–168.

Stange, M. M. R. Sánchez-Villagra, W. Salzburger, and M. Matschiner. 2018. Bayesian Divergence-Time Estimation with Genome-Wide SNP Data of Sea Catfishes (Ariidae) Supports Miocene Closure of the Panamanian Isthmus. *Systematic Biology,* syy006. https://doi.org/10.1093/sysbio/syy006.

Stehlin, H. G. 1928. Ein *Astrapotherium* fund aus Venezuela. *Eclogae Geologicae Helvetiae*, 21:227–232.

Suarez, C., A. M. Forasiepi, F. J. Goin, and C. Jaramillo. 2016. Insights into the Neotropics Prior to the Great American Biotic Interchange: New Evidence of Mammalian Predators from the Miocene of Northern Colombia. *Journal of Vertebrate Paleontology*, 36(1):e1029581. https://doi.org/10.1080/02724634.2015.1029581

Swofford, D. L. 2002. *Phylogenetic Analysis Using Parsimony (*and Other Methods). Version 4*. Sunderland: Sinauer Associates.

Tomassini, R. L., C. I. Montalvo, C. M. Deschamps, and T. Manera. 2013. Biostratigraphy and Biochronology of the Monte Hermoso Formation (Early Pliocene) at its Type Locality, Buenos Aires Province, Argentina. *Journal of South American Earth Sciences*, 48:31–42. https://doi.org/10.1016/j.jsames.2013.08.002.

Tonni, E. P. 2009. "Los mamíferos del Cuaternario de la región Pampeana de Buenos Aires, Argentina." In *Quaternário do Rio Grande do Soul: integrando conhecimentos*, ed. A. M. Ribeiro, S. G. Bauermann, and C. S. Scherer, pp. 193–205. Porto Alegre, Brazil: Monografias da Sociedade Brasilera de Paleontologia.

Townsend, K. E. B., and D. A. Croft. 2008. Diets of Notoungulates from the Santa Cruz Formation, Argentina: New Evidence from Enamel Microwear. *Journal of Vertebrate Paleontology*, 28:217–230. https://doi.org/10.1671/0272-4634(2008)28[217:donfts]2.0.co;2.

Trouessart, E. L. 1898. *Catalogus mammalium tam viventium quam fossilium: nova editio (prima completa). Tomus II*. Berolini: R. Friedländer & Sohn.

Tsubamoto, T. 2014. Estimating Body Mass from the Astragalus in Mammals. *Acta Palaeontologica Polonica*, 59:259–265. https://doi.org/10.4202/app.2011.0067.

Ubilla, M., D. Perea, and M. Bond. 1994. The Deseadan Land Mammal Age in Uruguay and the Report of *Scarrittia robusta* nov. sp. (Leontiniidae, Notoungulata) in the Fray Bentos Formation (Oligocene-?Lower Miocene). *Geobios*, 27:95–102. https://doi.org/10.1016/S0016-6995(06)80217-2.

Ubilla, M., D. Perea, M. Bond, and A. Rinderknecht. 2011. The First Cranial Remains of the Pleistocene Proterotheriid *Neolicaphrium* Frenguelli, 1921 (Mammalia, Litopterna): A Comparative Approach. *Journal of Vertebrate Paleontology*, 31:193–201. https://doi.org/10.1080/02724634.2011.539647.

Vallejo-Pareja, M. C., J. D. Carrillo, J. W. Moreno-Bernal, M. Pardo-Jaramillo, D. F. Rodriguez-Gonzalez, and J. Muñoz-Durán. 2015. *Hilarcotherium castanedaii*, gen. et sp. nov., a New Miocene Astrapothere (Mammalia, Astrapotheriidae) from the Upper Magdalena Valley, Colombia. *Journal of Vertebrate Paleontology*, 35:e903960. https://doi.org/10.1080/02724634.2014.903960.

Van Frank, R. 1957. A Fossil Collection from Northern Venezuela: 1. Toxodontidae (Mammalia, Notoungulata). *American Museum Novitates*, 1850:1–38.

Villafañe, A. L., E. Ortiz-Jaureguizar, and M. Bond. 2006. Cambios en la riqueza taxonómica y en las tasas de primera y última aparición de los Proterotheriidae (Mammalia, Litopterna) durante el Cenozoico. *Estudios Geológicos*, 62:155–166.

Villafañe, A. L., G. I. Schmidt, and E. Cerdeño. 2012. Consideraciones sistemáticas y bioestratigráficas acerca de *Thoatheriopsis mendocensis* Soria, 2001 (Litopterna, Proterotheriidae). *Ameghiniana*, 49:365–374.

Villarroel, C., and J. Colwell Danis. 1997. "A new Leontiniid Notoungulate." In *Vertebrate Paleontology in the Neotropics: The Miocene Fauna of La Venta*, ed. R. F. Kay, R. H. Madden, R. L. Cifelli, and J. J. Flynn, pp. 303–318. Washington, D.C.: Smithsonian Institution Press.

Villarroel, C., and J. Guerrero. 1985. Un nuevo y singular representante de la familia Leontiniidae? (Notoungulata, Mammalia) en el Mioceno de La Venta, Colombia. *Geologia Norandina*, 9:35–40.

Vizcaíno, S. F., G. H. Cassini, N. Toledo, and M. S. Bargo. 2012. "On the Evolution of Large Size in Mammalian Herbivores of Cenozoic Faunas of Southern South America." In *Bones, Clones, and Biomes: The History and Geography of Recent Neotropical Mammals*, ed. B. D. Patterson and L. P. Costa, pp. 76–101. Chicago: The University of Chicago Press.

Vucetich, M. G., A. A. Carlini, O. Aguilera, and M. R. Sánchez-Villagra. 2010. The Tropics as Reservoir of Otherwise Extinct Mammals: The Case of Rodents from a New Pliocene Faunal Assemblage from Northern Venezuela. *Journal of Mammalian Evolution*, 17:265–273. https://doi.org/10.1007/s10914-010-9142-x.

Webb, S. D. 1985. "Late Cenozoic Mammal Dispersal between the Americas." In *The Great American Biotic Interchange*, ed. F. G. Stehli and S. D. Webb, pp. 357–386. New York: Plenum Press.

Webb, S. D. 1991. Ecogeography and the Great American Interchange. *Paleobiology*, 17:266–280.

Webb, S. D. 2006. The Great American Biotic Interchange: Patterns and Processes. *Annals of the Missouri Botanical Garden*, 93:245–257. https://doi.org/10.3417/0026-6493(2006)93.

Webb, S. D., and J. Meachen. 2004. On the Origin of Lamine Camelidae Including a New Genus from the Late Miocene of the High Plains. *Bulletin of Carnegie Museum of Natural History*, 36:349–362. https://doi.org/10.2992/0145-9058(2004)36[349:otoolc]2.0.co;2.

Webb, S. D., and S. C. Perrigo. 1984. Late Cenozoic Vertebrates from Honduras and El Salvador. *Journal of Vertebrate Paleontology*, 4:237–254.

Weir, J. T., E. Bermingham, and D. Schluter. 2009. The Great American Biotic Interchange in Birds. *Proceedings of the National Academy of Sciences*, 106(51):21737–21742. https://doi.org/10.1073/pnas.0903811106

Welker, F., M. J. Collins, J. A. Thomas, M. Wadsley, S. Brace, E. Cappellini, S. T. Turvey, M. Reguero, J. N. Gelfo, A. Kramarz, J. Burger, J. Thomas-Oates, D. A. Ashford, P. D. Ashton, K. Rowsell, D. M. Porter, B. Kessler, R. Fischer, C. Baessmann, S. Kaspar, J. V. Olsen, P. Kiley, J. A. Elliott, C. D. Kelstrup, V. Mullin, M. Hofreiter, E. Willerslev, J.-J. Hublin, L. Orlando, I. Barnes, and R. D. E. MacPhee. 2015. Ancient Proteins Resolve the Evolutionary History of Darwin's South American Ungulates. *Nature*, 522:81–84. https://doi.org/10.1038/nature14249

Westbury, M., S. Baleka, A. Barlow, S. Hartmann, J. L. A. Paijmans, A. Kramarz, A. Forasiepi, M. Bond, J. N. Gelfo, M. A. Reguero, P. López-Mendoza, M. Taglioretti, F. Scaglia, A. Rinderknecht, W. Jones, F. Mena, G. Billet, C. de Muizon, J. L. Aguilar, R. D. E. MacPhee, M. Hofreiter. 2017. A Mitogenomic Timetree for Darwin's Enigmatic South American Mammal *Macrauchenia patachonica*. *Nature communications*, 8:15951. https://doi.org/10.1038/ncomms15951.

Weston, E. M., R. H. Madden, and M. R. Sánchez-Villagra. 2004. Early Miocene Astrapotheres (Mammalia) from Northern South America. *Special Papers in Palaeontology*, 71:81–97.

Wilf, P., N. R. Cúneo, I. H. Escapa, D. Pol, and M. O. Woodburne. 2013. Splendid and Seldom Isolated: The Paleobiogeography of Patagonia. *Annual Review of Earth and Planetary Sciences*, 41:561–603. https://doi.org/10.1146/annurev-earth-050212-124217.

Woodburne, M. 2010. The Great American Biotic Interchange: Dispersals, Tectonics, Climate, Sea Level and Holding Pens. *Journal of Mammalian Evolution*, 17:245–264. https://doi.org/10.1007/s10914-010-9144-8.

Woodburne, M. O., F. J. Goin, M. Bond, A. A. Carlini, J. N. Gelfo, G. M. López, A. Iglesias, and A. N. Zimicz. 2014a. Paleogene Land Mammal Faunas of South America: A Response to Global Climatic Changes and Indigenous Floral Diversity. *Journal of Mammalian Evolution*, 21:1–73. https://doi.org/10.1007/s10914-012-9222-1.

Woodburne. M. O., F. J. Goin, M. S. Raigemborn, M. Heizler, J. N. Gelfo, and E. V. Oliveira. 2014b. Revised Timing of the South American Early Paleogene Land Mammal Ages. *Journal of South American Earth Sciences*, 54:109–119. https://doi.org/10.1016/j.jsames.2014.05.003.

Wozniak, J., and M. H. Wozniak. 1987. Bioestratigrafía de la región nor-central de la Serranía de Falcón, Venezuela nor-occidental. *Boletín de Geología Venezuela*, 16:101–139.

Zurita, A. E., A. A. Carlini, D. Gillette, and R. Sánchez. 2011. Late Pliocene Glyptodontinae (Xenarthra, Cingulata, Glyptodontidae) of South and North America: Morphology and Paleobiogeographical Implications in the GABI. *Journal of South American Earth Sciences*, 31:178–185. https://doi.org/10.1016/j.jsames.2011.02.001.

SUMMARY OF REQUIREMENTS FOR SMITHSONIAN CONTRIBUTIONS SERIES

For comprehensive guidelines and specifications, visit https://scholarlypress.si.edu.

ABSTRACTS must not exceed 300 words.

TEXT must be prepared in a recent version of Microsoft Word; use a Times font in 12 point for regular text; be double spaced; and have 1" margins.

REQUIRED ELEMENTS are title page, abstract, table of contents, main text, and references.

FIGURES must be numbered sequentially (1, 2, 3, etc.) in the order called out; have components lettered consistently (in size, font, and style) and described in captions; include a scale bar or scale description, if appropriate; include any legends in or on figures rather than in captions. Figures must be original and must be submitted as individual TIF or EPS files.

FIGURE FILES must meet all required specifications in the Digital Art Preparation Guide. Color images should be requested only if required.

TAXONOMIC KEYS in natural history manuscripts should use the aligned-couplet form for zoology. If cross referencing is required between key and text, do not include page references within the key, but number the keyed-out taxa, using the same numbers with their corresponding heads in the text.

SYNONYMY IN ZOOLOGY must use the short form (taxon, author, year:page), with full reference at the end of the manuscript under "References."

REFERENCES should be in alphabetical order, and in chronological order for same-author entries. Each reference should be cited at least once in main text. Complete bibliographic information must be included in all citations. Examples of the most common types of citations can be found at SISP's website under Resources/Guidelines.